U.S. DEPARTMENT OF THE INTERIOR
U.S. GEOLOGICAL SURVEY

Petrology of Late Eocene Lavas Erupted in the Forearc of Central Oregon

A.S. Davis, P.D. Snavely, Jr., L.B. Gray, and D.L. Minasian

Open-File Report 95-40

Menlo Park, California
1995

ABSTRACT

Two prominent late Eocene volcanic centers are present within the Tertiary marine sedimentary sequences of the Central Oregon Coast Ranges. One, near Cape Perpetua, was formally named the Yachats Basalt (Snavely and MacLeod, 1974), the other, 120 km to the north, has been informally referred to as the basalt of Cascade Head (Snavely and Vokes, 1949). The late Eocene flows are intercalated with thin-bedded, tuffaceous, marine siltstone and fine-grained sandstone of the Nestucca Formation. At both centers, basal units are submarine breccias and pillow basalt but most of the flows were subaerially erupted. Both sequences consist of massive flows (typically < 10m), interbedded with thin layers of lapilli tuff, scoria, and conglomerate. Abundant W to NW-trending dikes are common in both units.

Conventional K-Ar ages of plagioclase separates range from ~30 to 36 Ma for the Yachats and from ~30 to 34 Ma for Cascade Head basalt. Most of the conventional K-Ar ages cluster between 30-32 Ma; ages which are too young based on the paleontological data. Concordant $^{40}Ar/^{39}Ar$ incremental heating ages for a sample each from the Yachats Basalt and the basalt of Cascade Head yielded ages of 36±1.4 Ma and 34±0.4 Ma, respectively, indicating that volcanism occurred in the uppermost Eocene.

Although minor amounts of alkalic basalt and basanite are present in the uppermost part of the Yachats Basalt, flows are predominantly tholeiitic whereas flows from Cascade Head are predominantly alkalic. Most flows, from both units, have undergone considerable crystal fractionation (MgO ~7% to 3%); nearly primitive mantle-derived compositions are rare. Extensively fractionated compositions of trachyandesite to rhyodacite are limited to margins of compositionally zoned dikes. Although crystal fractionation was clearly an important process at both centers, scatter in major and trace element trends suggest that it may not have occurred in a closed system. Trace element systematics indicate lavas were generated from variably enriched intraplate or OIB-type mantle sources. Chondrite-normalized REE patterns suggest smaller percentage of partial melting for the alkalic basalt of Cascade Head and the alkalic basalt representing the latest stage of eruptions in the Yachats Basalt.

Compared with the remarkably thick Paleocene and early Eocene basalt sequences (e.g. Crescent Formation and Siletz River Volcanics) that form the basement in much of the Oregon Coast Ranges, the late Eocene volcanics are more enriched in incompatible elements although they plot along the same MORB-OIB trend. Sparse, published Pb isotopic data for the late Eocene and Siletz River Volcanics are very similar to each other and to seamounts in the eastern Pacific. More enriched incompatible element abundances at comparable isotopic compositions are compatible with an origin by smaller percentage of melting from similar heterogeneous sources. Synchronous volcanism, similar orientation of dikes, and similar OIB source compositions are compatible with an origin in an extensional environment along a rifted continental margin. Although the late Eocene volcanism was coeval with arc-volcanism to the east, it was not geochemically related to subduction but instead appears to represent smaller percentage of melting of similar sources as for the Paleocene and early Eocene volcanism, possibly from upwelling asthenosphere from the accreted Siletzia mantle.

INTRODUCTION

Upper Eocene basaltic flows form two extensive units in the Tertiary sedimentary and volcanic sequences of the Oregon Coast Ranges. One unit near Cape Perpetua was named the Yachats Basalt (Snavely and MacLeod, 1974) and the other,120 km to the north at Cascade

Head (Fig. 1), was informally referred to as the basalt of Cascade Head (Snavely and Vokes, 1949). Isolated outcrops of basalt related to and apparently representing the last surge of volcanism in the Cascade Head area were informally referred to as the basalt of Cannery Hills (Snavely and others, 1990 a). The late Eocene flows intertongue laterally with bathyal to neritic siltstone of the Nestucca Formation (Fig. 2, Snavely, 1987).

The upper Eocene volcanism was contemporaneous with calc-alkaline volcanism of the early Cascade arc, that occurred about 100 km to the east. Plate tectonic reconstructions (Wells and others,1984) suggest that the parent magmas that produced the late Eocene volcanics rose in a transtensional environment along a broad zone of right-lateral shearing along the continental margin in a forearc setting. The Upper Eocene volcanics show no chemical evidence for subduction affinity but chemically resemble basalt erupted in intra-plate settings (Barnes and Barnes, 1992).

Descriptions and major element chemistry of selected samples of the Yachats Basalt were given by Snavely and MacLeod (1974) and major and trace element chemistry of selected samples of the basalt of Cascade Head have been given by Barnes and Barnes (1992).

This report presents major and trace element and mineral chemistry data as well as K-Ar and $^{40}Ar/^{39}Ar$ ages for a suite of samples from the Yachats and the Cascade Head basalts. The petrologic features of the two eruptive centers are compared with each other and with Paleocene and Early Eocene volcanism in the Oregon and Washington Coast Ranges in an attempt to better understand the magmatic history of this region.

GEOLOGIC SETTING

Major basaltic volcanic sequences occur within the Tertiary marine sedimentary sequences of the central Oregon Coast Ranges. The oldest volcanic unit consists of the Siletz River Volcanics (58-50 Ma, Duncan, 1982), which ranges in thickness from 1500 to 6000 m (Snavely and others, 1968). The Siletz River Volcanics consists of a thick lower unit of mostly submarine, low-K_2O, tholeiitic pillow lava and breccia and an upper unit which includes subaerial alkalic basalt and differentiates (Snavely and others, 1968). Similar massive basaltic sequences of Paleocene to lower Eocene age appear to form much of the basement of the Coast Ranges from British Columbia to southern Orgeon (e.g. Metchosin Volcanics, Crescent, and Roseburg Formations; Fig. 1). In the northern part of the Oregon Coast Ranges are basalt flows, dikes, agglomerates, and pyroclastics of the Tillamook Volcanics which are largely middle Eocene in age (46 - 42 Ma, Magill and others, 1981) although the lower unit may be correlative with parts of the Siletz River Volcanics (Duncan, 1985). These early to middle Eocene basaltic units have been interpreted as oceanic crust with associated volcanic islands that were accreted to the North American continent as a result of North American-Pacific plate convergence (Snavely and MacLeod, 1974; Duncan, 1982; Snavely, 1985). A regional unconformity separates the older volcanic units from the late Eocene units of the Yachats Basalt and the basalt of Cascade Head and Cannery Hills (Fig. 2). The youngest volcanic unit in the Oregon Coast Range consists of middle Miocene lava flows and breccia exposed along the coast at Depoe Bay, Yaquina Head, and Cape Foulweather (Snavely and others, 1973), about 50 km north of the Yachats Basalt.

The upper Eocene lavas comprise mappable units within the Nestucca Formation, a unit of tuffaceous, thin-bedded, marine siltstone and fine-grained sandstone. Foraminiferal assemblages from the Nestucca Formation indicate a late Eocene age (Narizian stage) and a bathyal to neritic environment (McKeel and Lipps, 1979; Rau, 1981).

The physical characteristics and stratigraphy of the Yachats Basalt are described by Snavely and MacLeod (1974) and of the basalt of Cascade Head by Barnes and Barnes (1981) and Snavely and others (1990 a,b). The major features of these basaltic units are briefly summarized below.

The Yachats Basalt (Fig. 3A) reaches a maximum thickness of about 750 m. The lowermost part consists largely of submarine breccias and pillow basalt but most of the unit was erupted subaerially. Flows are predominantly massive and generally 3 to 8 m thick but reach a maximum of 20 m. Some of the thicker flows exhibit columnar jointing. Thin beds (1 cm to 10 m) of scoria, lapilli tuff, and conglomerate are present between some flows. Dikes and dike swarms, trending commonly W to NW, cut all parts of the unit. Dikes are commonly 1 to 2 m wide, reaching a maximum of 8 m. Some dikes exhibit several sets of chilled margins and compositional zoning that ranges from basalt to trachyandesite or rhyodacite, indicates multiple intrusive surges moved through them.

The basalt of Cascade Head (Fig. 3B) reaches a maximum thickness of about 600 m. Like the Yachats Basalt, the basal portion is also largely submarine but most of the sequence consists of subaerial flows. Massive flows, 3 to 9 m thick, are interbedded with thin layers of lapilli tuff; however, thick columnar jointed flows appear to be rare. Abundant dikes and dike swarms cut the unit and may range from basalt to trachyandesite in composition. A distinctive feature of the basalt of Cascade Head, which is rare in the Yachats Basalt, is the presence of at least four intervals of ankaramite flows. These flows contain up to 50% phenocrysts of primarily clinopyroxene accompanied by variable amounts of olivine. Sills of similar ankaramite cropout more than 10 km east of the Cascade Head volcanic center (Snavely and others, 1990).

The final surge of lava at the Cascade Head center is referred to as the basalt of Cannery Hills (Snavely and others, 1990 a). This basalt is well exposed in isolated outcrops along the east shore of Nestucca Bay (Fig. 3B). These flows and breccias were erupted from small vents and spatter cones along a north-trending fault that cuts the uppermost part of the Nestucca Formation. Mollusk-bearing basaltic sandstone is often mixed with the basalt and red oxidized scoria and littoral cones of gritty sandstone, with dips up to 60°, occur in places along feeder dikes.

ANALYTICAL METHODS

The samples were studied in thin section and selected for bulk chemical analyses performed in the analytical laboratories of the U. S. Geological Survey. Major element chemistry was determined by wave-length dispersive X-ray fluorescence (XRF) and abundances of Rb, Sr, Zr, Ba, Y, and Nb by energy-dispersive XRF, using methods described in Baedecker (1987). FeO, CO_2, and H_2O were determined by standard wet chemical techniques (Peck 1964). All samples analyzed for major elements were also analyzed for rare earth element (REE) abundances by ICP-MS and the precision and accuracy of the method are described by Lichte and others (1987). A selected subset of samples were analyzed by INAA for Hf, Ta, Th, Sc, Co, Cr and for REE, using the methods described in Baedecker (1987). Feldspar, olivine, clinopyroxene, and amphibole were analyzed with a 9-channel ARL electron microprobe. Operating conditions, standards, and data reduction methods used are described in Davis and Clague (1987).

For conventional whole-rock K-Ar measurements, rock was crushed and sieved to retain the 0.5 to 1.0 mm size fraction. The ground material was then treated with 5% HF for two minutes and with 14% HNO_3 for thirty minutes to remove clay minerals that are present

in small amounts in the groundmass, vesicles, and along fractures. A second, more rigorous procedure was tried on a few samples (indicated in Table 3) in order to test whether this would remove alteration more efficiently. This procedure consisted of treating the sample with 10% HF in an ultrasonic bath for 10-15 minutes followed by rinsing and washing the samples in distilled water for five minutes. The dried, ground material was split into aliquants. One was used for the Ar analysis and the other was pulverized to a fine powder for duplicate K_2O analyses. K_2O analyses were performed by flame photometry (Ingamells, 1970) and Ar mass analyses were done either with a multiple collector mass spectrometer (Stacey and others, 1981) or with a 60° sector, 15.2-cm radius Nier-type spectrometer, both operated in the static mode. Details of the conventional K-Ar dating techniques have been described by Dalrymple and Lanphere (1969). For samples with replicate Ar analyses, weighted mean ages were calculated, with weighting proportional to the inverse of the variance for each analysis (Taylor, 1982).

For $^{40}Ar/^{39}Ar$ dating the samples were sealed in air in quartz vials and irradiated in the core of the U.S. Geological Survey TRIGA reactor following methods described by Dalrymple and others (1987). Incremental heating analyses were done using a conventional Ar extraction line with induction heating (Dalrymple and Lanphere, 1969) and a multicollector spectrometer (Stacey and others, 1981). The $^{40}Ar/^{39}Ar$ incremental heating analyses were reduced as both spectra and isochrons using criteria recommened by Lanphere and Dalrymple (1978). Concordant weighted mean plateau ages are used as the best estimate of the sample ages.

PETROGRAPHY AND MINERAL CHEMISTRY

Locations of analyzed samples are shown in figure 3 and latitude and longitude are given along with the petrographic descriptions in appendix 1. Mineral chemistry of primary phases is given in appendices 2 to 5. Rock names introduced in this section are based on the chemical classification of Cox and others (1979) described in the chemistry section.

Yachats Basalt

Lava flows in the Yachats Basalt are predominantly basalt but include minor amounts of more evolved compositions (see chemistry section). Most of the basalts are porphyritic or glomeroporphyritic. The most common phenocryst phase is plagioclase, which may comprise over 30% of the rock. The plagioclase is accompanied by variable amounts of clinopyroxene and/or olivine in a groundmass of plagioclase, anhedral clinopyroxene, and abundant Fe-Ti oxides. The plagioclase phenocrysts are frequently large (to 3 cm) and often show evidence of resorption, sieve-textured cores, and an abundance of inclusions that are presumably devitrified glass, whereas the smaller plagioclase crystals are typically euhedral. Plagioclase phenocrysts in basalts are typically labradorite but range from bytownite to andesine. In more fractionated basaltic andesite and trachyandesite, phenocryst cores are also predominantly labradorite but rims may be andesine or oligoclase and some microlites are anorthoclase. The feldspar composition of the most fractionated rhyolite sample (S91-11) from the margin of a compositionally zoned dike contain andesine and oligoclase microphenocrysts and anorthoclase microlites in the groundmass along with some anhedral quartz. The anhedral quartz grains may be a contaminant from the wall rock. Compositional zoning of feldspar is

typically normal and minor in most basalts but reaches over 30 mole percent (Appendix 2A) in some basaltic andesite. K_2O increases with decreasing An content (Fig.4A).

Anhedral clinopyroxene phenocrysts are present in minor amounts in most of the tholeiitic and mildly alkalic basalt samples. Sub- to euhedral clinopyroxene microphenocrysts are abundant in the two more strongly alkalic samples (S89-15, S91-14). Anhedral granules of clinopyroxene are abundant in the groundmass of most basalt samples; subophitic clinopyroxene enclosing plagioclase is present in some holocrystalline samples from flow interiors.

Compositionally, the clinopyroxene is typically augite (Fig. 5A) with low to moderate amounts of TiO_2 and Al_2O_3, ranging from 0.62 to 2.68% and from 1.36 to 5.24% in tholeiitic samples, respectively. Clinopyroxene in the alkalic basalt is typically more calcic with higher TiO_2 and Al_2O_3 contents, reaching maximums of 3.70 and 6.86%, respectively (S91-14, Appendix 3A). In accord with the differentiated nature of the host rock, Cr_2O_3 in the clinopyroxene is typically at, or below, detection limits, except for some crystals in alkalic samples which contain up to 0.81%. TiO_2 (Fig. 6A) increases with decreasing Mg number (100Mg/(Mg+Fe)) in the clinopyroxene of basalt but decreases in the trachyandesite, probably indicating significant amounts of Fe-Ti oxide fractionation.

Olivine phenocrysts are present in small amounts in many of the tholeiitic and mildly alkalic basalt and olivine microphenocrysts are very abundant in the two more strongly alkalic samples. The larger olivine pseudomorphs are generally euhedral to subhedral with some embayed margins and a few contain spinel inclusions, which are mostly oxidized. In most samples the olivine is completely replaced by clay minerals and Fe oxides/hydroxides. A few unaltered cores remain in sample SR58-17 and all of the olivine in the basanite sample (S89-15) is unaltered. For these two samples the compositional range in olivine is narrow ranging from $Fo_{60.3}$ to $Fo_{63.4}$ in the basanite (S89-15) and is $Fo_{69.1\pm0.2}$ in the few unaltered phenocryst cores in sample SR58-17. In accord with the differentiated nature of the host rocks no highly magnesian olivine is present.

Textures of the basalts and basaltic andesites are most commonly intergranular, pilotaxitic, or subtrachytic. Hyalopilitic textures occur in glassy samples and subophitic textures occur in holocrystalline samples from the interior of flows. The more fractionated samples typically have pronounced trachytic textures. Generally, the rocks are not badly altered but secondary minerals of calcite, zeolite, and clay minerals are common in amygdules, veins, and fractures.

Basalt of Cascade Head

The Cascade Head samples are also predominantly basalt in composition but in contrast to the Yachat Basalt, they are mostly alkalic (see chemistry section). Like the Yachats Basalt, most samples are porphyritic but the dominant phenocryst phase is clinopyroxene. However, some highly plagioclase-phyric units are also present. Some of the clinopyroxene-phyric samples are ankaramites with very high abundances of phenocrysts (to 50%) of mostly clinopyroxene, accompanied by varying proportions of olivine. The clinopyroxene phenocrysts in the ankaramites are frequently large (to 3 cm), euhedral to subhedral, and strongly colored pink-brownish pleochroic and unaltered; the accompanying olivine phenocrysts are typically pseudomorphed by clay minerals.

Compositionally the clinopyroxene crystals are mostly salite and augite (Fig. 5B) which are more calcic and higher in TiO_2 (Fig. 6B), Al_2O_3, and Na_2O at comparable Mg numbers than those in the tholeiitic Yachats basalts, although they overlap with compositions in

alkalic Yachats Basalt samples. Like for most Yachats Basalt, Cr_2O_3 contents are typically below or at detection limits in accord with their differentiated host rock compositions.

Although most olivine phenocrysts have been altered, some microphenocrysts are still fresh and have been analyzed (Appendix 4). Forsterite content (Fo mole%) shows a large range from about 82 to 46 and is positively correlated with NiO which is typically low but ranges from 0.01 to 0.24%. CaO is negatively correlated with Fo and ranges from 0.19 to 0.50%.

Plagioclase phenocrysts, although not as prominent as in many Yachats samples, also reach the cm-size range and have similar morphological features as those of Yachats samples. The compositional range is also similar (Fig. 4B) but extends to more sodic plagioclase compositions for some phenocrysts, and crystals of anorthoclase and rare sanidine are present in the groundmass of the trachyandesites (Appendix 2B). Compositional zoning reaches over 20 mole % in some samples and is typically normal, although pronounced reverse zoning (up to 11 mole%) is observed for some samples (SR62-160, MR68-80). No significant difference in K_2O contents is observed between the tholeiitic and alkalic basalts of Cascade Head, suggesting that samples plot in the tholeiitic field due to accumulation of clinopyroxene as discussed in the chemistry section below.

The trachyandesite samples contain amphibole phenocrysts. The phenocrysts are sub- to anhedral, pleochroic brown to yellow-brown with opaque reaction rims and some contain apatite inclusions. Compositionally they are kaersutite (using the nomenclature of Leake, 1978) in the less differentiated sample (MR68-80) and ferroan pargasitic hornblende or ferroan pargasite in the more differentiated one (S79-36, Appendix 5).

Titanomagnetite and ilmenite are highly abundant in all Cascade Head samples. As in Yachats samples, intergranular to subtrachytic textures are common in basalt and pronounced trachytic textures occur in more differentiated samples.

The basalt of Cannery Hills are sparsely to moderately porphyritic with small clinopyroxene phenocrysts accompanied by small, but variable amounts of olivine microphenocrysts in an intergranular to subtrachytic groundmass of abundant clinopyroxene and opaque minerals and only minor plagioclase. Some samples have considerable amounts of secondary alteration in veinlets and fractures crisscrossing the rocks; especially the SH64 samples look sheared with an abundance of veinlets and fractures. Secondary minerals include clays, zeolites, and calcite.

K-Ar AND $^{40}Ar/^{39}Ar$ AGES

Conventional whole-rock K-Ar ages for two whole rocks and one plagioclase separate from the Yachats Basalt yielded ages of 30.7±0.7, 34.0±0.7, and 36.1±0.7 Ma, respectively. Ages for 11 whole rock samples from the basalt of Cascade Head range from 30.5±0.6 to 33.0±0.7 Ma. Most conventional K-Ar ages cluster between 30 to 32 Ma, which is too young when compared to the paleontological ages obtained for microfossils in the interbedded siltstone of the Nestucca Formation (Rau, 1981; Bukry and Snavely, 1988). Conventional K-Ar ages of plagioclase and hornblende separates from the trachyandesite dike (S84-114) yielded slightly older ages of 34.0±1.0 and 33.9±0.8 Ma, respectively. Since this dike cuts several flows with younger ages, these ages are clearly too young and the flows are at least 34 Ma or older.

$^{40}Ar/^{39}Ar$ incremental heating ages for a sample from each the Yachats Basalt (S83-136) and from the basalt of Cascade Head (S83-50) yielded ages only slightly older than the corresponding conventional whole-rock ages (Table 3). Sample 83-136 which gave a whole-

rock age of 34.2 ±1.0 Ma gave an isochron age of 36.5 ±1.4 Ma and sample S83-50 which gave a whole-rock age of 32.9 ±0.8 gave a $^{40}Ar/^{39}Ar$ incremental heating age of 33.5 ±0.4 Ma. These incremental heating ages gave concordant isochrons and meet all of the criteria (e.g. atmospheric intercepts, low sums/N-2) established by Lanphere and Dalrymple (1978) for reliable ages.

The ages obtained for geographically widely separated samples are remarkably consistent and span a very narrow range, suggesting rapid, extrusion from multiple vents. The best ages are within the error of the age of the Eocene-Oligocene boundary (MacIntosh and others, 1992) indicating eruption during the uppermost Eocene, in agreement with the paleontological ages.

MAJOR ELEMENT CHEMISTRY

Major-element compositions for Yachats, Cascade Head, and Cannery Hills basalts are presented in Table 1. A plot of total alkalis versus SiO_2 (Fig. 7) shows compositions from both centers with similar trends, except that the Cascade Head and Cannery Hills compositions are displaced toward a more alkalic trend.

Yachats Basalt

Most of the Yachats flows are tholeiitic basalt and minor basaltic andesite (volatile-free; using the classification of Cox and others, 1979). The trachyandesite and rhyolite are found only in dikes. A few alkalic flows and dikes are present and one flow, in the upper part of the unit, is strongly alkalic basanite (S89-15, Fig. 7). No primitive compositions that could be considered primary mantle-derived magmas have been found; most compositions cluster between 5% to 3% MgO although the entire range is from about 7% to 3% (Fig. 8). SiO_2, Na_2O, Al_2O_3 and K_2O generally increase with decreasing MgO content (Fig. 8), whereas CaO, FeO*, and TiO2 generally decrease. Although there is considerable scatter reflecting variable proportions of phenocrysts, K_2O (Fig.8G) and Na_2O (Fig. 8E) show fairly well defined linear trends for the tholeiitic samples but the alkalic samples do not fit this trend well. P_2O_5 vs. MgO (Fig. 8H) also shows a linear trend for tholeiitic samples, increasing with decreasing MgO to about 3% MgO, but P_2O_5 is much lower in the rhyolitic dike sample presumably due to apatite fractionation. The mildly alkalic sample (SR63-117) is as low in K_2O and P_2O_5 as the tholeiitic samples, but the two more strongly alkalic samples (S89-15, S91-14) are greatly enriched in K_2O and P_2O_5 compared to the tholeiitic compositions.

K_2O vs. TiO_2 (Fig. 9A) shows a large amount of scatter probably reflecting at least in part different amounts of Fe-Ti oxide and feldspar fractionation. However, K_2O vs. P_2O_5 (Fig. 9B) shows a linear trend with similar K/P ratios, indicating that both elements were incompatible until apatite fractionation began in the more evolved trachyandesite magmas.

Basalt of Cascade Head

The Cascade Head samples are mostly alkalic basalts and trachyandesite (Fig. 7). The two samples (S83-117, S83-48) that plot in the tholeiitic field do so only because of the high abundance of mafic phenocryst phases, especially clinopyroxene. The compositions of groundmass feldspar and Fe-Ti oxides in these two rocks indicate alkalic host lava compositions similar to the other samples. The Cascade Head suite includes samples with

higher MgO contents than the Yachats Basalt (Fig. 8). MgO contents of nearly 10% would be considered near primary, however, all of the samples with MgO >7% are ankaramites wich may contain up to 50% phenocrysts of mostly clinopyroxene. The high MgO content appears to be due to the accumulation of mafic phenocrysts. As in the Yachats Basalt, highly fractionated compositions such as trachyandesite occur only in dikes. Fractionation trends are parallel to but higher in alkalis than theYachats Basalt (Fig. 7). The ankaramitic samples have a lot of scatter with low SiO_2, K_2O, and high TiO_2 over a narrow range of MgO (Fig. 8) that do not appear to reflect fractionation trends but instead appears to be due to the accumulation of mafic phenocrysts. P_2O_5 vs. MgO variation (Fig. 8H) suggests two different trends, one mildly and one more strongly alkalic, that are essentially parallel to the Yachats trend. K_2O vs. TiO_2 (Fig. 9A) show less scatter but higher abundances than for most Yachats basalts. With respect to K_2O vs. P_2O_5 (Fig. 9B) the basalt of Cascade Head plot along the same trend as the Yachats Basalt but lower abundances of P_2O_5 in the trachyandesite suggest apatite fractionation.

The basalt of Cannery Hills are similar to other moderately alkalic composition of Cascade Head (Fig. 7) but they are more primitive with considerably higher MgO (~9%) and some have very high TiO_2 contents (> 4.0%, Fig. 9). Their undifferentiated nature suggests that they may have bypassed the magma storage system in which most of the Cascade Head basalts were fractionated.

TRACE ELEMENT CHEMISTRY

Trace-element abundances for the Yachats Basalt are given in Table 2A and for the basalt of Cascade Head and Cannery Hills in Table 2B.

Yachats Basalt

Rb, Ba, Nb, Y, and Zr behaved largely incompatibly throughout the fractionation sequence (Fig. 10) but some scatter is evident, especially for Rb and Ba which are sensitive to secondary alteration. Nb vs. Zr (Fig.10E) shows a well defined linear trend from basalt to rhyolite; only the basanite (S89-15) and alkalic basalt from a dike (S91-14) deviate from this trend because of very high Nb contents. Sr vs. Zr (Fig.10 C) shows a large amount of scatter and a limited range of abundances in basalt and basaltic andesite presumably due to the variable abundance of plagioclase. Although Zr/Nb ratios range from 3.6 to 9.7, for most samples Zr/Nb ratios cluster around 5.5 ±1 (Fig. 10F) over a large range of Zr abundances that is consistent with crystal fractionation.

The chondrite-normalized rare earth element (REE) patterns (Fig. 11A) show pronounced light REE enrichment for all samples comparable to other intraplate volcanics (e.g. Basaltic Volcanism Project, 1980). The more differentiated basalt and basaltic andesite samples have higher overall REE abundances with patterns that are elevated but generally parallel to those of less fractionated samples. The rhyolite dike sample has the highest light REE enrichment but the pattern is not parallel to the other samples. The more erratic pattern may be due to contamination with wall rock and partial alteration of the groundmass. A plot of chondrite-normalized $(Ce/Yb)_N$ vs.Ce abundance (Fig. 12) shows a reasonably well defined trend compatible with crystal fractionation for the tholeiitic samples. Two more strongly alkalic samples have higher $(Ce/Yb)_N$ ratios, suggesting that they may have originated by smaller percentage of melting of a source similar to the tholeiitic basalt or by similar percentage of melting of a more enriched source.

Basalt of Cascade Head

Trace element compositions of Casacade Head samples show similar trends to the Yachats Basalt except that Rb, Ba, Sr, and Nb are higher and Y abundances lower at comparable Zr contents (Fig. 10). Zr/Nb ratios vs. Zr (Fig.10 F) abundance shows a similar trend as for Yachats Basalt except Zr/Nb ratios are typically lower, as is to be expected for alkalic compositions.

Chondrite-normalized REE patterns (Fig. 11B) are generally similar to those of Yachats samples but light REE enrichment is greater at comparable heavy REE abundance. $(Ce/Yb)_N$ vs. Ce abundance (Fig.12) shows an overall pattern indicative of crystal fractionation but $(Ce/Yb)_N$ ratios are higher and more variable than for Yachats Basalt, compatible with origin by smaller percentage of partial melting and more heterogeneous sources. The basalt of Cannery Hills have trace element abundances similar to other Cascade Head basalt (Fig. 10, 11). Chondrite-normalized REE patterns have similar LREE enrichment as the moderately alkalic Cascade Head basalt and similar $(Ce/Yb)_N$ ratios at lower Ce abundances (Fig. 12) are compatible with similar degree of partial melting from heterogeneous sources but more limited extent of fractionation.

DISCUSSION

Magmatic Processes

Most of the late Eocene lavas consist of fractionated basalt. Truly primitive compositions are absent although the basalt of Cannery Hills come close to being mantle-derived. Most of the Cascade Head basalts with MgO >7% do not appear to be primitive lavas but instead reflect accumulation of mafic phenocryst phases. The compositions of microphenocrysts and microlites of the ankaramitic samples indicate alkalic host lavas similar to the other samples. Magmas differentiated in crustal magma chambers but very extensive fractionation was limited to small volumes observed in dikes. These small volumes of extensively fractionated compositions could be derived from thin layers at the top of compositionally zoned magma chambers or be interstitial melt from boundary layer crystallization that was extracted by filter pressing. Compositional zoning and morphological features of some crystals suggest some magma mixing may have occurred. However, compared to the ubiquitous evidence of magma mixing observed at slow-spreading centers (e.g. Dungan and Rhodes, 1978; Rhodes and others, 1979; Davis and Clague, 1990), magma mixing was minor in the Yachats Basalt and the basalt of Cascade Head and fractionation trends observed are compatible with simple crystal fractionation and accumulation of observed phenocryst phases (Stormer and Nicholls, 1978). This appears to be especially true for the Yachats tholeiites, which show well defined fractionation trends. The two alkalic Yachats compositions in the upper part of the sequence do not fit this trend but instead are more similar to the alkalic lavas of Cascade Head indicating that similar small alkalic batches were erupted during the waning stage of volcanism.

The basalt of Cascade Head are alkalic with higher incompatible element abundances, suggesting origin by smaller percentage of partial melting. The Yachats Basalt represent either larger percentage of melting of a similar source or similar percentage of melting of a slightly more depleted source. Some source heterogeneities are indicated by trace element ratios for both volcanic centers. The preponderance of large euhedral clinopyroxene

phenocrysts in the ankaramitic Cascade Head samples that may have crystallized ahead of olivine suggest these magmas may have originated at greater depth (Bender and others, 1978) than the Yachats basalts which have accumulated primarily plagioclase.

Comparison with early Eocene basalts

The late Eocene volcanism is in many ways distinct from the mafic volcanism represented by the extensive Paleocene and early Eocene basalt sequences that comprise much of the basement of the Coast Ranges. The older basalt sequences have much larger volumes, reaching thicknesses of several km (Glassley, 1974; Snavely and MacLeod, 1974; Babcock and others, 1992). Typically these sequences consist of two units: a lower, more extensive unit of submarine, low-K_2O pillow basalts and breccias and an upper unit that is largely subaerial and includes alkalic basalts and minor differentiates (Snavely and MacLeod, 1974). The compositions of lower Eocene basalts (shown for comparison in the figures) are from the Crescent Formation because the most comprehensive published major-and-trace element data are from this sequence (Glassley, 1974; Babcock and others, 1992). The major-element compositions of Siletz River Volcanics, which forms the basement in the central Oregon Coast Range, are contained within the field shown for the Crescent Formation (Fig. 8, 9) but little trace-element data are available for the Siletz River Volcanics.

Compared to the late Eocene basalts, the more voluminous older units are much less fractionated and include many relatively primitive compositions (MgO >8%). In their low incompatible element abundances and the concave-downward REE profiles, basalts from the lower Crescent Formation (Fig. 11A) resemble normal mid-ocean ridge basalt (MORB). More enriched compositions from the upper Crescent Formation (not shown in figure) overlap with those of the late Eocene basalts and resemble typical intraplate basalts such as found on many oceanic islands and in some continental settings. The early Eocene basalt compositions are compatible with an origin as oceanic crust and associated islands as suggested by Snavely and others (1968) and Duncan (1982). Compositions of the lower Eocene basalts plot along the same trend as those shown for most of the late Eocene basalts but are more depleted in incompatible elements, suggesting an origin by larger percentages of partial melting from similar mantle sources or similar percentagee of melting from a highly depleted source.

No isotopic analyses were obtained from the late Eocene basalts in this study but Pb isotope compositions for a Yachats Basalt and for a trachyandesite from Cascade Head have been published by Tatsumoto and Snavely (1969) and are shown in figure 13, along with several analyses from the Siletz River Volcanics. Isotopic ratios of Yachats and Cascade Head lavas plot well within the range of the early Eocene basalts. The trachyandesite from Cascade Head has a composition similar to the tholeiitic basalt from the Siletz River Volcanics, indicating that the alkalic basalts could be derived by smaller percentage of melting from a similar source. The Pb isotopic ratios of a siltstone from the underlying Tyee Formation (Fig. 13) indicates that the enriched composition of Cascade Head sample is not due to assimilation of country rock. As suggested by the trace element ratios (e.g. Ce/Yb and Zr/Nb), source heterogeneities are confirmed by the range of isotopic ratios observed. Although major and most trace element abundances and ratios of the early Eocene basalts resemble depleted normal MORB, the Pb isotope compositions for most are more radiogenic than normal Pacific MORB, especially with respect to $^{207}Pb/^{204}Pb$ (Fig. 13). Compositions with more radiogenic $^{87}Sr/^{86}Sr$ have been interpreted as evidence for the influence of a hot spot (Duncan, 1982). However, similar enrichments and small scale heterogeneities have been observed for small seamounts near the East Pacific Rise (Fornari and others, 1988)

which do not appear to be related to a hot spot. The variable enrichment of small scale heterogeneities may be the result of metasomatism of a depleted peridotite mantle source related to subduction processes. Regardless of the origin of enrichment, the compositions clearly indicate that the late Eocene basalts could have been derived from similar sources as the Paleocene and early Eocene basalts.

Tectonic Implications

The Paleocene and early Eocene basaltic sequences forming the basement of the Coast Ranges from Washington to southern Oregon may have originated as oceanic crust with associated islands as suggested by Duncan (1982), and Snavely and others (1968). Snavely (1984), Wells and others (1984), and Babcock and others (1992) explored an alternative origin, suggesting the basaltic sequences may have formed in a continental margin rift system. Such an origin appears plausible for the upper Eocene units of Yachats and Cascade Head but appears less likely for the entire Paleocene and early Eocene volcanic sequence, especially the lower MORB-like unit. It is difficult to envision up to 16 km of mostly submarine basalts erupting over a period spanning 4 to 8 million years within a rift system extending from British Columbia to southern Oregon within an overall compressional environment of a convergent plate margin. An alternative model may incorporate aspects of both models. Fragments of oceanic crust with associated seamounts and islands were accreted to the continental margin in the Paleocene and early Eocene. The fragments, or microplates, originated close to the continental margin because they contain interbedded continental detritus (Snavely, 1987) and because paleomagnetic data do not show significant N-S translation but variable amounts of rotation (Wells and Coe, 1985). After accretion, smaller volumes of mafic magma, including subaerial alkalic basalts, are erupted on top of the accreted oceanic crust during periods of localized extension, possibly related to rotation of microplates.

A decrease in the rate of convergence between the Farallon and North American plates and plate reorganization may have resulted in episodes of extensional rifting and volcanism. One such episode may have occurred around 42 Ma (Wells and others, 1984) which may have generated the Tillamook and Grays River volcanics and another around 36 Ma may have produced the Yachats and Cascade Head basalts. The narrow range of ages for Yachats and Cascade Head basalts indicates that eruptions occurred more or less simultaneously at both centers and along the north-trending fault in the basalt of Cannery Hills. Unlike the Paleocene and early Eocene lavas which show the limited fractionation trend typically observed for MORB, most of these lavas have been fractionated in crustal magma chambers. The chemical continuity with the early Eocene volcanism shown by later eruptions may be due to tapping the same mantle wedge underlying the accreted oceanic crust but may have involved smaller percentages of melting. The dike swarms in the upper Eocene volcanics trended E-NE before being rotated by 75° to their present W-NW orientation (Wells and others, 1984; Snavely and others, 1992). Such an orientation would be expected for tension faults and fractures formed in response to right lateral shearing along the north-trending Fulmar fault zone (Snavely and Wells, 1991).

High $^{87}Sr/^{86}Sr$ isotopic ratios have been used as evidence for the existence of a hot spot that presumably generated symmetrical seamount chains (Duncan, 1982). Radiometric ages of some early Eocene volcanics are not consistent with a simple hot spot track (Babcock and others, 1992; Snavely, unpublished data). Without an age progression of a seamount chain, it is difficult to explain how a single hot spot could influence similar volcanism from British Columbia to southern Oregon. The isotopic enrichment, especially with respect to

$^{207}Pb/^{204}Pb$, could have resulted from metasomatism from the subducting slab if these lavas were generated in a continental margin rift system. Considering the tectonic complexity of microplate rotation and the possibility of different types of superposed volcanism for the early Eocene sequences, much more detailed isotopic and radiometeric data are required to interpret these thick, extensive volcanic units. However, small scale heterogeneities are ubiquitous in MORB sources and, although the present North Pacific MORB indicates very depleted sources (White and others, 1987; Church and Tatsumoto, 1975) more enriched heterogeneities may have been present in the early Eocene mantle. Enriched isoptopic compositions similar to those of the Eocene volcanics from the Oregon Coast Ranges have been observed for seamounts near the northern East Pacific Rise (Fig. 13, Fornari and others, 1988) where there is no evidence of a hot spot.

CONCLUSIONS

Late Eocene tholeiitic and alkalic basalts were erupted from two centers in the Oregon Coast Range. Although they erupted in a forearc, chemically these lavas are intraplate basalt similar to those found on oceanic islands or in some continental settings. Both sequences consist primarily of differentiated basalt; more felsic compositions, ranging from trachyandesite to rhyolite, are limited to dikes and sills. Lavas from the northern center at Cascade Head are generally more alkalic with higher incompatible element abundances suggesting an origin by smaller percentages of melting than for the Yachats Basalt. Presence of several ankaramitic units within the Cascade Head sequence, containing large euhedral clinopyroxene that apparently crystallized before or simultaneously with olivine, suggest that they may have originated at greater depths than most of the Yachats basalt which accumulated mostly plagioclase. Compared to the thick, extensive Paleocene and early Eocene basalt sequences that comprise much of the basement in the Oregon Coast Range these centers erupted smaller volumes of lavas that differentiated in crustal magma chambers. The narrow range of ages indicates rapid eruption from multiple vents occurred simultaneously at both centers and over a short period of time in the uppermost Eocene.

Incompatible element ratios of the late Eocene basalts are consistent with an origin by smaller percentage of partial melting of a source similar to the older volcanic units and the limited isotopic data indicates similar heterogeneous sources that are more enriched than MORB. The variable enrichment, especially with respect to $^{207}Pb/^{204}Pb$, may reflect metasomatism due to subduction-related processes. The late Eocene volcanism was coeval with volcanism at the Cascade Arc and may have resulted from upwelling and decompressional melting of accreted Siletzia mantle overlying the subducted slab during local extension and rifting in a forearc basin due to plate reorganization.

ACKNOWLEDGMENTS

We thank Russ Evarts for a very thorough and helpful review. Susan Vath helped draft the figures and Walt Friesen helped with sample preparation.

REFERENCES CITED

Babcock, R.S., Burmester, R.F., Engebretson, D.C., and Warnock, A., 1992, A rifted margin origin for the Crescent Basalts and related rocks in the northern Coast Range volcanic province, Washington and British Columbia: J. of Geophys. Res., v. 97, p. 6799-6821.

Baedecker, P. A., 1987, Methods for geochemical analyses: U.S. Geological Survey Bulletin 1770.

Barnes, M.A., 1981, The geology of Cascade Head, an Eocene volcanic center. MS thesis, University of Oregon, Eugene, 103 pp.

Barnes, M.A. and Barnes, C.G., 1992, Petrology of Late Eocene basaltic lavas at Cascade Head, Oregon Coast Range: J. Volcan. Geotherm. Res., v. 52, p.157-170.

Bender, J.F., Hodges, F.N., and Bence, A.E., 1978, Petrogenesis of basalts from the project FAMOUS area: Experimental study from 0 to 15 kbars: Earth and Planet. Sci. Let., v. 41, p. 277-302.

Bukry, D. and Snavely, P.D., Jr., 1988, Coccolith zonation for Paleogene strata in the Oregon Coast Range; *in* Filewicz, M.V. and Squires, R.L., (eds.), Paleogene statigraphy, West Coast of North America: Pacific Section, SEPM, West Coast Paleogene Symposium, v. 58, p. 251-263.

Church, S.E. and Tatsumoto, M., 1975, Lead isotope relations in oceanic ridge basalts from the Juan de Fuca -Gorda Ridge area, N.E. Pacific Ocean: Contrib. to Mineral. and Petrol., v. 53, p.253-279.

Cox, K.G., Bell, J.D., and Pankhurst, R.J., (1979), The interpretation of igneous rocks: Allen & Unwin, London: 450 p.

Dalrymple, G.B. and Lanphere, M.A., 1969, Potassium-argon dating. W.H. Freeman Co., San Francisco, California, 258 pp.

Dalrymple, G.B. and Lanphere, M.A., 1971, $^{40}Ar/^{39}Ar$ technique of K-Ar dating. A comparison with the conventional technique. Earth Planet. Sci. Lett., v. 12. p. 300-308.

Dalrymple, G.B., Alexander, E.C., Lanphere, M.A., and Kraker, G.P., 1981, Irradiation of samples for $^{40}Ar/^{39}Ar$ dating using the Geological Survey TRIGA reactor. U.S. Geol. Survey Prof. Paper 1176, p.1-55.

Davis, A.S., and Clague, D.A., (1987), Geochemistry, mineralogy, and petrogenesis of basalt from the Gorda Ridge: J. of Geophys. Res., v. 92, p. 10,467-10,483.

------, (1990), Gabbroic xenoliths from the northern Gorda Ridge: Implications for magma chamber processes under slow-spreading centers: J. of Geophys. Res., v. 95, p. 10,885-10,190.

Duncan, R.A., 1982, A captured island chain in the Coast Range of Oregon and Washington: J. Geophys. Res., v.87, p.827-837.

Dungan, M.A., and Rhodes, J.M., (1978), Residual glasses and melt inclusions in basalts from DSDP legs 45 and 46: Evidence for magma mixing: Contrib. to Mineral. and Petrol., v. 67, p. 417-431.

Fornari, D.J., Perfit, M.R., Allen, J.F., Batiza, R., Hayman, R., Barone, A., Ryan, W.B.F., Smith, T., Simkin, T., and Luckman, M., 1988, Geochemical and structural studies of the Lamont seamounts: seamounts as indicators of mantle processes: Earth and Planet. Sci. Lett., v.89, p.63-83.

Glassley, W.E., 1974, Geochemistry and tectonics of the Crescent volcanic rocks, Olympic Peninsula, Washington. Geol. Soc. Amer. Bull., v. 93, p. 785-794.

Haskin, L.A., Frey, F.A., Schmitt, R.A, and Smith, R.H., 1968, Meteoric, solar, and terrestrial rare-earth distributions: Phys. Chem. Earth, v.7, p.167-321.

Ingamells, C.O., 1970, Lithium metaborate flux in silica analysis: Anal. Chim. Acta, v. 52, p. 323-334.

Leake, B.E., 1978, Nomenclature of amphiboles: Mineral. Magazine, v. 63, p. 1023-1052.

Lichte, F.E., Meier, A.L., and Crock, J.G., 1987, Determination of the rare-earth elements in geological material by inductively coupled plasma mass spectrometry: Analytical Chemistry, v. 59, p. 1150-1157.

Magill, J., Cox, A., and Duncan, R., 1981, Tillamook volcanic series: Further evidence for tectpnic rotation of the Oregon Coast Range: J. Geophys. Res., v. 86, p. 2953-2970.

McKeel, D.R. and Lipps, J.H., 1975, Eocene and Oligocene planktonic foraminifera from the central and southern Oregon Coast Range: J. Foram. Res., v. 5, p. 249.

Peck, L.C., 1964, Systematic analyses of silicates: U.S. Geological Survey Bull. 1170.

Rau, W.W., 1981, Pacific Northwest Tertiary benthic foraminiferal biostratigraphic framework - An overview, in Armentrout, J.M. (ed.) Pacific Northwest Cenozoic biostratigraphy: GSA Special Paper 184, p. 67-84.

Rhodes, J.M., Dungan, M.A., Blanchard, D.P. and Long, P.E., 1979, Magma mixing at mid-ocean ridges: Evidence from basalts drilled near 22° N on the Mid-Atlantic Ridge: Tectonophysics, v. 55, p. 35-62.

Snavely, P.D. Jr., 1984, Sixty million years of growth along the Oregon continental margin. in Clarke, S.H. (ed.), Highlights in Marine Research of the U.S. Geol. Survey: U.S. Geological Survey Circular 938, p. 9-18.

Snavely, P.D. Jr., 1987, Tertiary geologic framework, neotectonics, and petroleum potential of the Oregon-Washington Continental Margin, *in* Scholl, D.W. and others (eds.), Geology and resource potential of the continental margin of western North America and adjacent ocean basins--Beaufort Sea to Baja California: Houston, Texas, Circum-Pacific Council for Energy and Mineral Resources, Earth Science Series, v. 6, p. 305-335.

Snavely, P.D., Jr., and MacLeod, N.S., 1974, Yachats basalt- An upper Eocene differentiated volcanic sequence in the Oregon Coast Range: J. Res. U.S. Geol. Survey, v.2, p. 395-403.

Snavely, P.D., Jr., MacLeod, N.S., and Minasian, D.L., 1990 a, Preliminary map of the Nestucca Bay Quadrangle, Tillamook County, Oregon: U.S. Geological Survey Open-File Report 90-202, scale 1:24,000.

Snavely, P.D., Jr., MacLeod, N.S., and Minasian, D.L., 1990 b, Geologic map of the Neskowin quadrangle, Tillamook County, Oregon: U.S. Geological Survey Open-File Report 90-413, scale 1:24,000.

Snavely, P.D.,Jr., MacLeod, N.S., and Wagner, H.C., 1968, Tholeiitic and alkalic basalts of the Eocene Siletz River Volcanics, Oregon Coast Range: Am. J. Sci., v. 266, p. 454-481.

Snavely, P.D., Jr., and Vokes, H.E., 1949, Geology of the coastal area between Cape Kiwanda and Cape Foulweather, Oregon: U. S. Geol. Survey, Oil and Gas Inv. Map, 97.

Snavely, P.D., Jr, and Wells, R.E., 1984, Tertiary volcanic and intrusive rocks or the Oregon and Washington continental shelf: U.S. Geological Survey Open-File Report 84-282, 17 pp.

Stacey, J .S., N .D. Sherrill, G. B. Dalrymple, M. A. Lanphere, and N. V. Carpenter, 1981, A five-collector system for the simultaneous measurement of argon isotope ratios in a static mass spectrometer: Int. J. Mass Spectrom. Ion Phys., v. 39, p. 167-180.

Steiger, R. H., and E. Jäger, 1977, Subcommission on geochronology: Convention on the use of decay constants in geo- and cosmochronology: Earth and Planet. Sci. Lett., v. 36, p. 545-362.

Stormer, J.C., and Nicholls, J., 1978, XLFRAC: A program for the interactive testing of magmatic differentiation models: Computer Geoscience, v. 4, p.143-159.

Tatsumoto, M., and Snavely, P.D., Jr., 1969, Isotopic composition of lead in rocks of the Coast Range, Oregon and Washington: J. of Geophys. Res., v. 74, p. 1087-1100.

Taylor, J. R., 1982, An introduction to error analysis, University Science Books, Mill Valley, California, 270 pp.

Wells, R.E., and Coe, R.S., 1985, Paleomagnetism and geology of Eocene volcanic rocks of southwest Washington, implications for mechanisms of tectonic rotation: J. Geophys. Res., v. 88, p. 10,371-10,383.

Wells, R.E., Engebretson, D.C., Snavely, P.D., Jr., and Coe, R.S., 1984, Cenozoic plate motions and the volcano-tectonic evolution of western Oregon and Washington: Tectonics, v. 3, p. 275-294.

White, M.W., Hofman, A.W., and Puchelt, H., 1987, Isotope geochemistry of Pacific mid-ocean ridge basalt: J. Geophys. Res., v. 92, p.4881-4893.

Table 1A. Major-element chemistry of Yachats Basalt

Sample	SR63-3	SR63-117	SR58-17	SR61-8A	SW58-4	S81-201C	S81-201A	SR61-106A	SR62-168A	SR61-109A
Rock type	Th. B.	A.B.	Th.B.	B.And.	Th.B.	T.And.	B.And.	Th. B.	B.And.	Th. B.
SiO_2	46.6	46.7	48.7	50.9	48.4	49.9	51.0	47.7	51.3	49.1
Al_2O_3	15.9	14.8	16.7	17.8	17.0	18.6	15.1	17.7	17.6	18.0
Fe_2O_3	3.3	4.9	11.1	5.2	12.2	8.05	11.7	4.3	4.8	4.3
FeO	8.5	8.8	n.d.	4.6	n.d.	n.d.	n.d.	6.6	6.6	5.6
MgO	3.5	4.0	3.95	3.2	3.71	1.63	2.78	4.4	2.3	3.4
CaO	8.1	8.9	10.3	7.1	9.59	7.45	5.64	9.9	2.8	9.6
Na2O	2.70	3.80	2.95	3.50	3.04	4.01	3.76	3.00	3.80	3.50
K_2O	0.79	0.57	0.64	1.20	0.67	1.33	1.24	0.38	1.20	1.00
H_2O (LOI)	3.00	4.11	1.92	4.00	1.90	5.56	6.41	2.90	1.26	2.38
TiO_2	2.70	2.80	2.98	2.20	2.82	1.91	1.38	2.80	2.70	2.80
P_2O_5	0.56	0.40	0.45	0.61	0.41	0.72	0.76	0.44	0.69	0.51
MnO	0.19	0.11	0.18	0.12	0.19	0.08	0.14	0.15	0.16	0.17
CO_2	4.00	<0.05	n.d.	<0.05	n.d.	n.d.	n.d.	<0.05	<0.05	<0.05
Total	99.8	99.9	99.9	100.4	99.9	99.2	99.9	100.3	100.2	100.4

Sample	SR61-106B	SW56-5	SW58-3	S89-15	SR90-35	S91-6	S91-11	S91-12	S91-13	S91-14
Rock type	Th.B.	Th.B.	T.And.	Bas.	Th.B.	Th.B.	Rhy.	Th.B.	T.And.	A.B.
SiO_2	47.2	48.6	54.9	44.7	50.5	49.1	64.5	50.6	55.2	42.8
Al_2O_3	16.3	17.1	16.4	14.0	17.1	17.9	15.5	15.9	15.6	10.7
Fe_2O_3	5.3	4.6	4.7	16.2	11.6	10.3	4.44	10.7	8.08	12.6
FeO	5.7	6.03	3.4	n.d.	n.d.	n.d.	n.d.	n.d.	n.d.	n.d.
MgO	5.6	3.45	2.3	5.01	3.42	3.83	0.64	2.98	1.85	6.38
CaO	8.3	9.51	5.5	7.18	8.81	10.3	1.69	8.12	4.57	13.1
Na_2O	2.80	3.54	4.20	4.48	3.50	2.99	5.32	3.46	4.56	2.36
K_2O	0.60	1.05	1.9	2.02	0.96	0.39	3.73	1.23	2.21	1.83
H_2O (LOI)	5.20	2.50	4.10	1.45	1.34	2.35	2.73	3.18	4.13	3.56
TiO_2	2.80	2.95	1.40	3.02	2.62	2.22	0.51	2.63	1.67	3.84
P_2O_5	0.45	0.48	0.71	1.48	0.49	0.34	0.12	0.58	0.72	0.72
MnO	0.19	0.16	0.10	0.25	0.16	0.11	0.12	0.16	0.10	0.23
CO_2	<0.05	<0.05	<0.05	n.d.	n.d.	n.d.	n.d.	n.d.	n.d.	n.d.
Total	100.4	99.9	100.4	99.8	100.5	99.8	99.0	99.5	98.7	98.1

Note: Th.B., tholeiitic basalt; A.B., alkalic basalt; Bas., basanite; B.And., basaltic andesite; T.And., trachyandesite; Rhy., rhyolite. n.d., not determined. Where FeO is not determined, all iron is reported as Fe_2O_3. LOI is loss on ignition at 925° C.

Table 1B. Major-element chemistry of Cascade Head and Cannery Hills basalt

	Cascade Head											
Sample	S83-20	SR83-86	SR83-94	MR68-81	SR83-48	SR62-160	SR61-5	S79-36	MR68-80	SR61-4	SR83-27	SR83-50
Rock type	Haw.	A.B.	A.B.	A.B.	Th.B.	A.B.	A.B.	T.And.	T.And.	AB	Th.B.	
SiO_2	48.5	44.6	45.4	44.7	46.9	48.5	46.8	61.3	54.4	46.2	46.2	47.6
Al_2O_3	17.0	14.2	13.8	15.1	12.2	16.5	16.4	16.9	18.2	16.0	13.2	15.1
Fe_2O_3	4.2	14.9	13.0	14.1	13.6	3.3	3.6	5.61	4.5	4.8	11.9	11.9
FeO	5.7	n.d.	n.d.	n.d.	n.d.	5.7	6.5	n.d.	1.4	7.5	n.d.	n.d.
MgO	4.2	5.43	7.94	3.63	7.12	4.5	5.8	0.61	1.6	5.2	6.68	4.36
CaO	7.9	10.4	10.2	10.9	10.4	8.7	8.5	2.55	5.5	8.8	11.1	9.30
Na_2O	4.00	3.15	3.17	2.96	2.27	3.70	3.30	5.76	5.10	3.20	2.25	3.44
K_2O	1.70	1.24	1.29	1.22	0.82	1.70	1.50	3.10	2.20	1.30	1.15	1.31
H_2O (LOI)	1.43	0.65	0.75	1.94	3.17	3.10	3.50	2.24	3.60	2.58	2.71	1.95
TiO_2	2.80	4.42	3.27	4.02	3.05	3.00	2.80	0.64	2.00	3.70	3.17	3.58
P_2O_5	0.91	0.74	0.93	0.80	0.46	0.90	1.1	0.26	0.78	0.74	0.59	0.75
MnO	0.31	0.19	0.19	0.24	0.19	0.30	0.23	0.25	0.18	0.30	0.38	0.17
CO_2	0.03	n.d.	n.d.	n.d.	n.d.	n.d.	n.d.	n.d.	<0.05	<0.05	n.d.	n.d.
Total	98.7	99.9	99.9	99.6	100.2	99.9	100.0	99.2	99.5	100.3	99.3	99.5

	Cascade Head					Cannery Hills					
Sample	SR83-157	S84-112	S91-10	S91-15	S91-16	SH64-1C	SH64-1D	SH64-1E	SR83-160	SR87-23	S87-83
Rock type	A.B.	A.B.	A.B.	A.B.	T.And.	A.B.	A.B.	A.B.	A.B.	A.B.	A.B.
SiO_2	48.0	44.2	45.3	45.6	51.9	43.8	43.1	42.7	41.3	43.9	42.7
Al_2O_3	16.2	11.6	14.8	15.6	17.0	13.8	13.8	13.8	13.3	12.4	12.9
Fe_2O_3	5.1	14.0	13.6	12.5	9.46	3.6	3.7	5.3	13.5	14.7	13.4
FeO	3.8	n.d.	n.d.	n.d.	n.d.	8.7	8.7	7.4	n.d.	n.d.	n.d.
MgO	4.0	9.29	6.41	4.68	1.86	9.0	8.8	8.6	8.22	8.54	7.93
CaO	10.2	11.3	10.4	10.7	5.23	10.2	10.9	10.8	10.5	10.5	11.8
Na_2O	3.40	2.09	2.85	2.99	5.03	2.50	2.30	2.00	1.60	2.17	2.07
K_2O	1.20	1.01	1.22	1.10	2.10	1.10	1.20	0.75	1.39	0.94	1.08
H_2O (LOI)	4.30	1.47	0.89	1.93	3.49	2.53	2.93	3.90	4.47	2.35	3.21
TiO_2	3.80	3.46	3.39	3.42	2.01	3.50	3.60	3.70	4.25	3.68	3.61
P_2O_5	0.72	0.73	0.61	0.64	0.33	0.80	0.70	0.80	0.90	0.62	0.74
MnO	0.36	0.18	0.18	0.18	0.13	0.18	0.18	0.20	0.22	0.19	0.20
CO_2	<0.05	n.d.	n.d.	n.d.	n.d.	0.09	0.05	0.06	n.d.	n.d.	n.d.
Total	101.1	99.3	99.7	99.3	99.1	99.8	99.9	100.0	98.4	98.5	98.3

Note: Th.B., tholeiitic basalt; A.B., alkalic basalt; Haw., hawaiite; T.And., trachyandesite. n.d., not determined. Where FeO is not determined, all iron is reported as Fe_2O_3. LOI is loss on ignition at 925° C.

Table 2A. Trace-element chemistry of Yachats Basalt

Sample	SM 63-3	SR63-117	SR58-17	SR61-8	SW58-4	S81-201C	S81-201A	SR61-106A	SR62-168A	SR61-109A
XRF Analysis										
Nb	57	37	54	57	43	60	80	40	71	50
Rb	22	15	14	32	12	19	32	<10	12	12
Sr	460	370	520	510	440	580	490	510	465	500
Zr	255	192	245	325	230	350	495	215	330	255
Y	29	32	30	57	39	44	51	25	47	28
Ba	315	200	290	270	215	370	580	138	255	305
Zr/Nb	4.5	5.2	4.5	5.7	5.4	5.8	6.2	5.4	4.7	5.1
ICP-MS Analysis (INAA)										
La	24. (32.4)	21. (24.8)	23.	17.	19. (25.6)	40.	42.	13.	31. (42.4)	26.
Ce	49. (65.2)	41. (50.5)	46.	38.	40. (54.3)	85.	87.	30.	62. (88.3)	53.
Nd	25. (32.0)	23. (24.0)	24.	19.)	23. (29.0)	45.	43.	17.	35. (43.0)	28.
Sm	4.8 (7.5)	5.4 (6.8)	5.2	3.8	5.1 (7.3)	9.4	8.4	3.3	7.1 (11.3)	5.5
Eu	1.8 (2.2)	1.8 (2.1)	1.4	1.3	1.8 (2.3)	3.2	2.8	1.2	2.7 (3.2)	1.8
Tb	0.76 (0.96	0.81 (1.0)	0.70	0.71)	0.75 (1.0)	1.4	1.2	0.50	1.1 (1.6)	0.86
Yb	1.5 (2.1)	1.7 (2.3)	1.4	1.5	1.6 (2.4)	2.4	2.5	1.1	2.7 (3.6)	1.6
$(La/Sm)_N$	2.7 (2.4)	2.1 (1.5)	2.4	2.5	2.0 (1.9)	2.3	2.7	2.2	2.4 (2.1)	2.6
$(Ce/Yb)_N$	7.4 (7.0)	5.5 (5.0)	7.5	5.8	5.7 (5.1)	8.1	7.9	6.2	5.2 (5.5)	7.5
INAA Analysis										
Hf	5.65	4.56	n.d.	7.20	5.22	n.d.	10.0	n.d.	7.45	n.d.
Ta	3.05	2.14	n.d.	3.57	2.42	n.d.	4.68	n.d.	3.86	n.d.
Th	4.05	2.9	n.d.	4.63	2.74	n.d.	6.56	n.d.	4.90	n.d.
Sc	18.7	20.7	n.d.	15.6	21.2	n.d.	11.2	n.d.	24.3	n.d.
Cr	18.7	54.1	n.d.	2.9	48.7	n.d.	2.2	n.d.	7.6	n.d.
Co	50.9	47.4	n.d.	25.6	42.3	n.d.	18.8	n.d.	55.6	n.d.

Table 2A. Continued

Sample	SR61-106B	SW56-5	SR90-35	S89-15	S91-6	S91-11	S91-12	S91-13	S91-14
XRF Analysis									
Nb	44	49	48	148	38	106	56	74	102
Rb	<10	<10	27	54	11	85	29	41	36
Sr	450	280	480	1300	530	210	500	450	690
Zr	220	295	465	720	184	800	325	465	365
Y	21	28	32	58	20	64	37	45	36
Ba	130	265	265	n.d.	n.d.	n.d.	n.d.	n.d.	n.d.
Zr/Nb	5.0	6.0	9.7	4.9	4.8	7.6	5.8	6.3	3.6
ICP-MS Analysis (INAA)									
La	15.	22.	25. (33.20	95.	27.	92. (80.0)	46.	72.	65.
Ce	33.	48.	52. (67.9)	190.	52.	170. (155)	92.	140.	130.
Nd	17.	28.	27. (34.0)	92.	26.	68. (63.0)	44.	65.	60.
Sm	3.3	5.7	5.6 (8.6)	17.	5.5	13. (13.8)	9.3	13.	12.
Eu	1.3	2.2	2.2 (2.6)	5.4	1.9	2.8 (3.1)	2.7	3.6	3.5
Tb	0.48	0.76	0.85 (1.1)	2.0	0.83	1.7 (1.8)	1.3	1.7	1.4
Yb	1.1	1.8	1.5 (2.6)	3.5	1.8	5.1 (5.3)	2.7	3.9	2.0
$(La/Sm)_N$	2.5	2.1	2.5 (2.1)	3.1	2.7	3.9 (3.2)	2.7	3.0	3.0
$(Ce/Yb)_N$	6.8	6.1	7.9 (5.5)	12.3	6.7	7.5 (6.7)	7.7	8.2	14.8
INAA Analysis									
Hf	n.d.	n.d.	5.92	n.d.	n.d.	18.1	n.d.	n.d.	n.d.
Ta	n.d.	n.d.	2.98	n.d.	n.d.	6.27	n.d.	n.d.	n.d.
Th	n.d.	n.d.	3.6	n.d.	n.d.	13.7	n.d.	n.d.	n.d.
Sc	n.d.	n.d.	18.5	n.d.	n.d.	8.9	n.d.	n.d.	n.d.
Cr	n.d.	n.d.	4.7	n.d.	n.d.	2.9	n.d.	n.d.	n.d.
Co	n.d.	n.d.	32.0	n.d.	n.d.	5.2	n.d.	n.d.	n.d.

Note: N, chondrite-normalized using the values of Haskins and others (1968). n.d., not determined.

Table 2B. Trace-element chemistry of Cascade Head and Cannery Hills basalts

	Cascade Head								
Sample	S83-20	SR83-86	SR83-94	MR68-81	SR83-48	SR62-160	SR61-5A	S79-36	MR68-80
<u>XRF Analysis</u>									
Nb	95	80	94	89	58	124	94	124	148
Rb	38	28	35	30	20	38	38	70	41
Sr	800	760	860	880	430	990	840	495	1000
Zr	410	350	385	345	240	510	435	790	750
Y	32	34	33	37	28	42	36	37	49
Ba	500	890	465	425	255	700	495	840	810
Zr/Nb	4.3	4.4	4.1	3.9	4.1	4.1	4.6	6.4	5.1
<u>ICP-MS Analysis (INAA)</u>									
La	57 (72.4)	45	60	61	25 (36.9)	94	47	100	120
Ce	110 (142)	89	120	120	50 (75.4)	180	98	180	220
Nd	53 (64.0)	46	53	59	27 (37.0)	79	44	62	87
Sm	9.6 (13.1)	8.1	8.6	10.	5.2 (8.5)	12	6.9	8.7	13
Eu	2.9 (3.6)	2.7	3.1	3.5	1.8 (2.5)	4.0	2.2	2.6	4.3
Tb	1.2 (1.4)	1.1	1.2	1.3	0.79 (1.0)	1.5	0.79	1.1	1.5
Yb	2.2 (3.0)	1.8	1.8	2.3	1.3 (2.3)	2.8	1.3	2.9	3.6
$(La/Sm)_N$	3.3 (3.0)	3.1	3.8	3.4	2.6 (2.7)	4.3	3.7	6.3	5.1
$(Ce/Yb)_N$	11.4 (10.8	11.2	15.2	11.9	8.7 (8.7)	14.6	17.1	14.1	13.9
<u>INAA Analysis</u>									
Hf	8.67	n.d.	n.d.	n.d.	5.47	10.3	n.d.	14.9	n.d.
Ta	6.12	n.d.	n.d.	n.d.	3.30	8.57	n.d.	9.23	n.d.
Th	8.00	n.d.	n.d.	n.d.	3.78	12.8	n.d.	18.1	n.d
Sc	10.7	n.d.	n.d.	n.d.	32.7	14.4	n.d.	1.4	n.d.
Cr	2.4	n.d.	n.d.	n.d.	46.7	39.9	n.d.	1.4	n.d.
Co	25.9	n.d.	n.d.	n.d.	79.5	29.3	n.d.	6.2	n.d.

Table 2B. Continued

	Cascade Head							Cannery Hills		
Sample	SR61-4	S91-10	S91-15	S91-16	SR83-27	S83-50	S84-112	SR86-160	S87-23	S87-87
XRF Analysis										
Nb	29	74	73	146	74	92	86	90	58	70
Rb	13	31	24	44	28	32	26	31	24	27
Sr	340	710	770	840	590	660	640	870	600	880
Zr	285	270	295	570	295	395	310	380	275	295
Y	33	26	28	45	31	42	31	25	23	21
Ba	152	n.d.	n.d.	n.d.	n.d.	n.d.	n.d.	540	280	520
Zr/Nb	9.8	3.7	4.0	3.9	4.0	4.3	3.6	4.2	4.7	4.2
ICP-MS Analysis (INAA)										
La	21 (27.4)	55	65	120	55 (52.7)	72	67	72.4	47.3	61.1
Ce	46 (59.4)	110	130	220	110 (104)	140	130	140	98.2	117
Nd	26 (29.)	48	58	91	48 (48.0)	62	59	61.0	43.0	52.0
Sm	4.8 (7.6)	9.0	11	15	9.3 (9.9)	12.	11.	13.2	9.4	11.4
Eu	1.8 (2.1)	2.7	3.3	4.2	2.7 (2.8)	3.5	3.1	3.8	2.8	3.4
Tb	0.84 (1.0)	1.1	1.2	1.7	1.1 (1.2)	1.5	1.3	1.5	1.1	1.3
Yb	2.3 (3.0)	2.0	2.6	3.8	2.1 (2.2)	3.2	2.2	2.2	2.3	2.1
$(La/Sm)_N$	2.4 (2.0)	3.4	3.2	4.4	3.2 (2.9)	3.3	3.3	3.0	2.8	2.9
$(Ce/Yb)_N$	4.6 (4.4)	12.5	11.4	13.2	11.9 (10.8	9.9	13.4	15.9	9.7	12.7
INAA Analysis										
Hf	5.82	n.d	n.d.	n.d.	6.49	n.d.	n.d.	8.32	6.25	6.37
Ta	1.91	n.d	n.d.	n.d.	4.88	n.d.	n.d.	6.38	4.40	4.64
Th	2.17	n.d.	n.d.	n.d.	5.9	n.d.	n.d.	8.08	4.70	6.88
Sc	26.9	n.d.	n.d.	n.d.	23.4	n.d.	n.d.	23.3	27.0	24.5
Cr	82.6	n.d.	n.d.	n.d.	230	n.d.	n.d.	173	376	317
Co	36.1	n.d.	n.d.	n.d.	63.2	n.d.	n.d.	49.1	61.5	55.4

Note: N, chondrite-normalized using the values of Haskins and others (1968). n.d., not determined.

Table 3 A. K-Ar ages of late Eocene basalts

Sample No.	Material	K_2O (wt.%)	^{40}Ar rad (x10-	$^{40}Arrad/^{40}Artotal$	Calculated Age (Ma)	Weighted Mean Age
Yachats Basalt						
S79-7	WR	1.524	6.848	0.708	30.9±0.8	30.7±0.6
		1.529	6.736	0.595	30.4±0.8	
SR83-136	Plag	0.361	1.793	0.226	34.2±1.0	34.0±0.7
		0.361	1.770	0.309	33.7±1.0	
S84-86	WR	0.719	3.77	0.693	36.0±1.1	36.1±0.7
		0.705	3.79	0.670	36.1±0.9	
		0.733				
		0.728				
Basalt of Cascade Head						
SR83-20	WR	1.976	9.182	0.572	31.9±0.8	31.9±0.7
		1.988	9.189	0.327	31.9±1.2	
SR83-20*	WR	1.862	8.669	0.481	32.1±1.3	
		1.851				
SR83-27	WR	1.190	5.204	0.588	30.1±0.8	30.5±0.6
		1.195	5.342	0.555	30.8±0.8	
SR83-27*	WR	1.216	5.667	0.535	31.8±0.8	
		1.236				
SR83-50	WR	1.450	6.883	0.493	32.9±0.8	32.8±0.6
		1.432	6.821	0.413	32.6±0.8	
SR83-73	WR	1.595	7.403	0.461	32.1±0.9	31.6±0.6
		1.576	7.169	0.371	31.1±0.9	
SR83-88	WR	1.483	6.736	0.573	31.4±0.8	31.5±0.6
		1.471	6.751	0.642	31.5±0.8	
SR83-94	WR	1.273	5.690	0.454	30.9±0.8	30.5±0.6
		1.263	5.540	0.408	30.1±0.9	
SR83-145	WR	1.409	6.473	0.468	32.0±1.0	32.6±0.8
		1.380	6.773	0.161	33.4±1.2	
SR83-146	WR	1.504	6.794	0.597	30.9±0.9	31.3±0.7
		1.523	6.976	0.480	31.7±1.0	

Table 3 A. Continued

Sample No.	Material	K_2O (wt.%)	^{40}Ar rad (x10-	$^{40}Arrad/^{40}Artotal$	Calculated Age (Ma)	Weighted Mean Age
SR83-157	WR	1.311	6.618	0.563	32.2±1.0	32.0±0.7
		1.322	6.081	0.549	31.8±1.0	
S84-112	WR	0.697	3.342	0.247	33.1±1.0	32.4±0.6
		0.691	3.290	0.582	32.6±1.3	
			3.212	0.791	31.9±0.8	
S79-36	WR	3.11	14.89	0.858	33.0±0.7	
		3.10				
S79-36	Plag	0.524	2.439	0.536	32.0±0.8	
		0.524				
S84-114	Plag	0.451	2.234	0.378	33.7±1.4	34.0±1.0
		0.461	2.275	0.424	34.3±1.4	
S84-114	Hbl	0.743	3.663	0.207	33.6±1.3	33.9±0.8
		0.756	3.701	0.243	34.0±1.0	
Cannery Hills basalt						
SR83-160	WR	0.351	1.532	0.519	30.5±1.5	31.0±1.1
		0.342	1.591	0.286	31.6±1.6	

Note: WR, whole rock; Plag, plagioclase; Hbl, hornblende. * indicates more severe acid treatment (see text).

Table 3B. $^{40}Ar/^{39}Ar$ ages of late Eocene basalt

Temp. (°C)	$^{40}Ar/^{39}Ar$	$^{37}Ar/^{39}Ar$*	$^{36}Ar/^{39}Ar$	$^{36}Ar_{ca}$ (%)	$^{40}Ar_K$ (%)	$^{40}Ar_R$ (%)	^{39}Ar (%of total)	Apparent Age (Ma)
Yachats Basalt								
	S83-136	Plagioclase						
400	1568.5	15.85	5.428	0.1	0.0	-2.2	0.5	-141.3±302
500	948.1	15.02	3.467	0.1	0.0	-7.9	3.1	-328.7±36
600	79.97	14.92	0.2455	1.6	0.0	10.8	11.3	34.01±1.98
660	107.6	15.25	0.3397	1.2	0.0	7.8	14.3	33.36±1.95
800	65.88	15.26	0.1945	2.1	0.0	14.6	20.5	37.92±1.26
860	16.86	14.74	0.0303	13.2	0.0	53.9	9.7	35.89±1.96
1050	20.79	14.68	0.0432	9.2	0.0	44.2	13.1	36.27±1.47
1200	34.37	14.95	0.0900	4.5	0.0	26.1	10.8	35.37±1.81
1350	45.03	15.13	0.1265	3.3	0.0	19.7	16.6	34.95±1.29
							Recalculated total fusior age=	34.41±1.79
Basalt of Cascade Head								
	SR83-50 Whole Rock							
550	12.74	1.33	0.0286	1.3	0.3	34.3	5.5	38.47±0.79
620	5.71	0.992	0.0062	4.5	0.6	68.8	16.7	34.59±0.27
680	4.62	0.872	0.0027	8.8	0.7	83.2	21.5	33.84±0.21
740	4.39	0.882	0.0021	11.5	0.8	86.5	28.2	33.50±0.18
810	4.99	1.54	0.0042	10.2	0.7	77.1	15.2	33.88±0.28
860	7.00	2.66	0.0108	6.9	0.5	56.8	5.4	34.89±0.73
970	7.34	2.94	0.0013	6.3	0.5	50.8	4.1	32.88±0.97
1065	8.23	21.63	0.0231	26.1	0.4	38.5	3.4	28.33±1.20
1125	311.5	158.0	1.0303	0.0	0.0	6.4	0.0	189.8±214
							Recalculated total fusior age =	34.01±0.22

NOTES: Subscripts indicate radiogenic (R), calcium-derived (Ca), and potassium-derived (K) argon. λ_e= 0.581E-10/yr; λ_b=4.692E-10/yr. Errors are estimates of the standard deviation of analytical precision.

*Corrected for ^{37}Ar decay, half-life=35.1 days.

Summary of age spectrum and isochron analyses

Sample Number	Increments Used (°C)	Weighted mean plateau age (Ma)	^{39}Ar (%)	Isochron age (Ma)	$^{40}Ar/^{36}Ar$ Intercept	Sums/(N-2)
S83-136	600-1350	35.74±0.64	96.4	36.49±1.45	294.2±2.1	1.48
	800-1350	36.21±0.71	70.7	35.25±1.30	297.7±2.9	0.65
SR83-50	680-970	33.70±0.61	74.4	33.52±0.37	302.7±11.5	1.54
	620-970	33.84±0.20	91.1	33.39±0.47	310.8±13.0	2.08

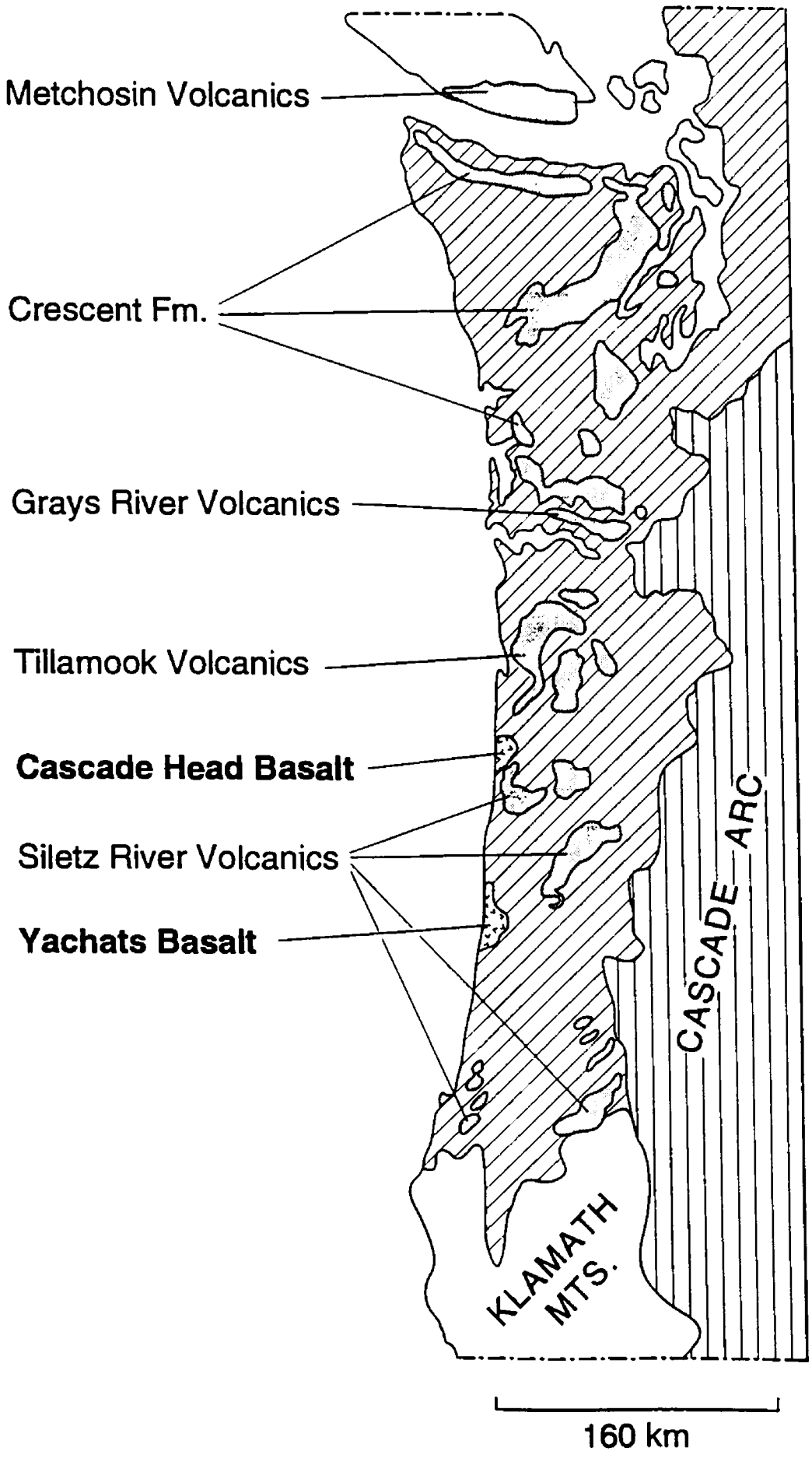

Figure 1. Generalized geologic map of the continental margin of the Pacific Northwest showing locations of late Eocene basalts (v-shaped pattern). Distribution of older basalt sequences that comprise much of the basement of the Coast Ranges are also shown (stippled). Tertiary sedimentary rocks are shown by diagonal lines and pre-Tertiary rocks by white areas. Modified from Wells and others (1984).

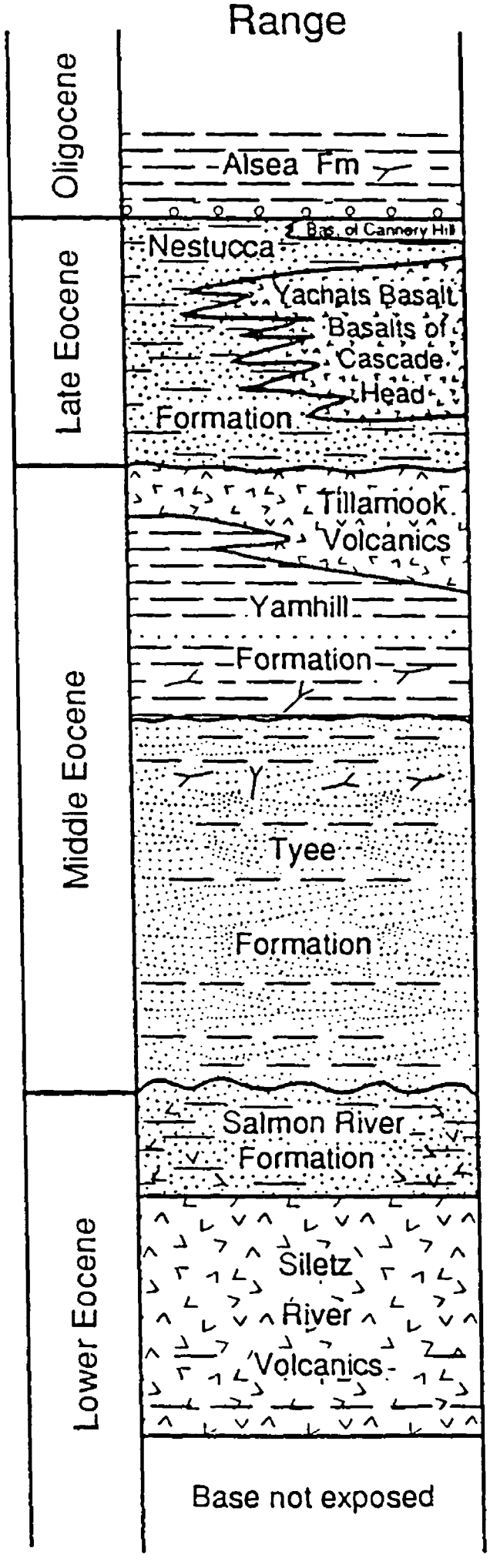

Figure 2. Generalized stratigraphic section of lower Eocene to Oligocene units in the central Oregon Coast Range.

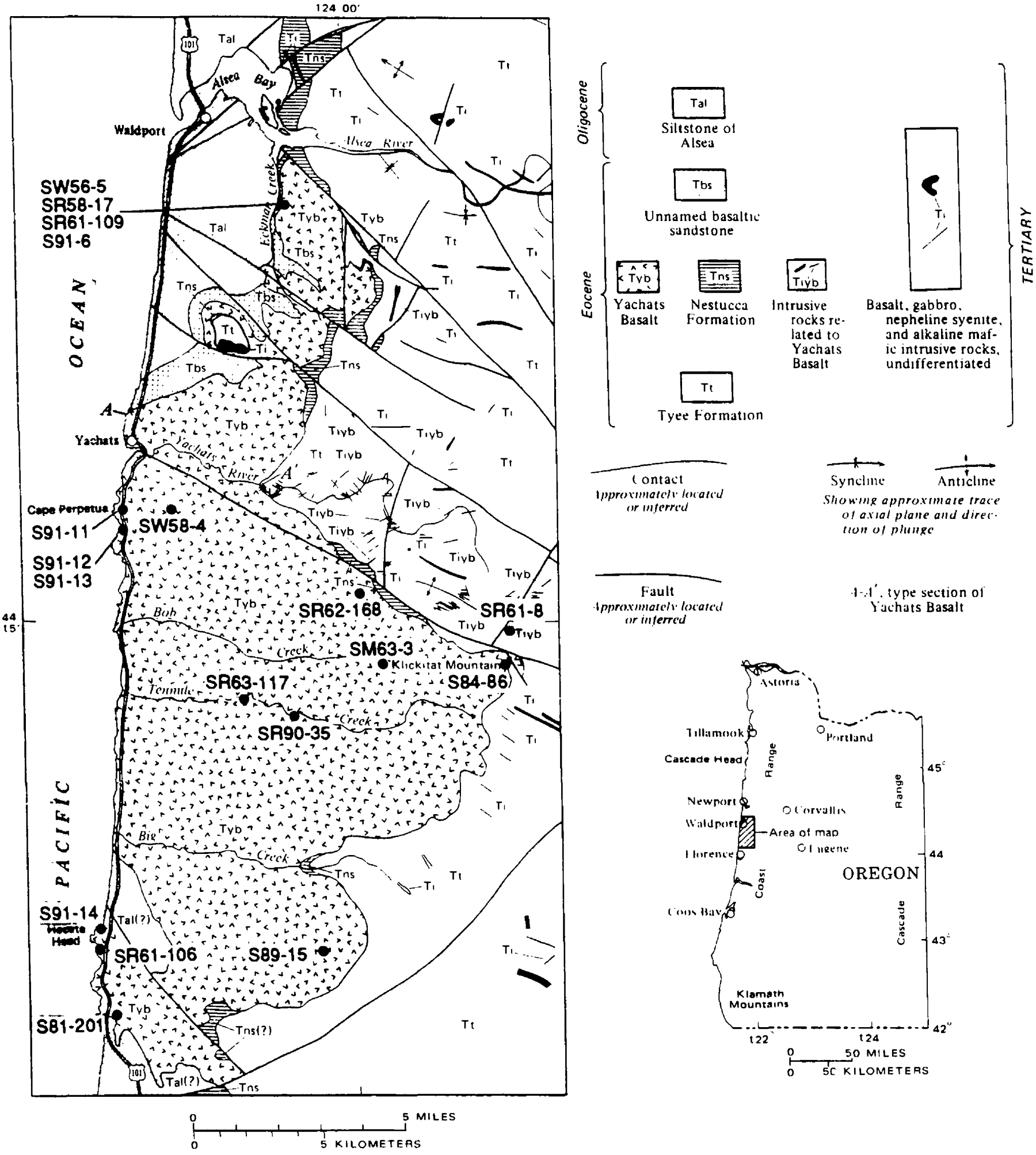

Figure 3A. Geologic map showing volcanic outcrops and locations of analyzed samples for Yachats Basalt. (Modified from Snavely and MacLeod, 1974).

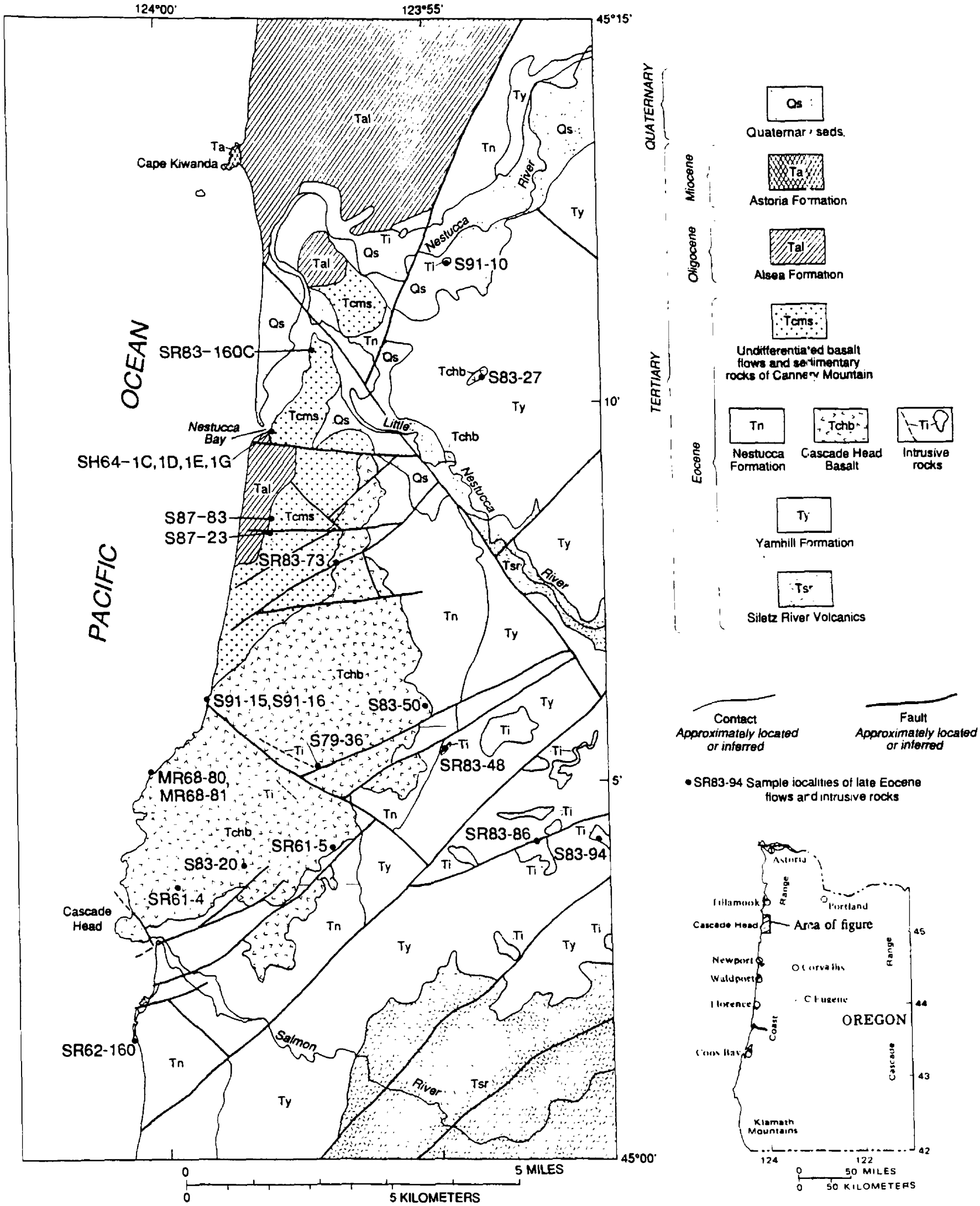

Figure 3B. Geologic map showing volcanic outcrops and locations of analyzed samples for basalt of Cascade Head and Cannery Hills. (Modified from Snavely and others, 1990a,b).

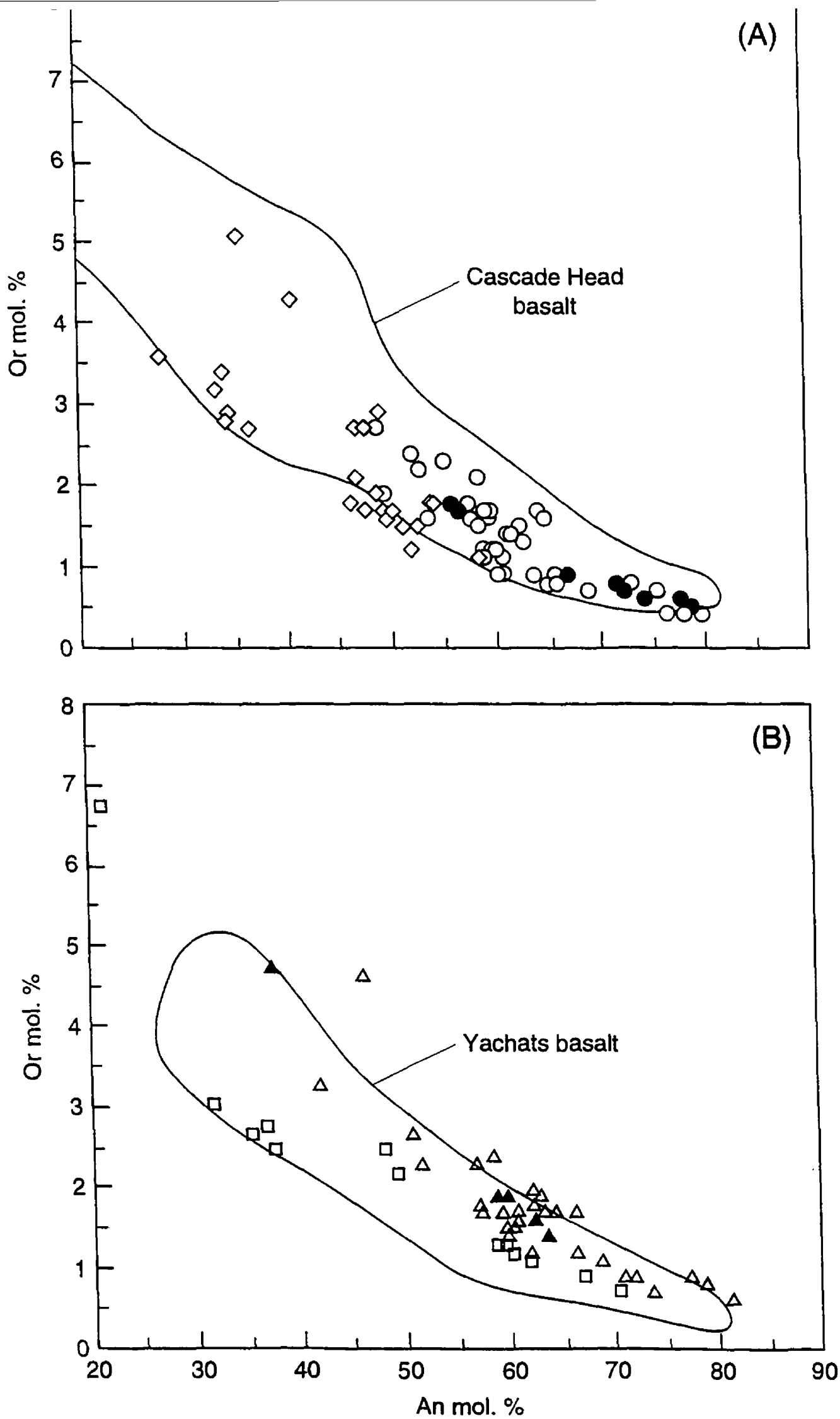

Figure 4. Or vs. An (mol.%) plot for feldspar phenocrysts from (A) Yachats and (B) Cascade Head basalts showing similar compositional ranges. Or increases with differentiation. Yachats Basalt: tholeiitic basalt, open circles; alkalic basalt, filled circles; basaltic andesite to rhyolite, diamonds. Cascade Head: alkalic basalt, open triangles: tholeiitic basalt, filled triangles; hawaiite to trachyandesite, squares.

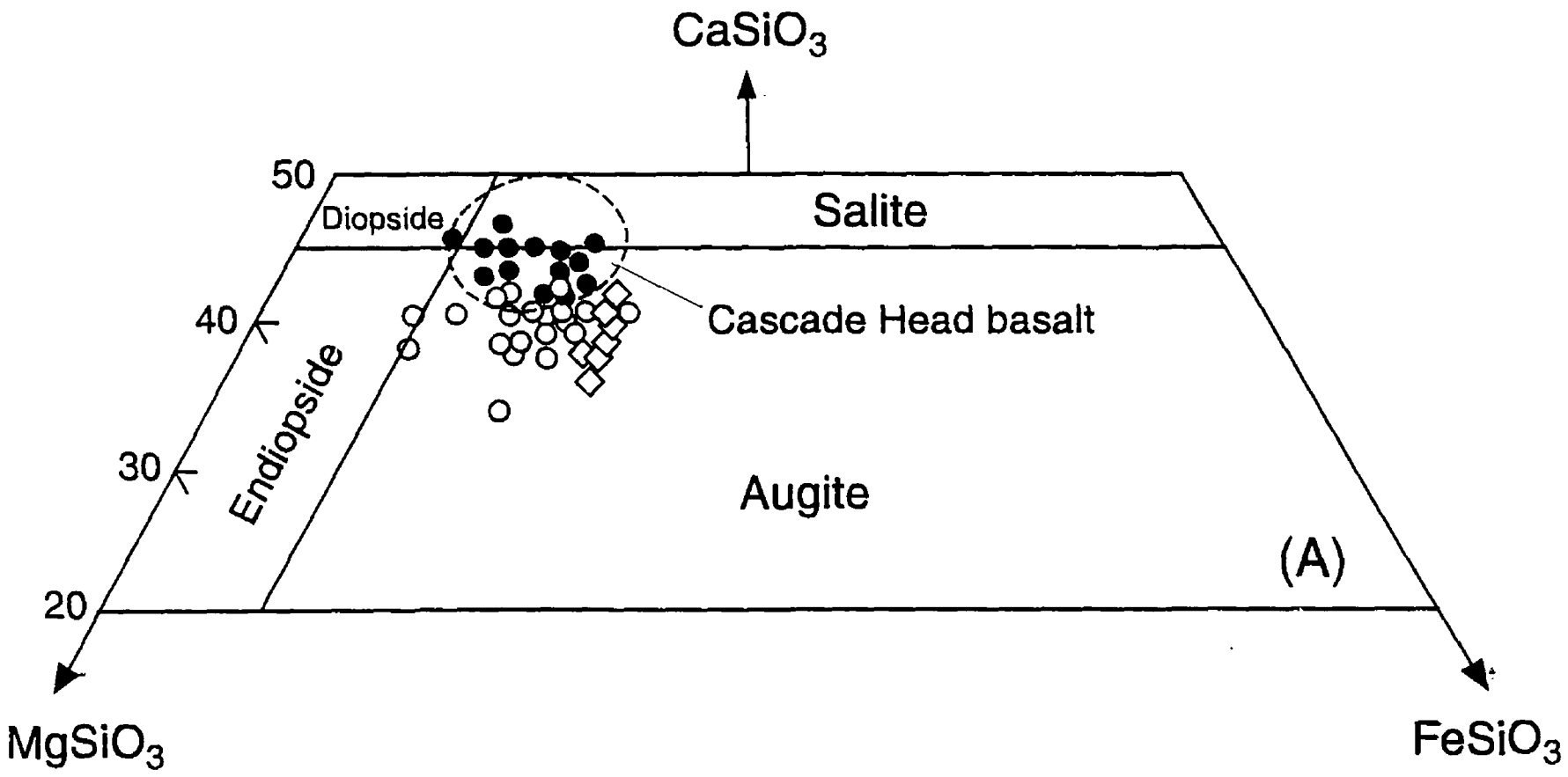

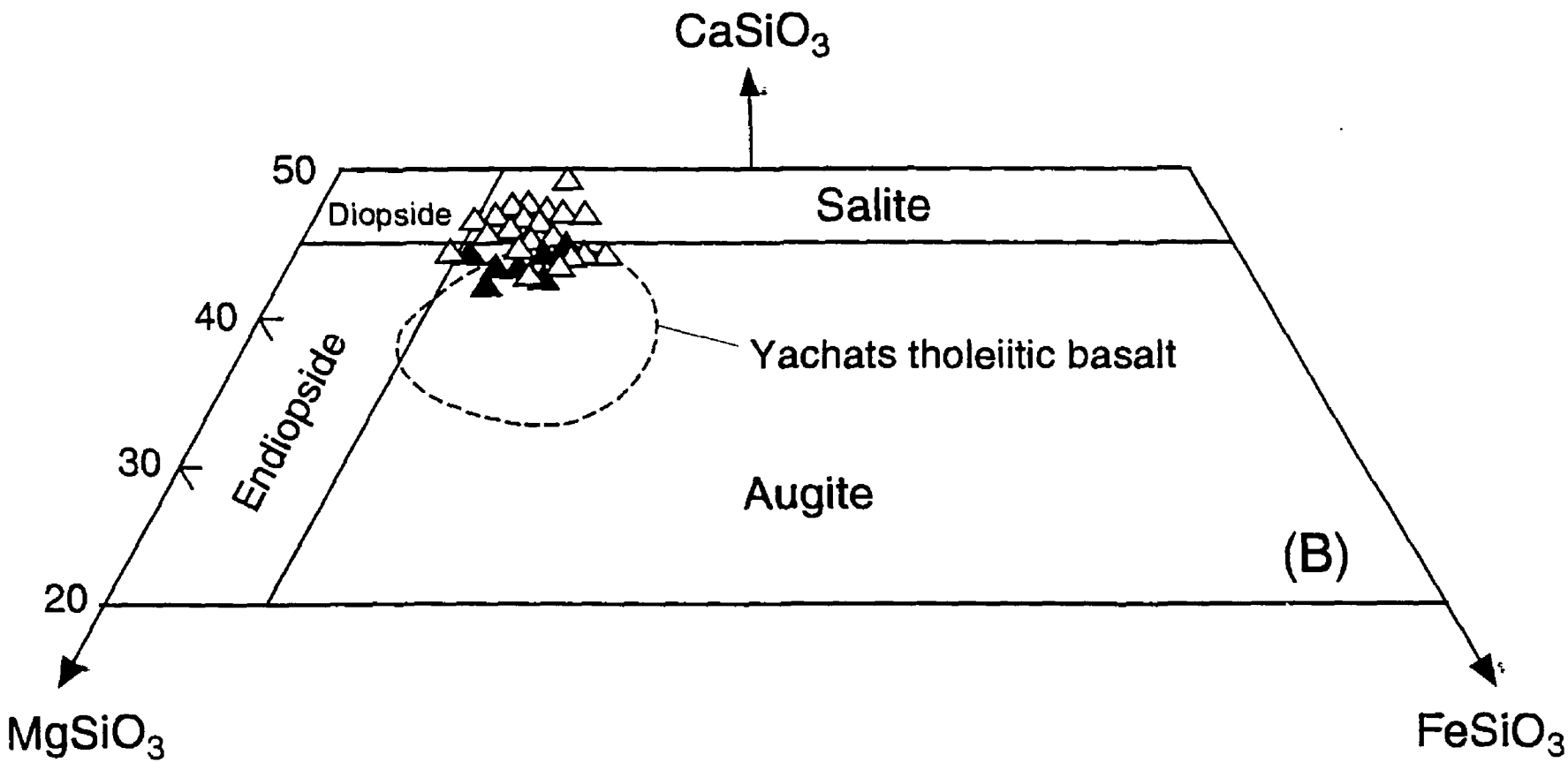

Figure 5. Ca-Mg-Fe ternary plot for pyroxene from (A) Yachats and (B) Cascade Head basalts. Clinopyroxene of Yachats basalts are mostly augite whereas those of Cascade Head basalts are mostly salite. Symbols as in figure 4.

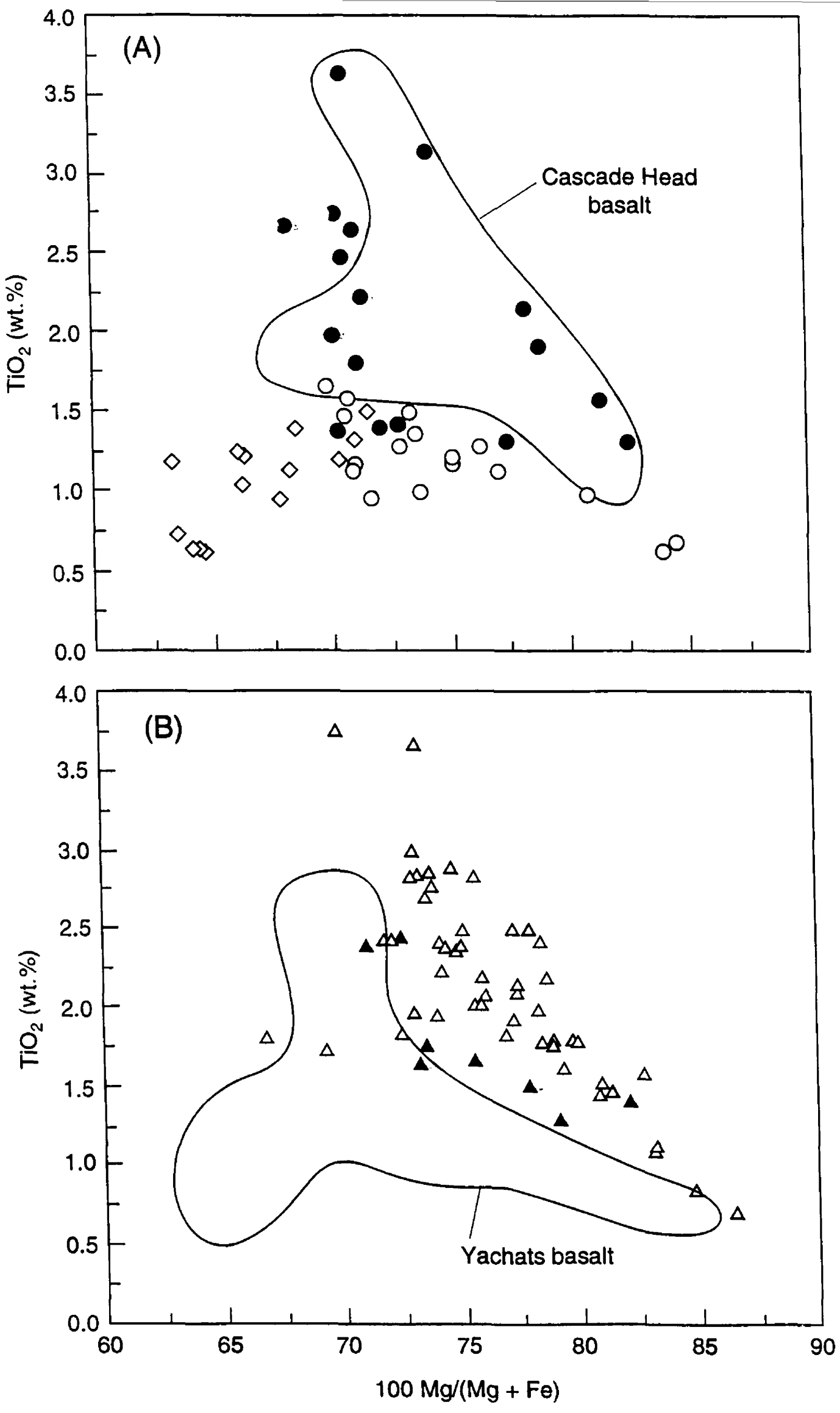

Figure 6. TiO_2 vs. Mg number (100Mg/(Mg+Fe)) for clinopyroxene of (A) Yachats and (B) Cascade Head basalts show tholeiitic compositions are lower in TiO_2 at comparable Mg number than the alkalic ones. TiO_2 decreases in clinopyroxene of more evolved compositions, indicating significant Fe-Ti oxide fractionation. Symbols as in figure 4.

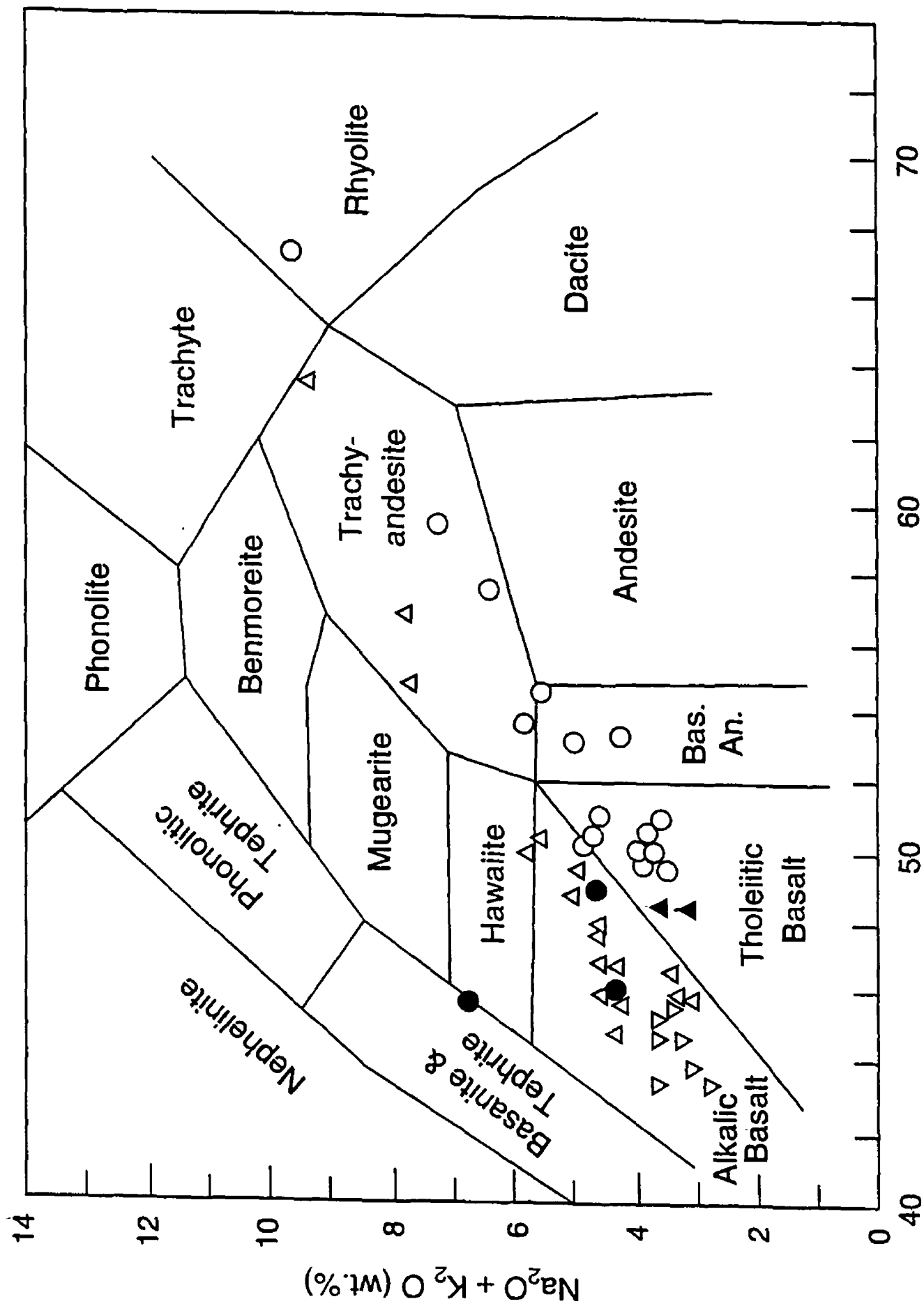

Figure 7. Alkalis vs. SiO_2 shows most of the Yachats samples are tholeiitic basalt and minor basaltic andesite (open circles) but include some alkalic compositions (filled circles). Basalt of Cascade Head are mostly alkalic (open triangles) but include a few tholeiitic compositions (filled triangles). Basalt of Cannery Hills (inverted triangles) are relatively primitive, alkalic basalt. Compositions are normalized to 100% and volatile-free, using the classification of Cox and others (1979).

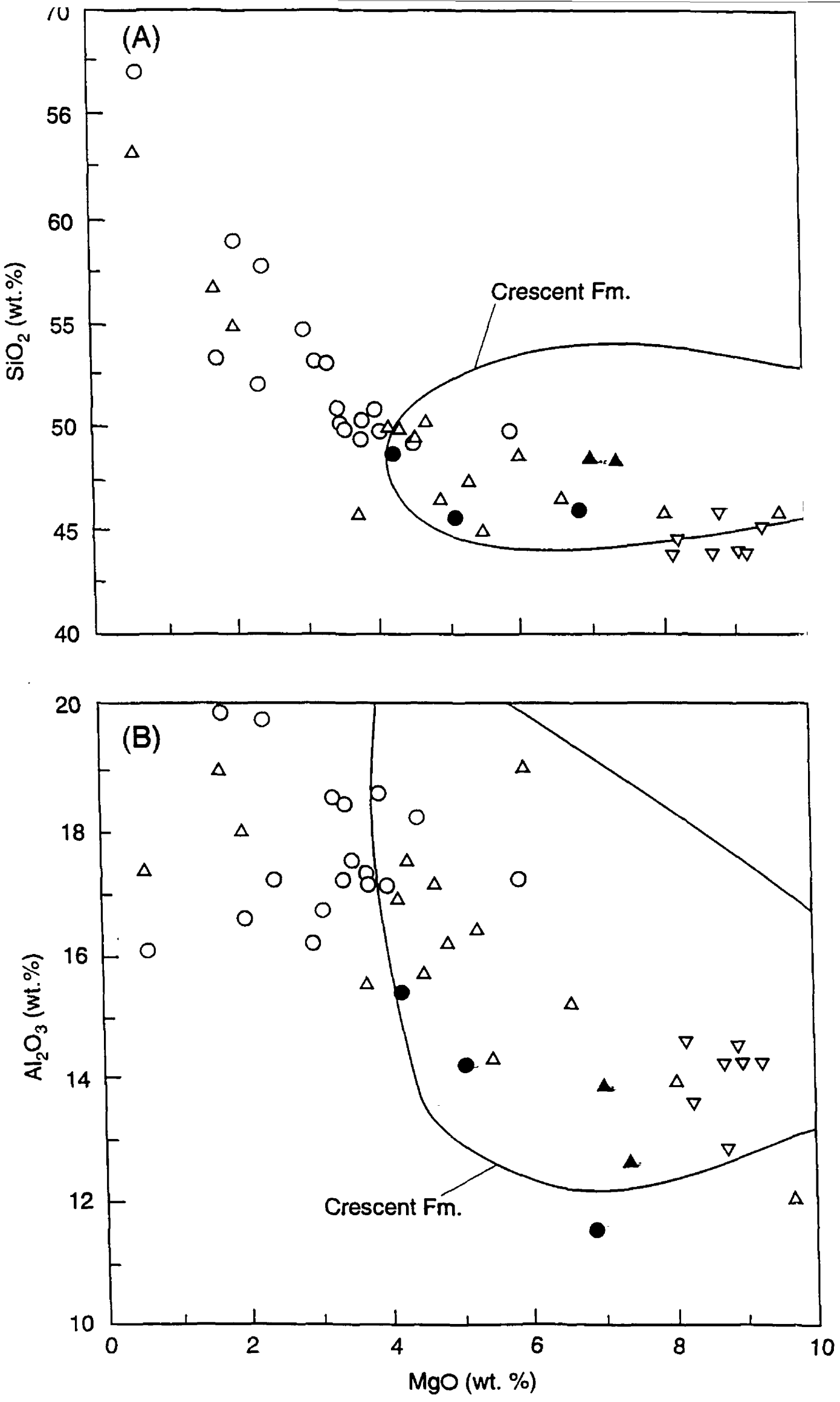

Figure 8. Major-element variation as a function of MgO content for Yachats Cascade Head and Cannery Hills lavas. Early Eocene basalts of the Crescent Formation (shown as field) are much less fractionated and include many primitive compositions. Symbols as in figure 7. Data for Crescent Formation from Glassley (1974) and Babcock and others (1992).

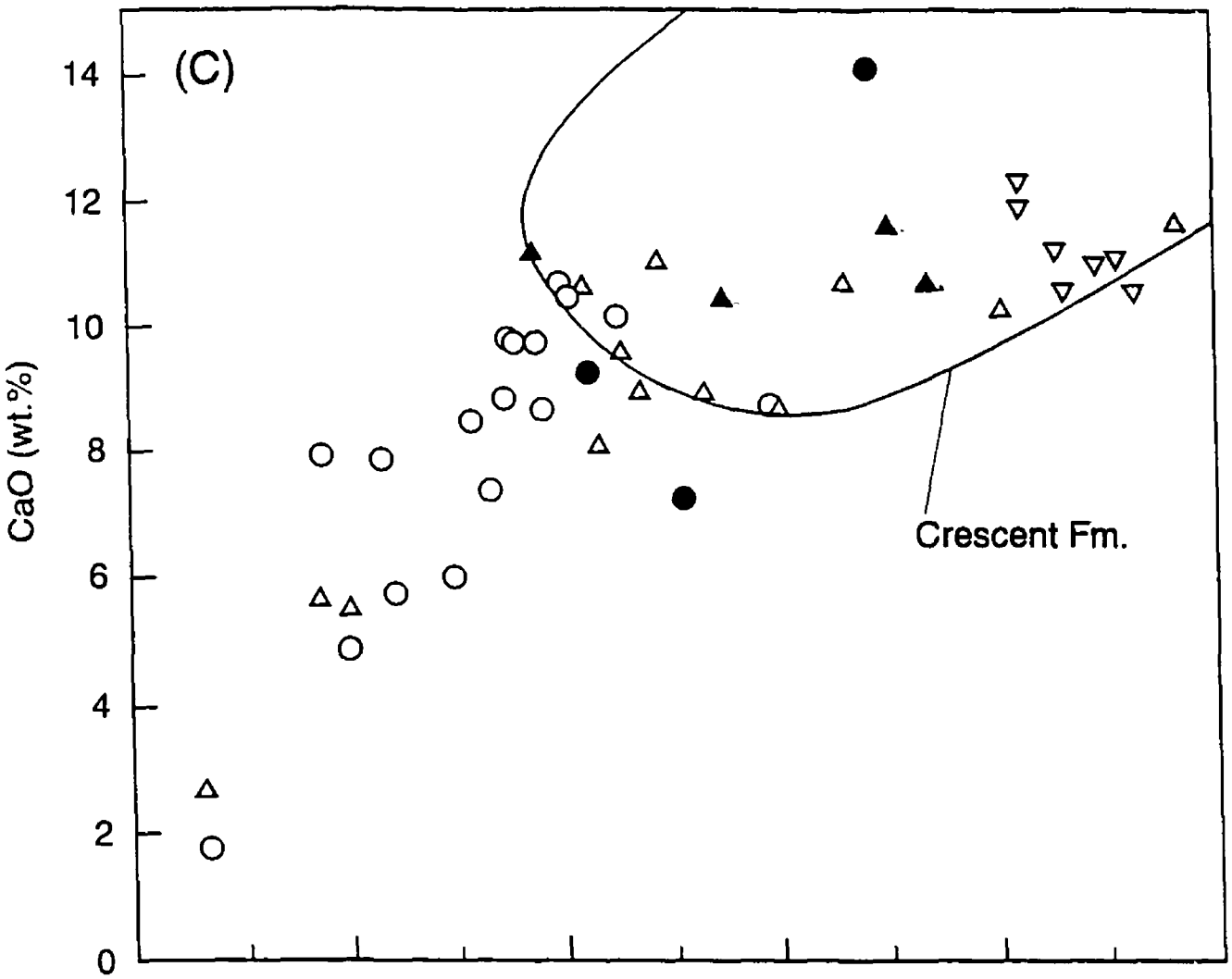

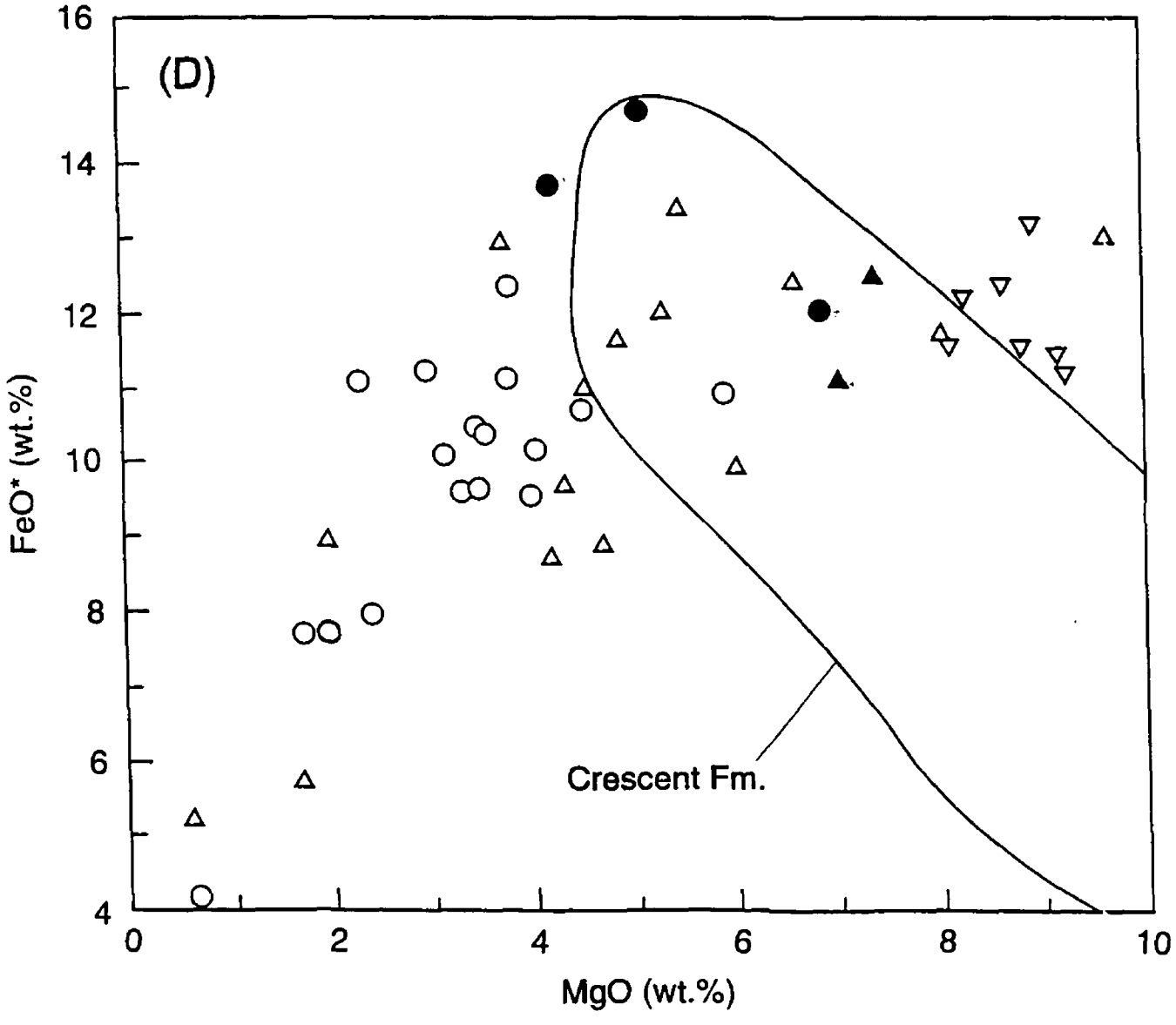

Figure 8. Continued.

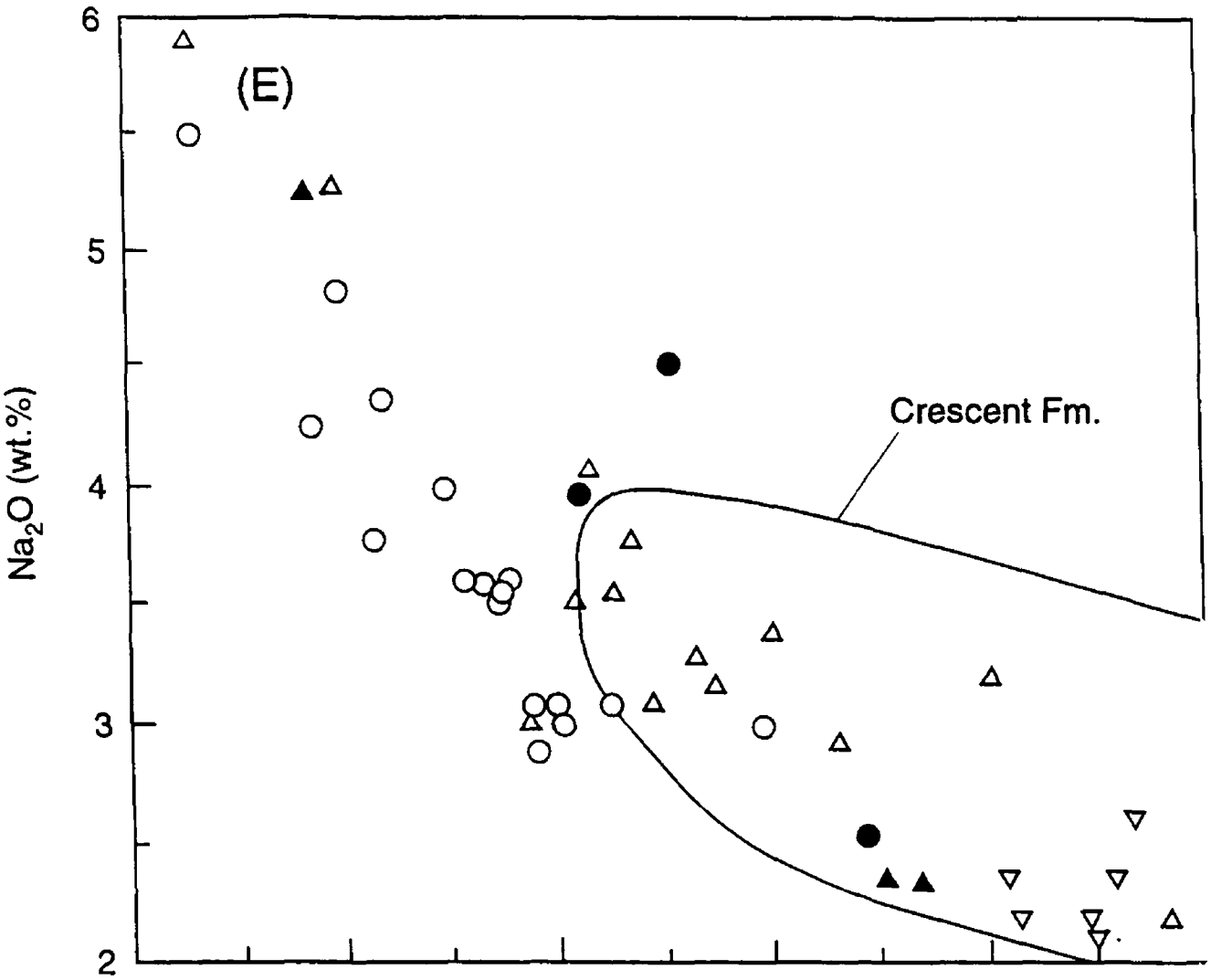

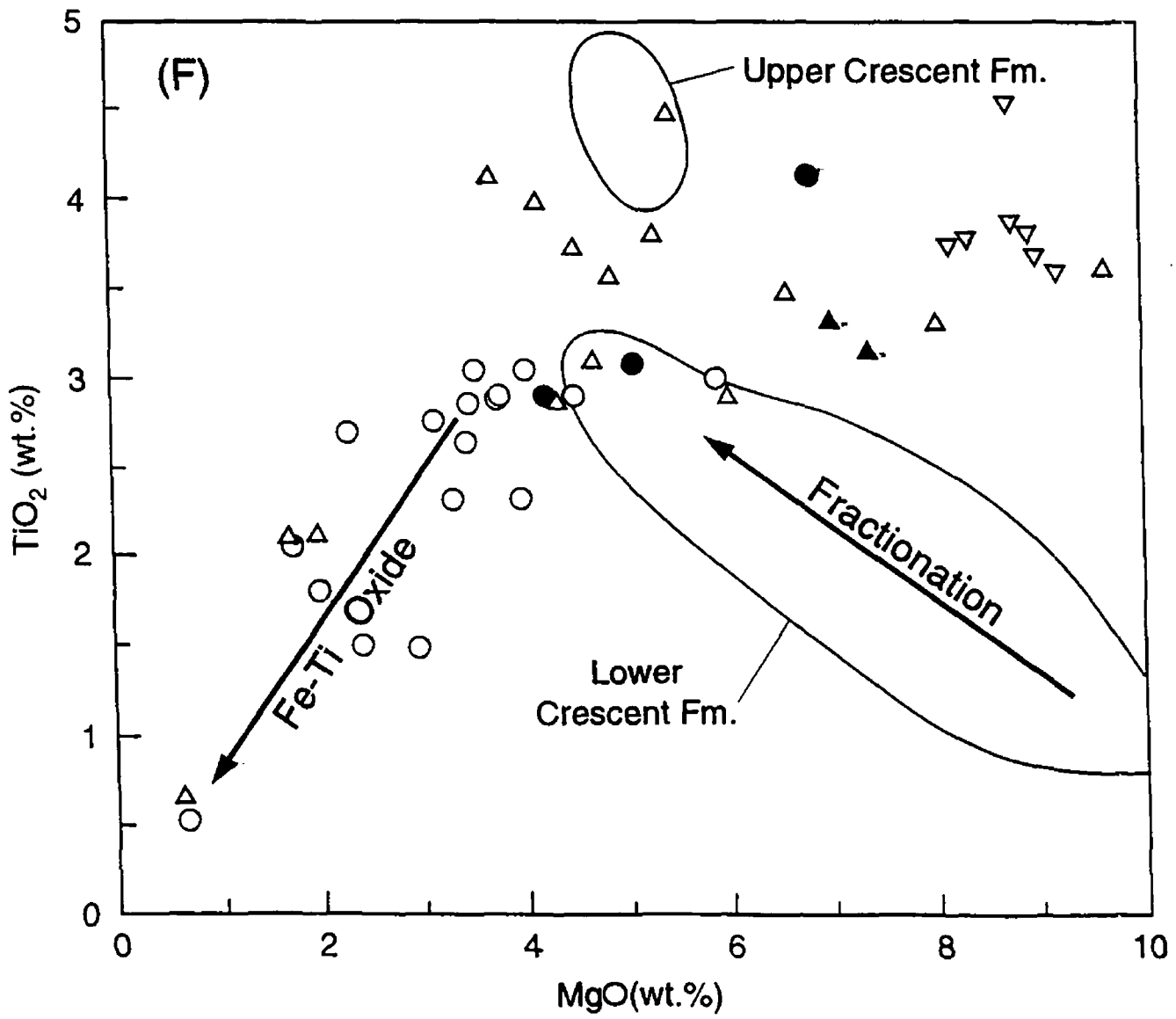

Figure 8. Continued.

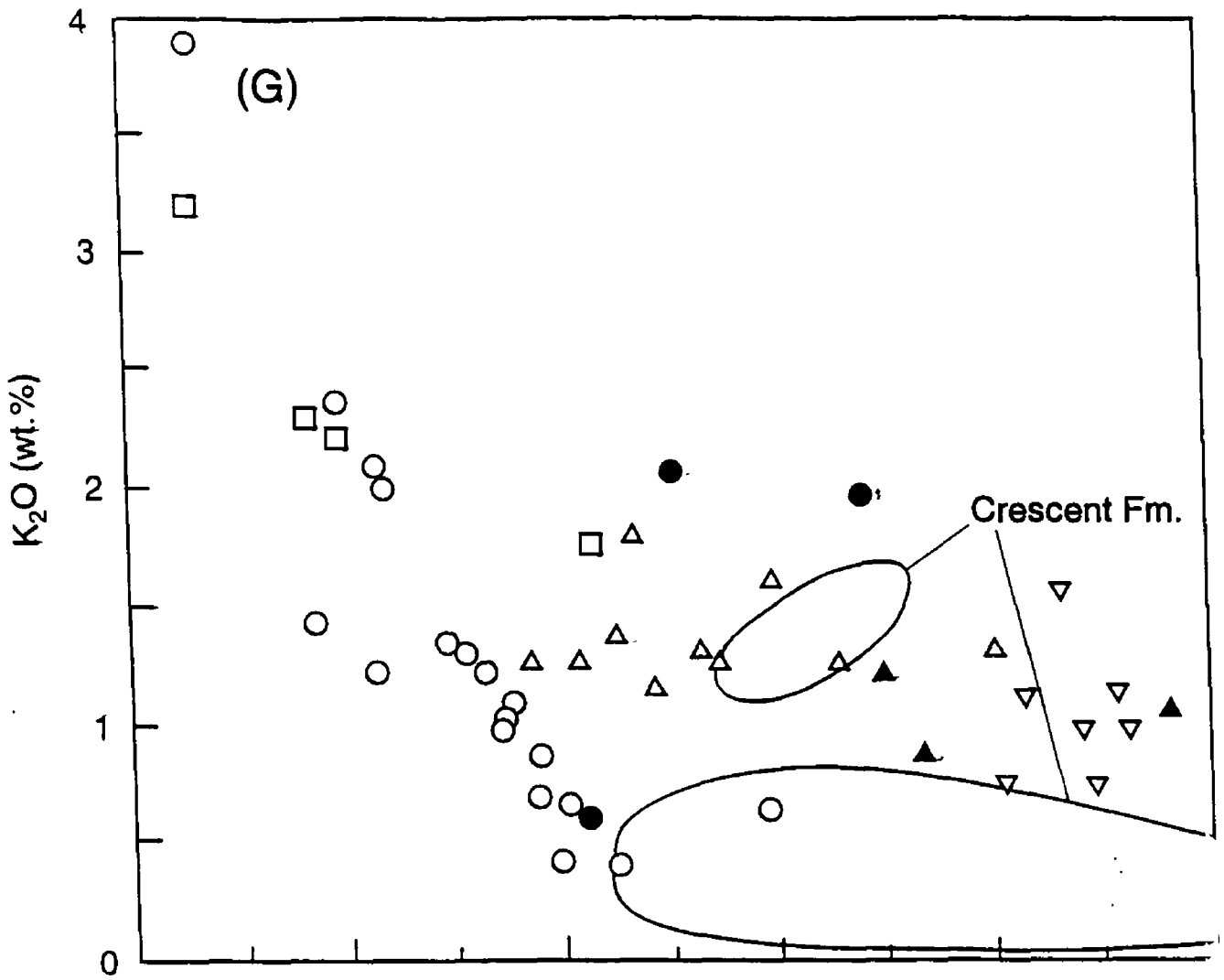

Figure 8. Continued.

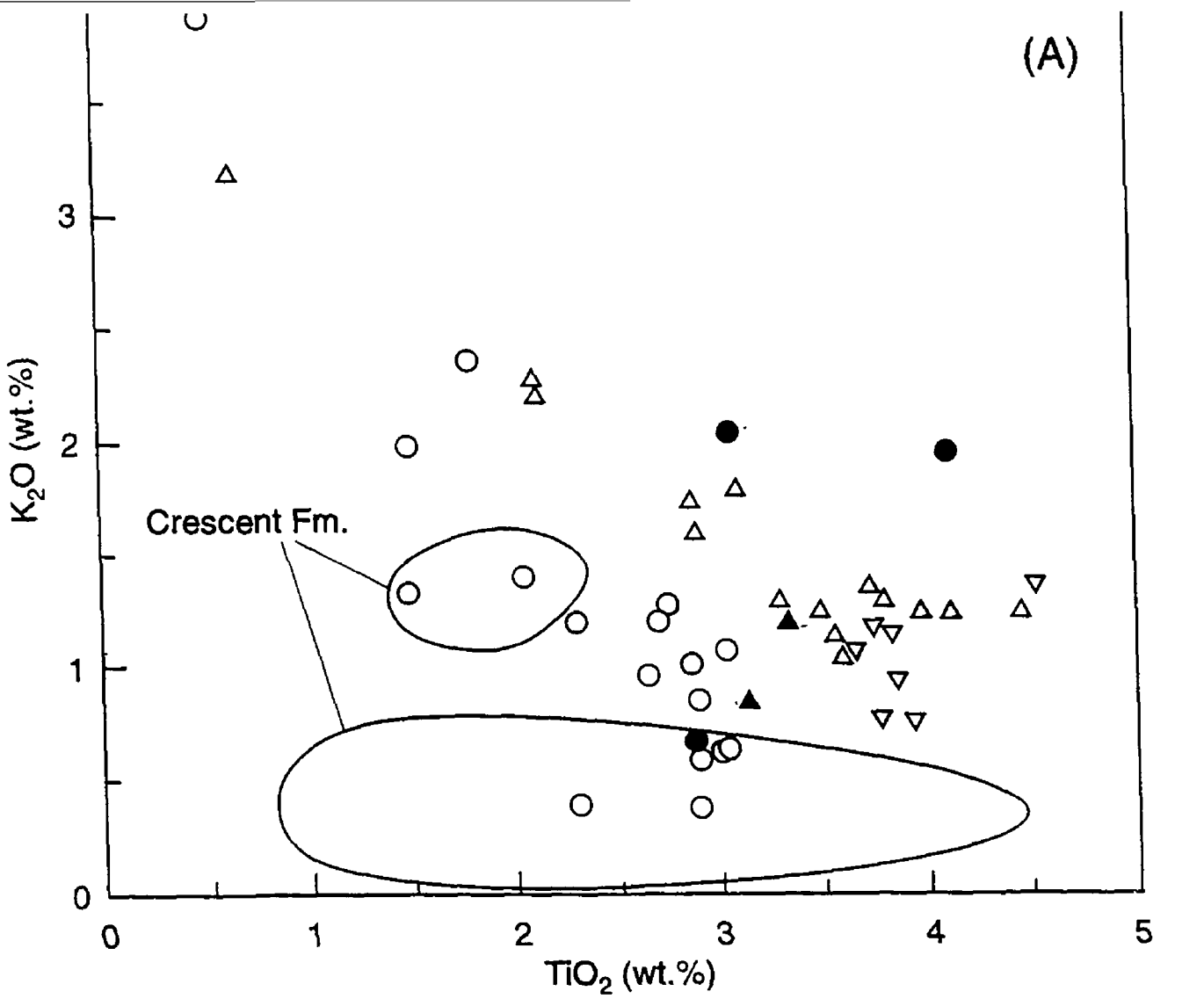

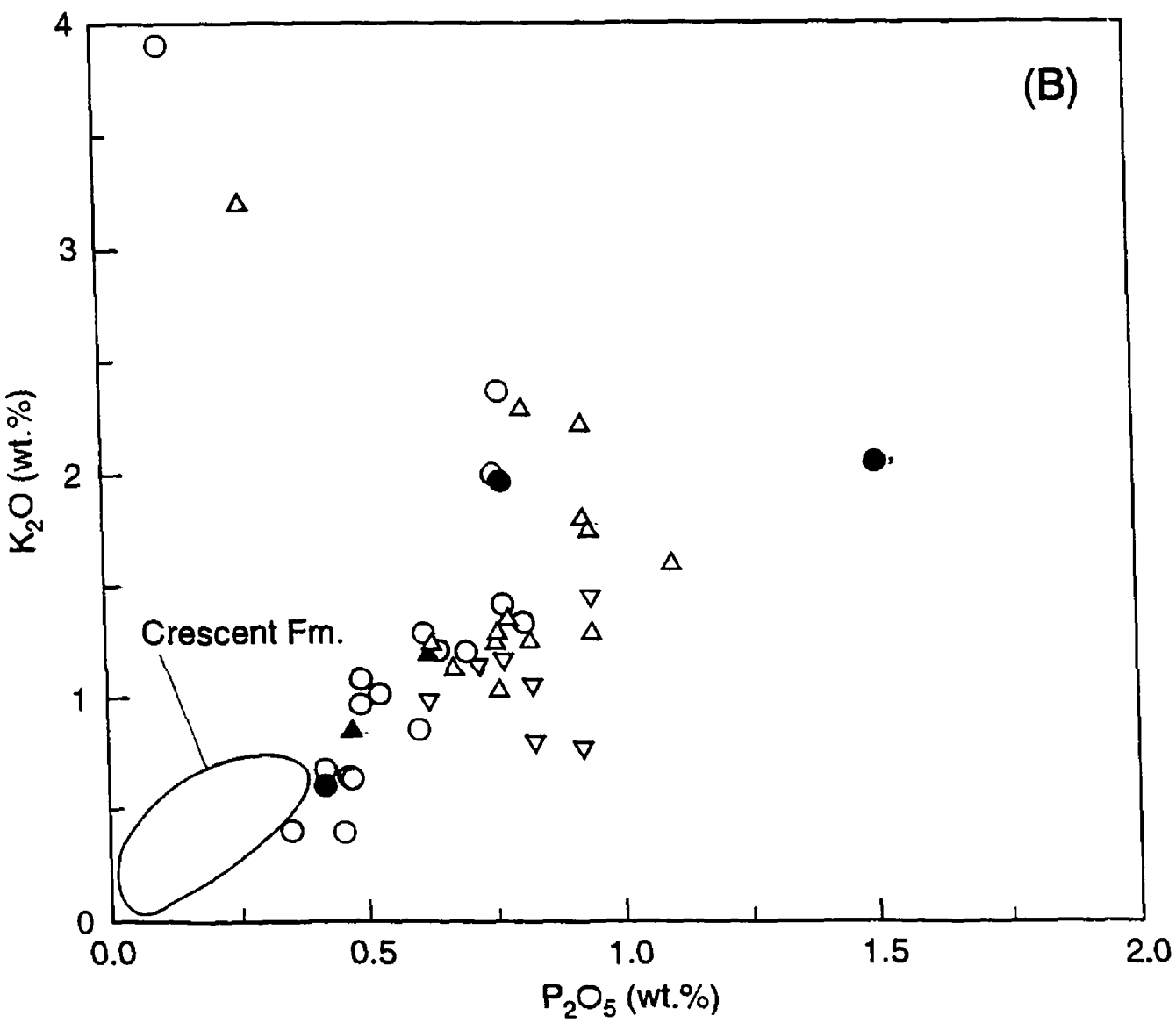

Figure 9. (A) K_2O vs. TiO_2 and (B) K_2O vs. P_2O_5 for late Eocene lavas. Samples from the early Eocene Crescent Basalt are shown for comparison. Symbols and data sources as in figure 8.

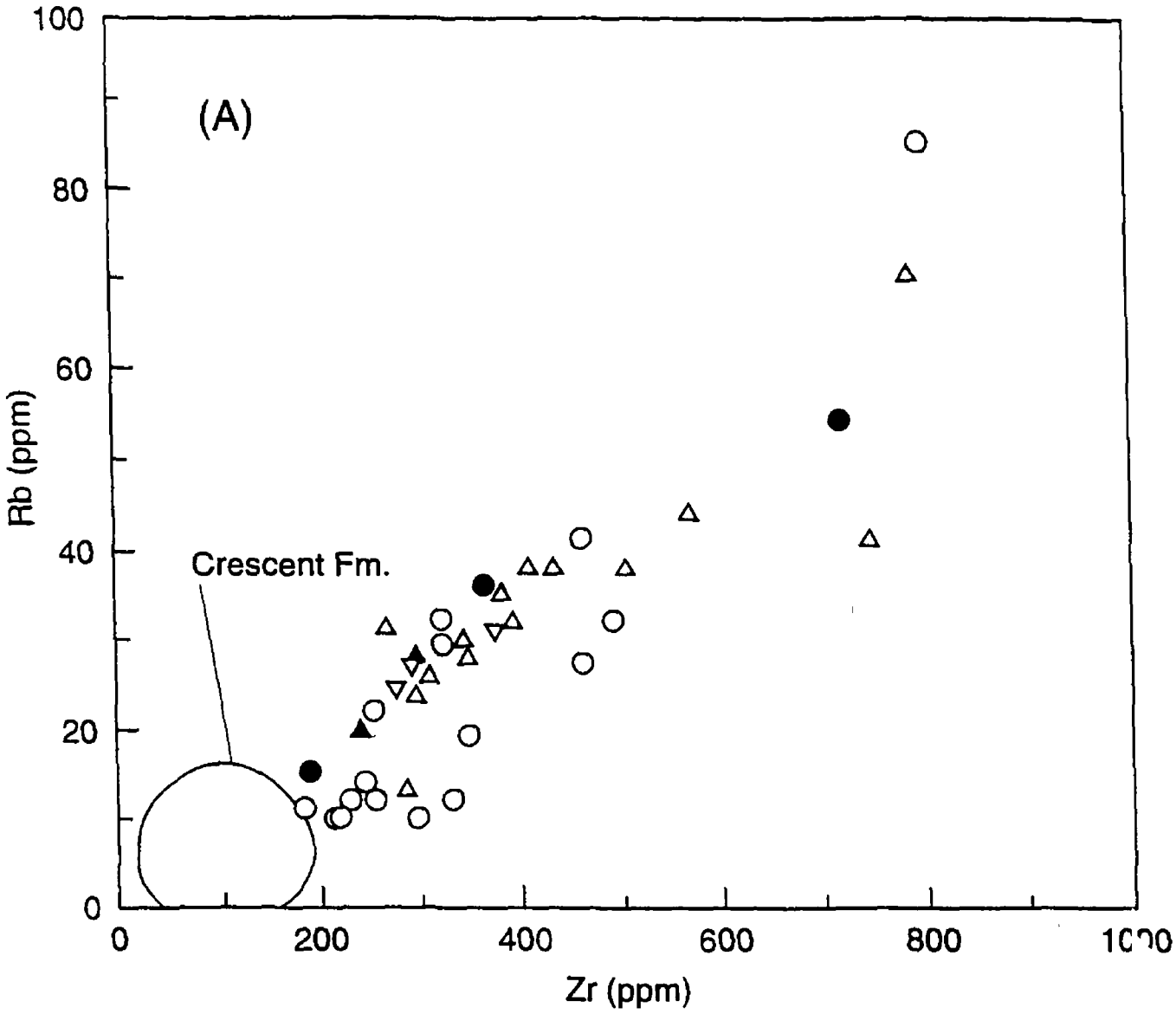

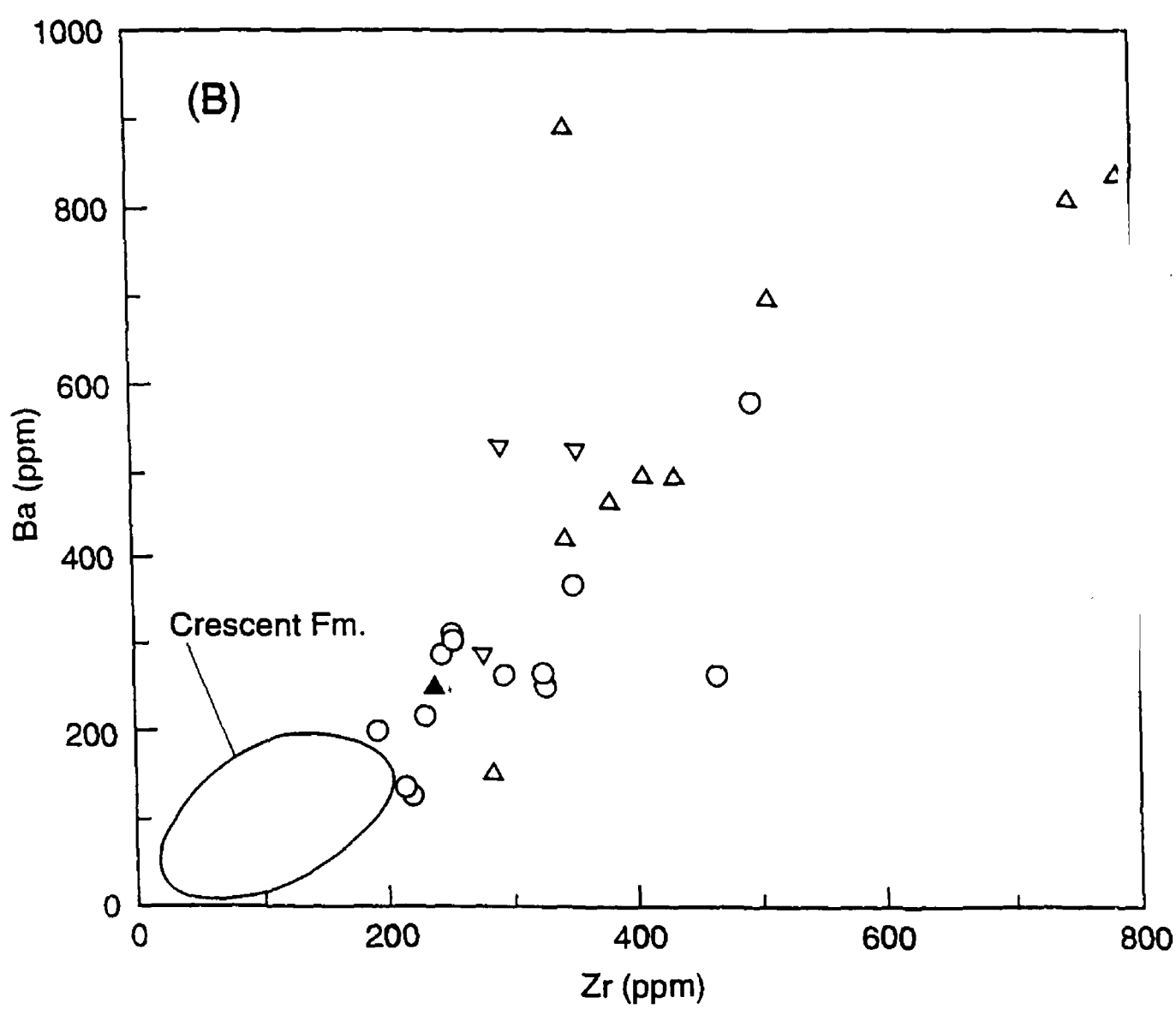

Figure 10. Trace-element variations as a function of Zr content for the late Eocene lavas. Early Eocene basalts of the Crescent Formation plot at the very depleted end of the spectrum. Symbols and data sources as in figure 8.

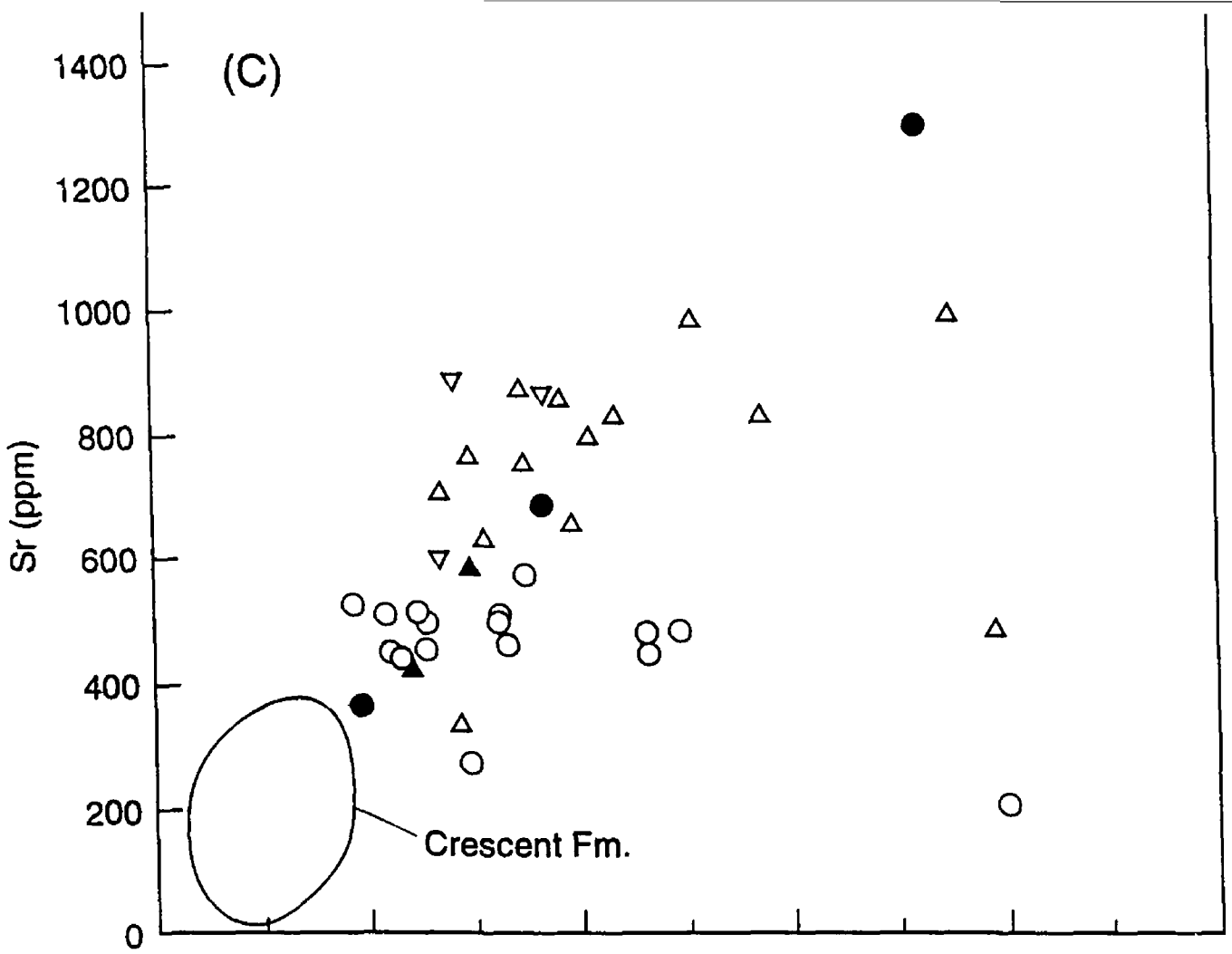

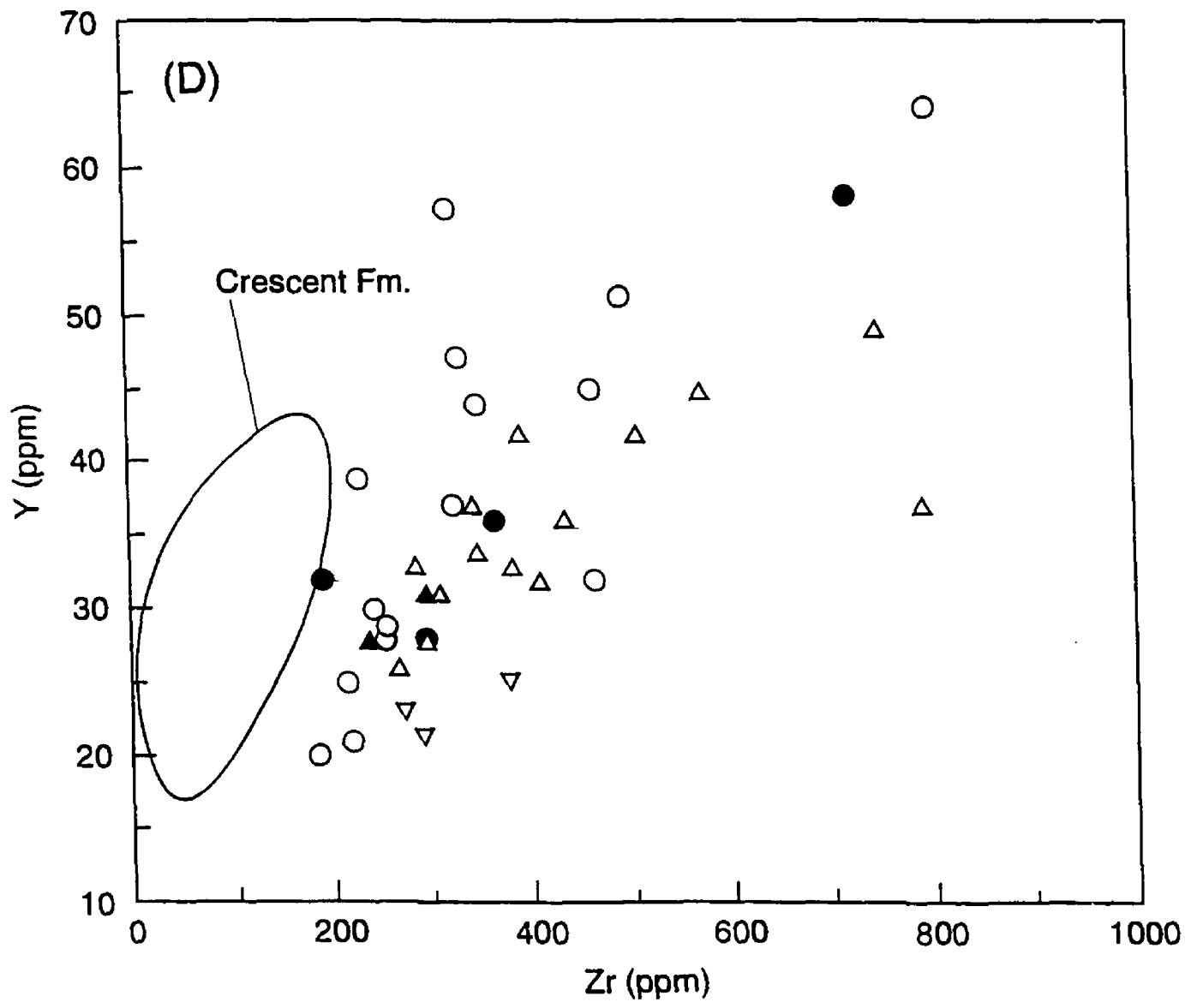

Figure 10. Continued.

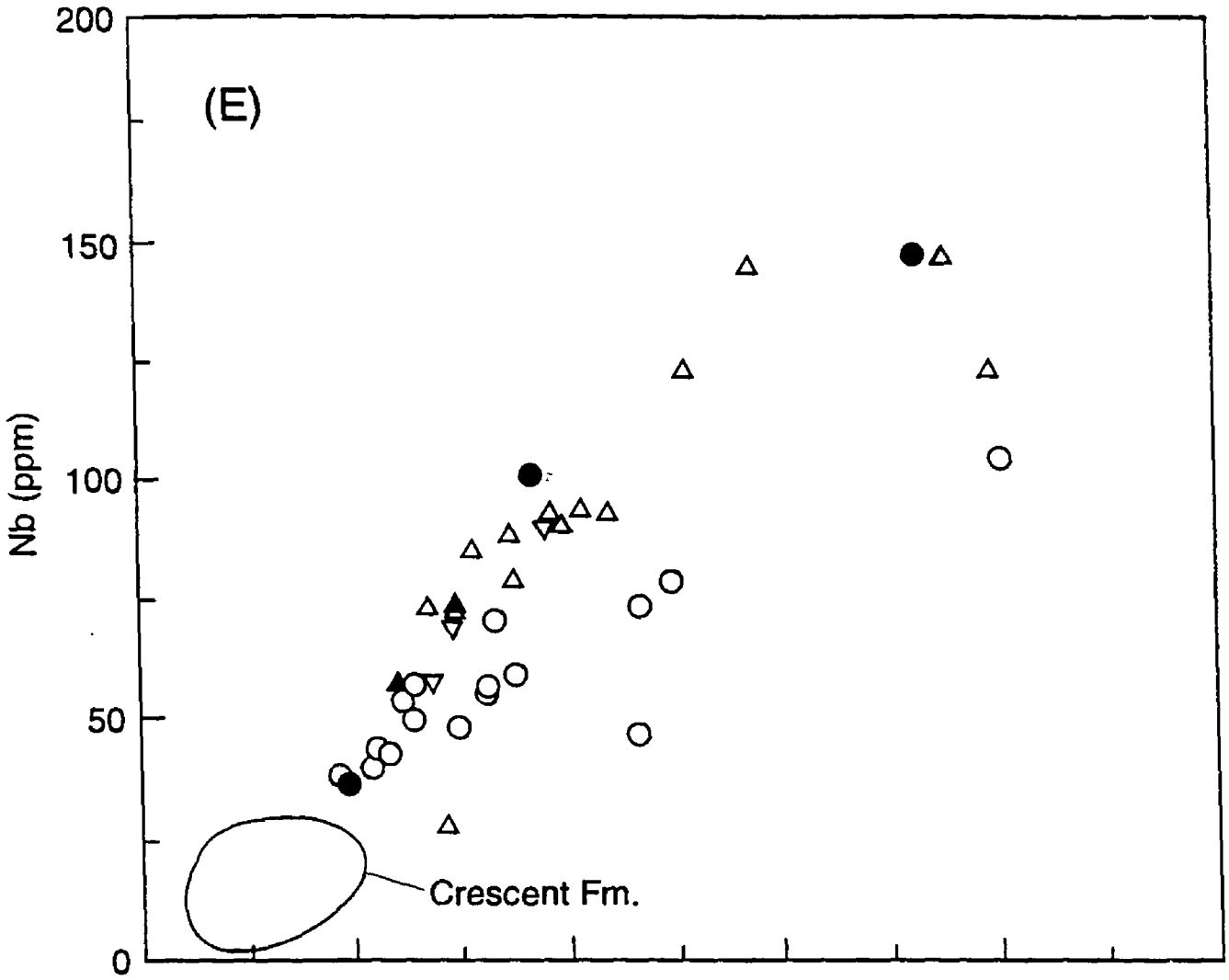

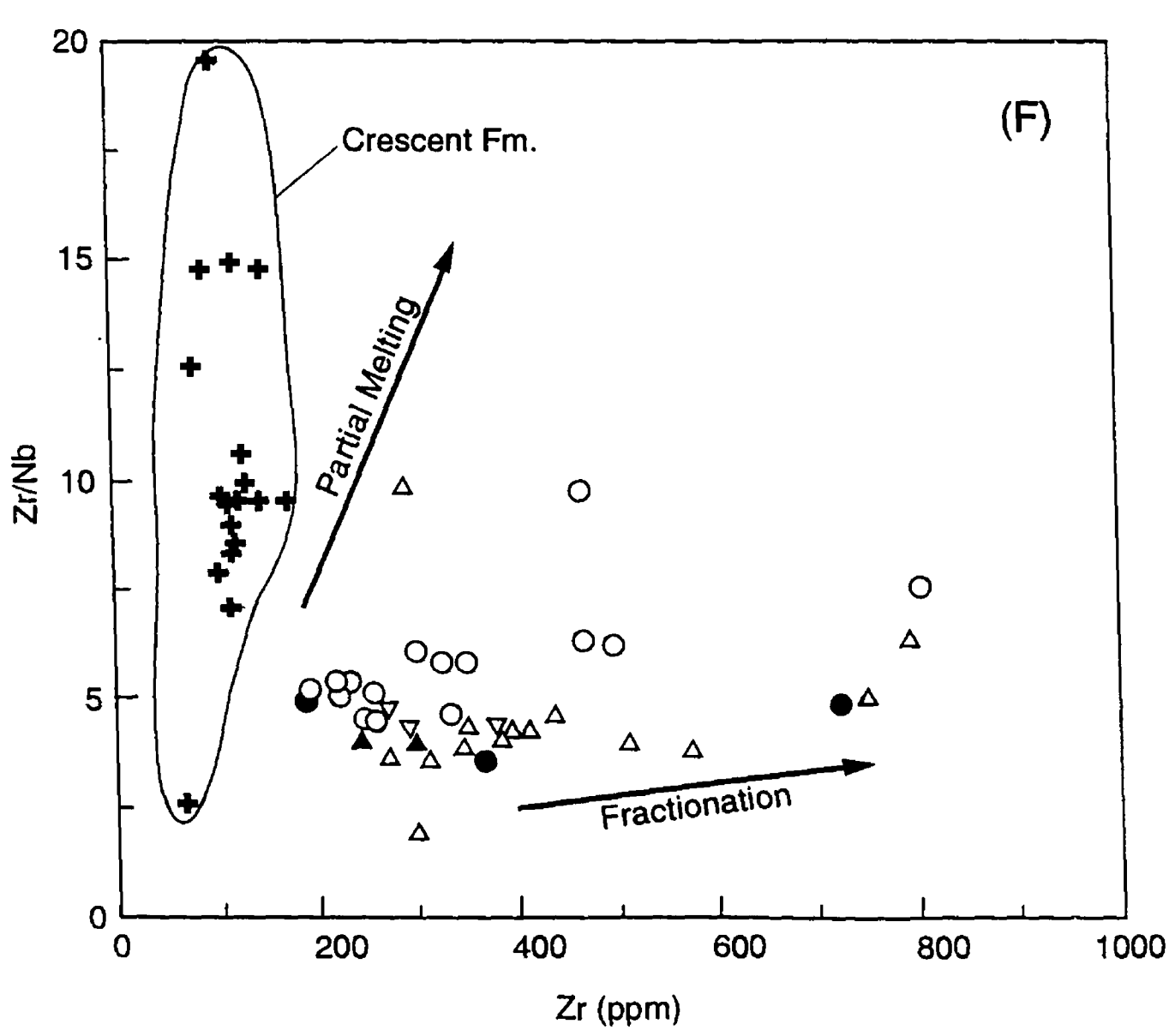

Figure 10. Continued.

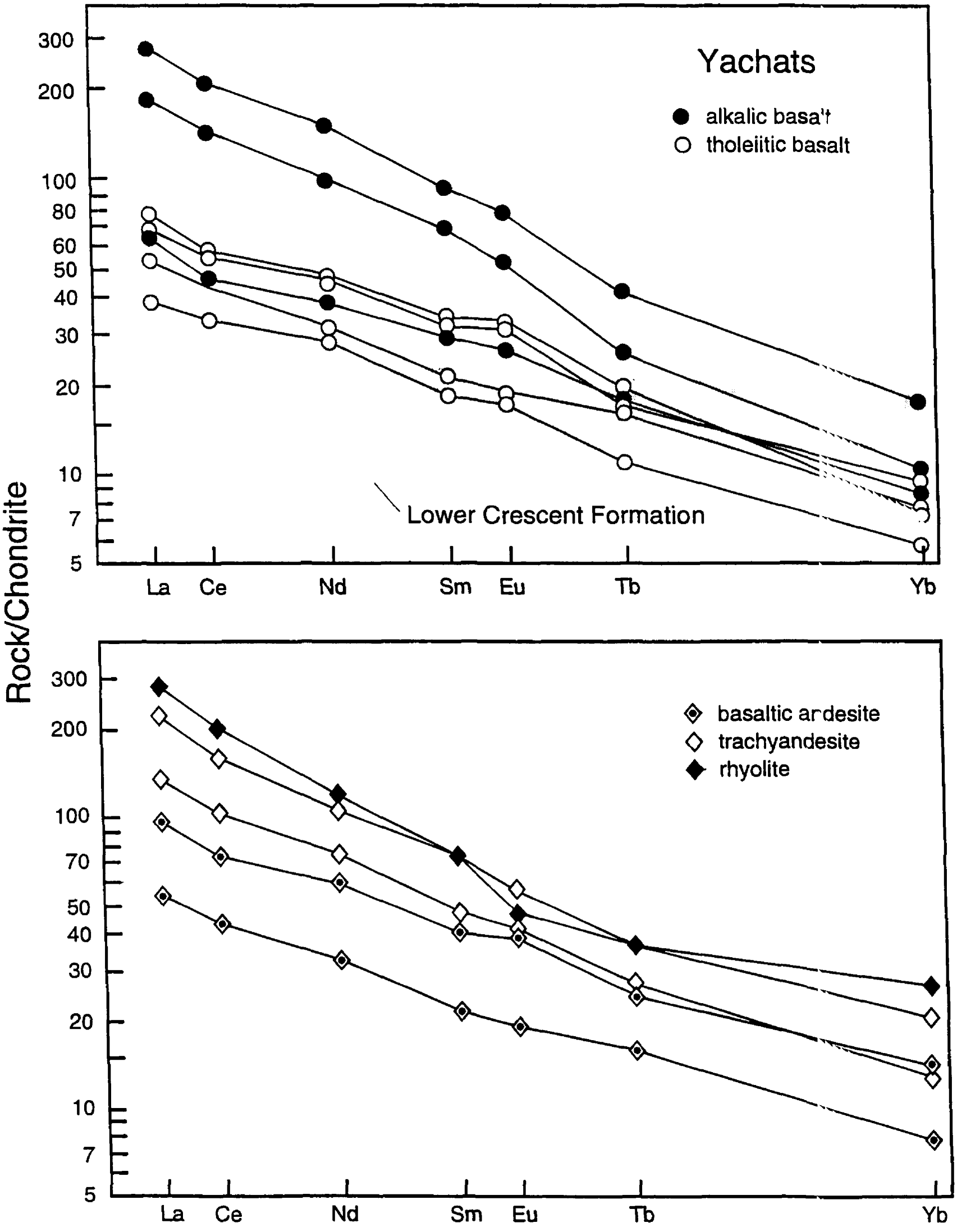

Figure 11A. Chondrite-normalized REE patterns for Yachats Basalt show light REE-enriched patterns for all samples but LREE enrichment is greater for alkalic compositions. Early Eocene basalts from the lower Crescent Formation (shown as a field) have light REE-depleted patterns similar to N-MORB. Normalizing values are from Haskin and others, (1968). Data for the lower Crescent Basalt from Glassley (1974).

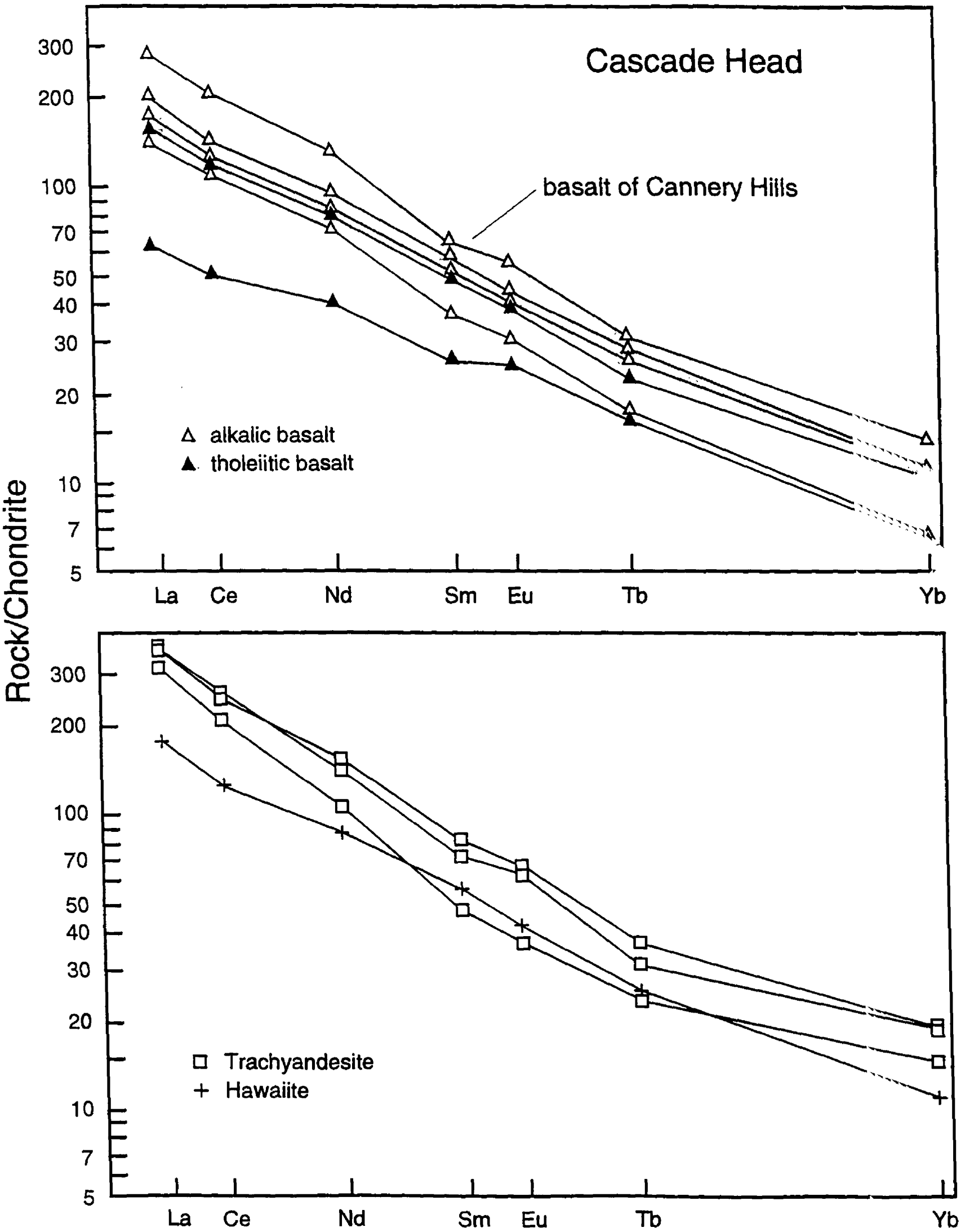

Figure 11B. Chondrite-normalized REE patterns for basalt of Cascade Head and Cannery Hills (shown as field) have light REE enriched patterns comparable to alkalic compositions from the Yachats Basalt. Normalizing values and data sources as in figure 11A.

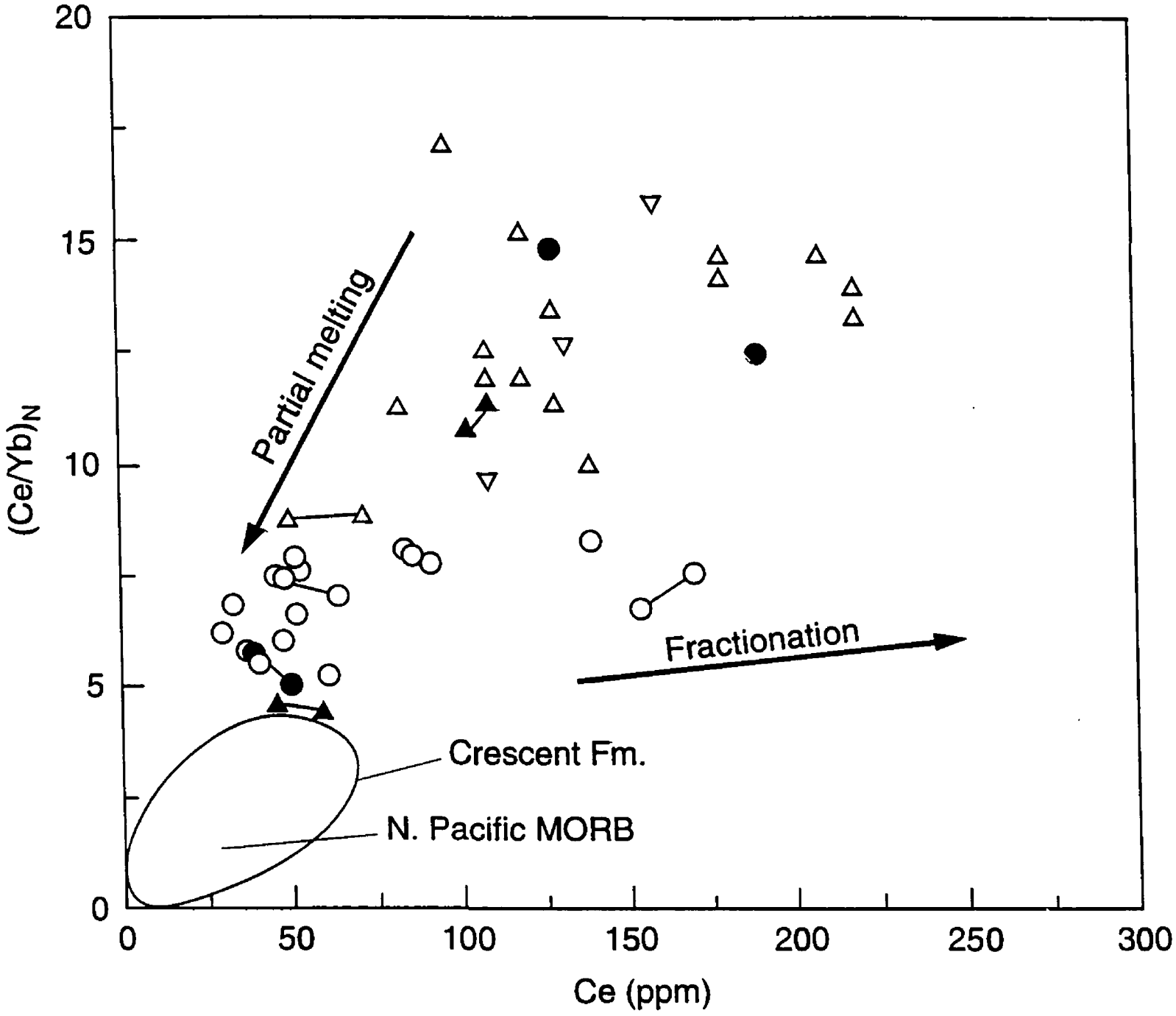

Figure 12. Chondrite-normalized Ce/Yb ratios vs. Ce abundance show similar ratios over a large range of Ce abundances that is compatible with crystal fractionation. The Cascade Head and Cannery Hills basalts have higher Ce/Yb ratios suggesting origin by smaller percentage of melting. Samples for which duplicate analyses by ICP-MS and INAA were available have been connected by tie lines. The early Eocene basalts from the lower and upper Crescent Formation (shown as one field) and mid-ocean ridge basalt are shown for comparison. Symbols and data sources as in Figure 8.

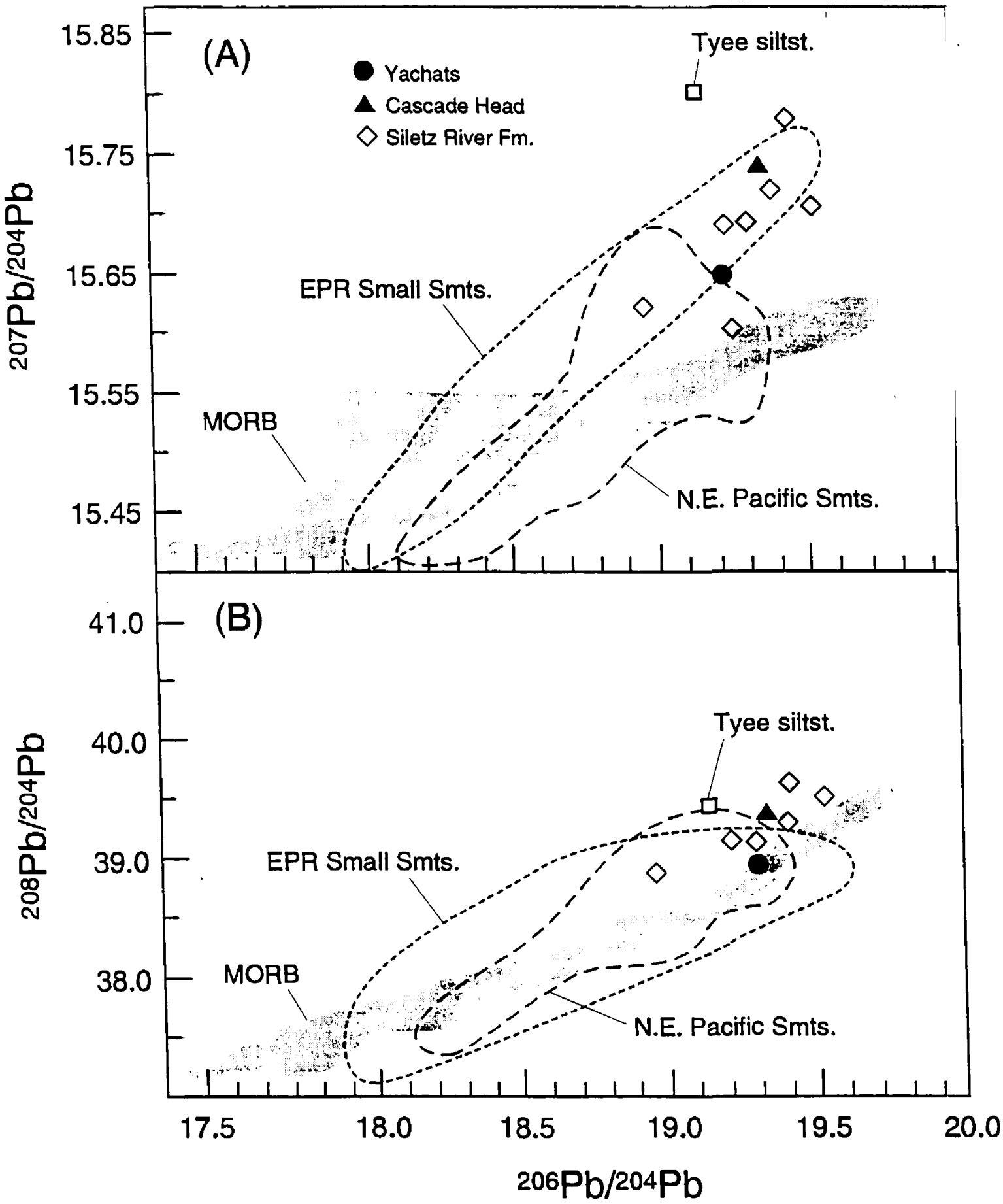

Figure 13. Pb isotopic compositions for a Yachats basalt (filled circle) and for a trachyandesite from Cascade Head (filled triangle) are similar to those of the older Siletz River Volcanics (diamonds) and to basalt from seamounts in the eastern Pacific. Data sources for EPR seamounts from Fornari and others (1984) and for MORB from Church and Tatsumoto (1975) and White and others (1987).

Appendix 1A: Location and Petrography of Yachats Basalt

SW58-4: 44° 17.29' N Lat., 124° 04.90' W Long. Tholeiitic basalt. Highly porphyritic with large (to 1 cm) plagioclase glomerocrysts and rare olivine and very rare clinopyroxene phenocrysts in intergranular groundmass of plagioclase, anhedral clinopyroxene, and abundant opaque minerals. Plagioclase phenocrysts have abundant inclusions and olivine phenocrysts are replaced by clays and Fe-oxide/hydroxide.

SR58-17: 44° 23.48' N Lat., 124° 01.86' W Long. Tholeiitic basalt breccia. Highly porphyritic with large (to 2 cm) plagioclase phenocrysts and rare olivine microphenocrysts in glassy to hyalopilitic groundmass. Plagioclase phenocrysts have resorbed looking margins and sieve-textures. Some glass is still fresh brown sideromelane. Olivine partly replaced with calcite. Moderate amounts of vesicles also filled with calcite.

SR61-8A: 44° 15.60' N Lat., 123° 54.48' W Long. Basaltic andesite feeder dike in Tyee Formation. Highly porphyritic with plagioclase glomerocrysts in an intergranular groundmass of anhedral clinopyroxene, feldspar, and abundant opaque minerals. Plagioclase phenocrysts are anhedral, complexly zoned with many inclusions.

SM63-3: 44° 14.13' N Lat., 123° 14.29' W Long. Tholeiitic basalt feeder dike. Sparsely plagioclase phyric with seriate texture, very sparsely vesicular. Groundmass of plagioclase, anhedral clinopyroxene, and abundant opaque minerals. Clay and calcite alteration in vesicles and groundmass.

S81-201A: 44° 06.17' N Lat., 124° 07.18' W Long. Basaltic andesite flow. Highly plagioclase phyric and with rare anhedral clinopyroxene phenocrysts in groundmass of seriate to subtrachytic texture of plagioclase and opaque minerals. Moderately vesicular. Brown clay in groundmass and in vesicles.

S81-201C: 44° 06.17' N Lat., 124° 07.18' W Long. Trachyandesite dike. Highly porphyritic with abundant plagioclase and very rare clinopyroxene phenocrysts in trachytic groundmass of feldspar and opaque minerals. Big, round vesicles are abundant.

SR63-117: 44°13.41' N Lat., 124° 03.13' W Long. Tholeiitic basalt flow. Moderately porphyritc with abundant plagioclase, minor olivine, and rare clinopyroxene phenocrysts in intergranular groundmass of plagioclase, clinopyroxene and minor opaque minerals. Olivine pseudomorphed by clay; clay abundant in groundmass.

SR61-106A: 44° 08.06' N Lat., 124°07.41' W Long. Tholeiitic basalt breccia. Highly porphyritic with large plagioclase and rare olivine phenocrysts in intergranular groundmass of plagioclase and anhedral clinopyroxene. Sparsely vesicular. Olivine replaced by clay minerals and clay in vesicles and groundmass.

SR61-106B: 44° 08.06' N Lat., 124°07.41' W Long. Tholeiitic basalt flow. Highly porphyritic with abundant euhedral plagioclase glomerocrysts and olivine and very rare clinopyroxene microphenocrysts in glassy to hyalopilitic groundmass. Highly vesicular. Clay mineral alteration in vesicles and groundmass.

SR62-168A: 44° 15.04' N Lat., 123° 58.86' W Long. Tholeiitic basalt transitional to basaltic andesite. Sparsely porphyritic with plagioclase glomerocrysts (to 0.5 cm) in trachytic groundmass of plagioclase and small anhedral clinopyroxene and very abundant oxidized opaques. Moderately altered.

SR61-109A: 44° 23.45' N Lat., 124° 01.91' W Long. Tholeiitic, columnar-jointed flow. Moderately porphyritic with euhedral plagioclase phenocrysts in intergranular to subtrachytic groundmass of plagioclase and anhedral clinopyroxene and opaque minerals. Some yellow-brown clay alteration in groundmass.

SW56-5: 44° 23.62' N Lat., 124° 01.87' W. Transitional basalt, columnar-jointed flow. Highly porphyritic with large sub- to euhedral plagioclase and rare rounded, anhedral clinopyroxene glomerocrysts accompanied by very rare olivine pseudomorphs in intergranular groundmass of plagioclase, clinopyroxene, and opaque minerals. Olivine replaced by green-brown clay mineral which is also abundant in the groundmass.

SR90-35: 44° 13.70'N Lat, 124° 01.50' W Long. Tholeiitic basalt flow. Moderately porphyritic with sub- to anhedral plagioclase glomerocrysts and rare olivine pseudomorphs in intergranular groundmass of plagioclase, clinopyroxene, and opaque minerals

S89-15: 45° 08.10' N Lat., 124° 00.10' W Long. Basanite flow. Highly porphyritic with abundant olivine and rare clinopyroxene microphenocrysts in intergranular groundmass of clinopyroxene, olivine, and opaque minerals. Olivine unaltered. Clinopyroxene deep purplish-pink pleochroic.

S91-6: 44° 23.48' N Lat., 124° 01.86' W Long. Tholeiitic basalt. Moderately plagioclase-phyric with small phenocrysts and rare clinopyroxene and olivine microphenocrysts in trachytic groundmass of plagioclase microlites, rare anhedral clinopyroxene, and abundant oxidized opaques in tachylitic glass.

S91-11: 44° 17.33' N Lat., 124° 06.69' W Long. Rhyolite from margin of compositionally zoned dike. Moderately porphyritic, with sub- to anhedral plagioclase phenocrysts in pilotaxitic groundmass of feldspar microlites and anhedral quartz in brownish devitrified glass. Very abundant Fe-Ti oxide microphenocrysts.

S91-12: 44° 17.07' N Lat., 124° 06.62' W Long. Tholeiitic basalt flow. Moderately porphyritic with small subhedral plagioclase phenocrysts and lesser amounts of clinopyroxene and olivine (pseudomorphed) in a groundmass of plagioclase and opaque minerals. Rare vesicles filled with brown clay minerals which are also relatively abundant in the groundmass.

S91-13 (MR68-64) : 44° 17.06' N Lat., 124° 06.64' W Long. Trachyandesite dike. Sparsely plagioclase-phyric with very rare, anhedral clinopyroxene microphenocrysts in a groundmass of brown altered glass with plagioclase microlites and abundant opaque minerals.

S91-14: 44° 08.55' N Lat., 124° 07.40' W Long. Alkalic basalt dike. Moderately porphyritic with clinopyroxene microphenocrysts and rare olivine pseudomorphs in groundmass of clinopyroxene, plagioclase, and abundant opaque minerals. Brown clay alteration in the groundmass.

Appendix 1B: Location and Petrography of Cascade Head and Cannery Hills basalts

S83-20: 45° 03.85' N Lat., 123° 58.57' W Long. Hawaiite. Nearly aphyric, with extremely rare broken clinopyroxene crystal fragments in a trachytic groundmass of feldspar and Fe-Ti oxides.

SR83-86: 45° 04.17' N Lat., 123° 53.20' W Long. Alkalic basalt flow. Sparsely clinopyroxene-phyric, with sub- to anhedral phenocrysts of pink-brownish clinopyroxene (to 0.3 cm) and rare olivine in intergranular groundmass of anhedral clinopyroxene, plagioclase, and abundant opaque minerals.

SR83-94: 45° 04.24' N Lat., 123°51.98' W. Alkalic basalt flow. Clinopyroxene and olivine phyric ankaramite. Large (to 0.8 cm) euhedral to subhedral clinopyroxene and olivine phenocrysts. Clinopyroxene pink-brown pleochroic. Olivine is unaltered. Groundmass intergranular to subtrachytic consisting of feldspar and anhedral clinopyroxene and opaques.

MR68-80: 44° 05.07' N Lat., 124° 00.28' W Long. Trachyandesite dike. Sparsely plagioclase and amphibole-phyric. Amphibole phenocrysts have opaque reaction rims. Groundmass consists of trachytic feldspar and abundant tiny opaque minerals.

MR68-81: 44° 05.07' N Lat., 124° 00.28' W. Alkalic basalt flow. Highly plagioclase-phyric, with big (to 1 cm) sub- to euhedral plagioclase phenocrysts and rare olivine (pseudomorphs) in intergranular groundmass of anhedral clinopyroxene, feldspar, and opaque minerals.

SR83-48: 45° 05.41' N Lat., 123° 54.81' W Long. Tholeiitic basalt flow. Clinopyroxene, olivine and plagioclase-phyric ankaramite with large (to 2 cm), euhedral, pink-brown, clinopyroxene phenocrysts and less abundant olivine, which is pseudomorphed by greenish clay minerals. Groundmass is intergranular, consisting mostly of clinopyroxene and opaque minerals.

SR62-160: 45° 01.56' N Lat., 124° 00.66' W Long. Hawaiite blocks in breccia. Sparsely plagioclase phyric with sub- to anhedral microphenocrysts and very rare anhedral or broken clinopyroxene phenocrysts in a trachytic groundmass of feldspar and tiny opaque minerals.

SR61-5: 45° 04.05' N Lat., 123° 56.93' W Long. Alkalic basalt feeder dike in Nestucca Formation. Plagioclase, olivine and clinopyroxene-phyric. Olivine are all replaced by greenish clay (saponite?). Intergranular texture of anhedral clinopyroxene, feldspar, and opaque minerals.

S79-36 (S84-114): 45° 05.13' N Lat., 123° 57.22' W Long. Trachyandesite dike. Plagioclase and amphibole phyric with large, complexly zoned plagioclase and sub- to euhedral amphibole phenocrysts in trachytic groundmass of feldspar and opaque minerals.

SR61-4: 45° 04.56' N Lat., 123°59.82" W Long. Alkalic basalt flow. Sparsely plagioclase and clinopyroxene phyric with subhedral microphenocrysts and very rare large olivine phenocrysts, which are pseudomorphed by clay minerals. Intergranular texture of clinopyroxene, plagioclase, and abundant opaque minerals.

S83-27: 45° 10.31' N Lat., 123° 54.02' W Long. Transitional between tholeiitic and alkalic basalt. Clinopyroxene and olivine phyric ankaramite with abundant, large clinopyroxene phenocrysts and rare olivine pseudomorphs. Groundmass subtrachytic to intergranular with anhedral clinopyroxene, plagioclase, and opaque minerals.

S83-50: 45° 05.97' N Lat., 123° 55.17' W Long. Alkalic basalt. Nearly aphyric with very rare plagioclase and clinopyroxene phenocrysts in fine-grained, trachytic groundmass of feldspar and opaque minerals.

S83-73: 45° 08.30' N Lat, 123° 56.70' W Long. Ankaramitic basalt. Large, pinkish-brown clinopyroxene phenocrysts (to 1 cm) and minor olivine, pseudomorphed by green clay (saponite?), in an intergranular groundmass of anhedral clinopyroxene and opaque minerals.

S84-86: 44° 14.07' N Lat and 123° 55.12'W Long. Alkalic basalt. Moderately porphyritic with olivine and clinopyroxene microphenocrysts in intergranular groundmass of clinopyroxene and plagioclase and abundant opaque minerals. Olivine crystals look shattered; some are unaltered.

S84-112: 45° 02.79' N Lat., 123° 46.78' W Long. Ankaramite basalt flow. Highly porphyritic with large (to 1 cm) pink clinopyroxene phenocrysts and small fresh olivine phenocrysts in intergranular groundmass of clinopyroxene and opaque minerals.

S91-10: 45° 11.83' N Lat., 123° 54.63' W Long. Ankaramite basalt flow. Highly porphyritic with big, pink clinopyroxene phenocrysts accompanied by rare plagioclase and olivine microphenocrysts in an intergranular groundmass of clinopyroxene, olivine, minor plagioclase, and opaques. Some olivine is unaltered.

S91-15: 45° 06.04' N Lat., 123° 59.23' W Long. Alkalic basalt dike. Moderately porphyritic with large (to 3 cm) plagioclase and smaller clinopyroxene glomerocrysts in holocrystalline groundmass of subophitic clinopyroxene enclosing plagioclase and minor olivine and abundant opaque minerals. Olivine pseudomorphed by clay minerals.

S91-16: 45° 06.04' N Lat., 123° 59.23' W Long. Trachyandesite dike. Sparsely porphyritic with large, euhedral plagioclase and very rare clinopyroxene microphenocrysts in trachytic groundmass of feldspar and abundant opaque minerals and brown clay minerals.

Basalt of Cannery Hills

SR83-160C: 45° 11.1'N Lat., 123° 57.1'W Long. Moderately porphyritic basalt with sub-to anhedral olivine and clinopyroxene microphenocrysts in an intergranular groundmass of clinopyroxene, olivine, sparse plagioclase, and abundant opaque minerals. Olivine altered to clay minerals.

S87-23: .45° 08.3'N Lat., 123° 58.0'W Long. Moderately porphyritic basalt with sub- to euhedral olivine and clinopyroxene phenocrysts (to 0.5 cm) in an intergranular to subtrachytic groundmass of plagioclase, clinopyroxene, olivine, and abundant opaque minerals.

S87-83: 45° 09.7'N Lat., 123° 57.8'W Long. Sparsely porphyritic basalt with small clinopyroxene and olivine phenocrysts in an intergranular to subophitic groundmass of plagioclase, clinopyroxene, and opaque minerals. Olivine completely and clinopyroxene partially altered. Patches of clay minerals in the groundmass and sparse vesicles are filled with concentric layers of fiberous brown clay minerals.

SH64-1C: 45° 09.7'N Lat., 123° 57.8'W Long. Fine-grained, ankaramitic basalt with abundant euhedral clinopyroxene microphenocrysts in a intergranular goundmass of anhedral clinopyroxene, minor plagioclase, and abundant opaque minerals. Small veinlets and fractures filled with clay minerals.

SH64-1D: 45° 09.7'N Lat., 123° 57.8'W Long. Same lithology as above but more severely altered with abundant veins and fractures filled with greenish-yellow clay minerals, zeolites, and calcite.

SH64-1E: 45° 09.7'N Lat., 123° 57.8'W Long. Similar lithology as above but with fewer clinopyroxene microphenocrysts, most of which are altered. Severe alteration in veins and fractures of clays, zeolites, and calcite.

SH64-1G: 45° 09.7'N Lat., 123° 57.8'W Long. Same lithology as 1E; equally altered but rock looks even more brecciated.

Appendix 2A:. Representative analyses of feldspar from the Yachats Basalt

Sample	SW58-4 R	SW58-4 C	SW58-4 R	SW58-4 C	SW58-4 Gms	SW56-5 R	SW56-5 C	SW56-5 R	SW56-5 C	SW56-5 Gms	SR61-8A R	SR61-8A C	SR61-8A R
SiO_2	52.80	51.12	53.35	52.48	53.24	49.18	50.34	48.49	51.49	53.89	53.05	52.27	60.16
Al_2O_3	29.52	31.32	29.81	31.08	29.11	31.72	30.96	32.0	30.49	28.00	29.71	30.99	23.61
FeO	0.95	0.64	0.76	0.57	1.03	0.55	0.62	0.59	0.54	0.83	0.60	0.54	0.44
MgO	0.21	0.13	0.17	0.11	0.12	0.15	0.12	0.16	0.14	0.14	0.12	0.13	0.04
CaO	12.05	14.14	12.08	12.30	11.97	15.02	14.60	15.97	13.67	11.40	11.96	13.24	5.86
K_2O	0.20	0.12	0.20	0.18	0.26	0.11	0.13	0.09	0.16	0.32	0.19	0.14	0.64
Na_2O	4.39	3.44	4.54	4.29	4.55	2.82	3.14	2.34	3.65	4.84	4.59	3.82	7.91
Total	100.13	100.91	100.91	101.02	100.27	99.54	99.92	99.62	100.13	99.43	100.22	101.12	98.67
An	59.5	68.9	58.8	60.6	58.3	74.1	71.4	78.6	66.8	55.5	58.4	65.2	27.9
Ab	39.3	30.4	40.0	38.3	40.2	25.3	27.8	20.9	32.3	42.7	40.5	34.0	68.4
Or	1.2	0.7	1.1	1.1	1.5	0.6	0.8	0.5	0.9	1.8	1.1	0.8	3.6

Sample	SR61-8A C	SR61-8A Gms	SR61-106 R	SR61-106 C	SR61-106 R	SR61-106 C	SR61-106 Gms	SR61-109A R	SR61-109A C	SR61-109A R	SR61-109A C	SR61-109A Gms	S81-201A R
SiO_2	50.63	60.00	53.35	53.54	53.79	53.10	56.29	50.71	49.17	54.51	51.62	56.01	55.06
Al_2O_3	30.25	25.87	30.15	29.88	29.23	29.97	27.95	32.28	32.94	28.60	31.05	27.83	27.86
FeO	0.57	0.52	0.70	0.52	0.66	0.62	0.90	0.68	0.64	0.77	0.59	0.85	0.44
MgO	0.10	0.05	0.17	0.19	0.21	0.27	0.17	0.12	0.10	0.14	0.14	0.12	0.07
CaO	13.45	7.10	12.45	12.50	12.15	12.57	10.60	14.80	15.14	10.74	13.39	10.01	10.35
K_2O	0.14	0.49	0.25	0.25	0.27	0.26	0.39	0.13	0.12	0.38	0.16	0.48	0.29
Na_2O	3.80	7.23	4.23	4.19	4.44	4.06	5.17	2.93	2.67	5.08	3.77	5.53	5.54
Total	98.94	101.32	101.28	101.06	100.76	100.87	101.48	101..64	100.78	100.23	100.73	100.84	99.61
An	65.6	34.2	61.0	61.4	59.3	62.2	51.9	73.0	75.3	52.7	65.7	48.6	50.0
Ab	33.6	63.1	37.6	37.2	39.1	36.3	45.7	26.2	24.0	45.0	33.4	48.6	48.4
Or	0.8	2.8	1.4	1.4	1.6	1.5	2.4	0.8	0.7	2.2	0.9	2.7	1.7

Appendix 2A: Feldspar analyses continued

Sample	S81-201A C	S81-201A R	S81-201A C	S81-201A Gms	S81-201C R	S81-201C C	S81-201C R	S81-201C C	S81-201C Gms	S90-35 R	S90-35 C	S90-35 R
SiO_2	54.80	55.89	55.89	56.64	55.98	52.67	55.39	55.74	58.51	51.82	47.66	54.34
Al_2O_3	28.16	26.87	26.96	26.89	26.96	28.87	27.06	26.99	24.99	30.24	33.04	28.74
FeO	0.44	0.48	0.39	0.76	0.58	0.53	0.72	0.57	0.79	0.70	0.63	0.86
MgO	0.07	0.06	0.07	0.19	0.11	0.08	0.09	0.08	0.06	0.13	0.14	0.12
CaO	10.77	9.82	10.14	9.50	9.82	12.01	10.03	9.61	7.31	13.06	16.31	11.12
K_2O	0.26	0.29	0.29	0.37	0.46	0.26	0.51	0.46	0.90	0.16	0.07	0.27
Na_2O	5.24	5.82	5.63	5.78	5.75	4.58	5.49	5.77	6.80	4.00	2.24	5.15
Total	99.74	99.23	99.37	100.13	99.67	99.0	99.28	99.22	99.36	100.11	100.08	100.60
An	52.4	47.4	49.0	46.5	47.3	58.3	48.8	46.6	35.3	63.7	79.8	53.5
Ab	46.1	50.9	49.2	51.3	50.0	40.2	48.3	50.7	59.5	35.4	19.8	44.9
Or	1.5	1.7	1.7	2.1	2.7	1.5	2.9	2.7	5.1	0.9	0.4	1.6

Sample	S90-35 C	S90-35 Gms	S91-6 R	S91-6 C	S91-6 R	S91-6 C	S91-6 Gms	S91-11 R	S91-11 C	S91-11 R	S91-11 C	S91-11 Gms
SiO_2	47.45	54.99	53.36	51.07	52.08	52.67	53.01	58.95	59.13	58.97	58.31	61.76
Al_2O_3	33.04	27.57	29.30	30.05	29.88	29.26	29.26	25.11	25.02	25.95	25.76	21.72
FeO	0.70	1.32	0.64	0.43	0.55	0.49	0.77	0.26	0.33	0.24	0.33	0.60
MgO	0.12	0.35	0.22	0.11	0.17	0.11	0.17	0.03	0.04	0.03	0.03	0.05
CaO	16.09	9.98	12.13	13.22	12.87	11.98	12.16	6.94	6.98	7.22	7.53	3.39
K_2O	0.06	0.33	0.29	0.30	0.23	0.35	0.29	0.57	0.58	0.51	0.47	1.91
Na_2O	2.25	5.46	4.39	3.93	4.12	4.50	4.54	7.38	7.13	7.28	6.95	8.31
Total	99.71	100.00	100.33	99.10	99.88	99.37	100.21	99.34	99.21	100.20	99.37	97.86
An	79.5	49.3	59.4	63.9	62.5	58.3	57.5	33.1	33.9	34.4	36.4	16.4
Ab	20.1	48.8	38.9	34.4	36.2	39.7	39.7	63.7	62.7	62.7	60.9	72.6
Or	0.4	1.9	1.7	1.7	1.3	2.1	1.7	3.2	3.4	2.9	2.7	11.0

R and C, rim and core of phenocrysts. Gms, crystals in groundmass.

Appendix 2B:. Representative analyses of feldspar from Cascade Head basalts

Sample	S79-36 R	S79-36 C	S79-36 R	S79-36 C	S79-36 Gms	SR61-5 R	SR61-5 C	SR61-5 R	SR61-5 C	SR61-5 Gms	SR62-160 R	SR62-160 C	SR62-160 C
SiO_2	58.66	59.18	59.72	57.86	62.27	52.27	49.36	53.02	49.05	65.83	49.70	53.47	49.45
Al_2O_3	26.05	26.23	25.23	26.61	23.35	26.68	32.99	29.98	32.65	20.13	31.03	28.19	31.41
FeO	0.22	0.22	0.36	0.26	0.33	1.39	0.54	0.63	0.49	0.38	0.60	0.56	0.47
MgO	0.03	0.02	0.02	0.03	0.01	0.61	0.11	0.13	0.10	0.00	0.10	0.11	0.07
CaO	7.62	7.37	6.60	7.76	4.49	11.98	14.96	12.29	14.86	0.90	13.98	11.69	14.50
K_2O	0.48	0.47	0.55	0.44	1.20	0.27	0.13	0.26	0.13	6.66	0.19	0.32	0.15
Na_2O	7.02	7.17	7.57	6.93	8.35	4.15	2.90	4.33	2.91	6.76	3.43	4.75	3.05
Total	100.09	100.65	100.11	99.87	100.01	100.35	100.99	100.5	100.18	100.65	99.22	99.07	99.11
An	36.5	35.2	31.5	37.3	21.3	60.4	73.5	60.1	73.3	4.3	68.5	56.8	71.8
Ab	60.8	62.1	65.4	60.2	71.9	37.9	32.8	38.4	26.0	58.1	30.4	41.4	27.3
Or	2.8	2.7	3.1	2.5	6.8	1.7	1.2	1.5	0.7	37.6	1.1	1.8	0.9

Sample	SR62-160 R	SR62-160 Gms	MR68-80 R	MR68-80 C	MR68-80 R	MR68-80 C	MR68-80 Gms	MR68-81 R	MR68-81 C	MR68-81 R	MR68-81 C	MR68-81 Gms	SR83-48 R
SiO_2	49.35	64.36	49.71	52.44	52.50	51.71	54.96	51.59	51.14	54.65	51.40	56.39	52.11
Al_2O_3	31.45	20.59	31.02	29.18	29.10	30.05	27.41	30.42	30.49	28.36	29.99	26.72	29.12
FeO	0.60	0.51	0.58	0.50	0.53	0.52	0.72	0.64	0.52	0.50	0.54	0.47	0.57
MgO	0.10	0.10	0.11	0.10	0.10	0.10	0.13	0.14	0.15	0.10	0.13	0.07	0.17
CaO	14.28	2.53	14.30	12.28	12.10	12.58	10.12	13.25	12.90	10.67	12.98	8.67	13.03
K_2O	0.16	3.84	0.13	0.21	0.23	0.19	0.39	0.29	0.30	0.40	0.30	0.57	0.24
Na_2O	3.17	7.41	3.26	4.41	4.45	4.17	5.55	3.89	4.17	5.32	4.13	6.35	3.98
Total	99.12	99.33	99.12	99.11	98.99	99.32	99.25	100.21	99.67	100.27	99.46	99.45	99.23
An	70.7	12.4	70.3	59.9	59.2	61.8	49.1	64.2	62.0	51.4	62.4	41.6	63.5
Ab	28.4	65.3	29.0	38.9	39.4	37.1	48.7	34.1	36.2	46.3	35.9	55.1	35.1
Or	0.9	22.3	0.7	1.2	1.3	1.1	2.2	1.7	1.8	2.3	1.7	3.3	1.4

Appendix 2B: Feldspar analyses continued

Sample	SR83-48 C	SR83-48 R	SR83-48 C	SR83-48 Gms	S83-86 Gms	S83-86 Gms	SR83-94 Gms	SR83-94 Gms	S91-10 R	S91-10 C	S91-10 R	S91-10 C	S91-10 Gms
SiO_2	53.04	52.38	53.19	58.40	51.45	62.97	52.27	53.71	52.40	47.25	51.36	47.59	51.24
Al_2O_3	28.56	29.50	28.99	25.20	30.12	21.51	28.94	28.28	29.29	33.85	29.76	32.48	29.70
FeO	0.51	0.64	0.60	0.43	0.77	0.39	1.35	0.80	0.61	0.52	0.75	0.56	0.88
MgO	0.15	0.14	0.17	0.06	0.04	0.01	0.08	0.08	0.10	0.10	0.14	0.09	0.11
CaO	12.17	12.68	12.22	7.81	12.15	2.88	11.55	9.23	11.81	16.34	12.78	15.84	12.62
K_2O	0.33	0.27	0.33	0.84	0.29	3.47	0.29	0.78	0.41	0.10	0.33	0.13	0.34
Na_2O	4.56	4.07	4.40	6.68	4.46	7.72	4.61	5.46	4.40	2.06	3.98	2.29	4.05
Total	99.32	99.69	99.89	99.42	99.14	98.96	99.09	98.33	99.02	100.22	99.10	98.98	98.93
An	58.5	62.2	59.4	37.4	59.1	13.7	57.1	46.0	58.3	81.0	62.7	78.6	62.0
Ab	39.6	36.2	38.7	57.9	39.2	66.6	41.2	49.3	39.3	18.5	35.3	20.6	36.0
Or	1.9	1.6	1.9	4.8	1.7	19.7	1.7	4.7	2.4	0.6	1.9	0.8	2.0

R and C, rim and core of phenocrysts. Gms, crystals in groundmass.

Appendix 3 A:. Representative analyses of clinopyroxene from Yachats Basalt

Sample	SW58-4 R	SW58-4 C	SW58-4 R	SW58-4 C	SW58-4 Gms	SW56-5 Gms	SW56-5 Gms	SR61-106 R	SR61-106 C	SR61-106 R	SR61-106 C	SR61-106 Gms
SiO_2	50.67	51.57	51.02	51.85	51.66	48.09	48.70	51.79	51.41	53.34	53.00	51.68
TiO_2	1.48	1.29	1.59	0.96	1.28	2.68	2.49	1.15	1.37	0.62	0.68	1.67
Al_2O_3	2.61	2.73	2.75	3.78	2.14	5.24	4.78	2.13	2.90	2.76	2.32	2.21
FeO	11.02	8.63	10.54	7.07	9.99	10.77	10.38	9.29	9.78	6.19	5.77	10.94
Cr_2O_3	0.00	0.10	0.00	0.31	0.00	0.01	0.10	0.20	0.25	0.56	0.77	0.01
MnO	0.25	0.19	0.25	0.16	0.24	0.24	0.21	0.22	0.24	0.15	0.14	0.26
MgO	14.85	15.52	14.27	16.53	15.12	12.93	13.95	15.65	15.25	17.95	17.50	14.20
CaO	18.81	20.13	19.46	19.32	19.51	20.01	19.50	18.44	17.99	18.36	19.60	19.30
Na_2O	0.35	0.34	0.38	0.38	0.32	0.37	0.38	0.36	0.39	0.36	0.36	0.38
Total	100.03	100.49	100.26	100.35	100.25	100.33	100.47	99.24	99.56	100.28	100.15	100.64
Wo	39.1	41.6	40.9	40.4	40.3	43.1	41.5	38.9	38.4	38.1	40.4	40.6
En	43.0	44.5	41.7	48.1	43.5	38.8	41.3	45.9	45.3	51.8	50.3	41.5
Fs	17.9	13.9	17.3	11.5	16.1	18.1	17.2	15.3	16.3	10.0	9.3	17.9
Mg#	70.6	76.2	70.7	80.7	72.9	68.2	70.6	75.0	73.5	83.8	84.4	69.8

Sample	SR61-109 Mr	SR61-109 Mc	SR61-8A R	SR61-8A C	SRr61-8A Gms	S81-201C R	S81-201C C	S81-201C Mc	S81-201C R	S81-201C C	S81-201C Mc	S90-35 Gms
SiO_2	50.95	51.79	51.30	51.18	50.96	51.75	52.12	51.19	52.0	52.11	50.64	49.26
TiO_2	0.97	1.14	1.34	1.51	1.39	1.26	1.04	1.22	0.74	0.62	0.64	2.00
Al_2O_3	1.75	1.87	2.99	3.27	3.26	1.95	1.36	1.51	4.23	1.92	2.03	3.85
FeO	11.63	11.83	10.06	9.91	11.23	12.90	13.48	12.79	12.33	13.30	13.13	10.10
Cr_2O_3	0.00	0.00	0.00	0.01	0.00	0.00	0.01	0.00	0.00	0.00	0.01	0.00
MnO	0.37	0.39	0.26	0.23	0.32	0.36	0.38	0.36	0.42	0.50	0.46	0.24
MgO	13.70	14.23	13.81	13.94	13.69	14.13	14.79	14.07	11.97	13.53	13.23	13.18
CaO	19.30	18.78	19.98	19.89	19.08	18.51	17.71	18.47	17.64	18.59	18.80	20.71
Na_2O	0.30	0.33	0.34	0.36	0.35	0.34	0.28	0.32	1.10	0.34	0.35	0.41
Total	98.94	100.35	100.06	100.30	100.30	101.19	101.16	99.93	100.43	100.91	99.28	99.74
Wo	40.7	39.3	42.4	42.3	40.7	38.4	36.3	38.5	40.2	38.9	39.6	44.1
En	40.2	41.4	40.9	41.3	40.6	40.7	42.2	40.8	37.9	39.4	38.8	39.1
Fs	19.2	19.3	16.7	16.4	18.7	20.9	21.6	20.8	21.9	21.7	21.6	16.9
Mg#	67.7	68.2	71.0	71.5	68.5	66.1	66.2	66.3	63.4	64.4	64.2	70.0

Appendix 3 A:. Continued

Sample	S89-15 mc	S89-15 mc	S89-15 mc	S91-13 R	S91-13 C	S91-14 R	S91-14 C	S91-14 R	S91-14 C	S91-14 R	S91-14 C	S91-14 Gms
SiO_2	49.95	48.51	49.82	50.70	49.12	45.60	49.69	46.31	49.99	50.18	50.27	49.61
TiO_2	1.45	2.15	1.41	0.95	1.42	3.71	1.58	3.20	1.40	1.93	1.27	1.46
Al_2O_3	2.99	3.70	3.02	2.62	3.61	6.86	4.06	6.02	3.70	3.01	3.69	4.47
FeO	8.54	9.41	8.63	9.52	11.71	9.17	6.17	7.92	5.67	7.17	5.65	7.56
Cr_2O_3	0.01	0.00	0.01	0.00	0.00	0.00	0.81	0.02	0.66	0.01	0..77	0.04
MnO	0.27	0.25	0.29	0.24	0.28	0.18	0.12	0.10	0.15	0.14	0.10	0.16
MgO	13.03	13.28	13.10	14.35	13.33	12.05	15.33	12.93	15.32	15.02	15.40	14.79
CaO	21.64	20.73	21.81	20.50	19.13	21.10	21.21	21.81	21.57	21.59	21.37	20.51
Na_2O	0.69	0.49	0.66	0.35	0.38	0.62	0.57	0.46	0.50	0.36	0.52	0.62
Total	98.563	98.51	98.74	99.23	98.98	99.28	99.54	98.76	98.94	99.41	99.04	99.22
Wo	46.6	44.5	46.6	42.8	40.9	46.9	44.8	47.4	45.6	44.9	45.3	43.6
En	39.0	39.7	39.0	41.7	39.6	37.2	45.0	39.1	45.0	43.5	45.4	43.8
Fs	14.4	15.8	14.4	15.5	19.5	15.9	10.2	13.4	9.4	11.6	9.3	12.6
Mg#	73.1	71.6	73.0	72.9	67.0	70.1	81.6	74.4	82.8	78.9	82.9	77.7

R, C and Mr, Mc are Rims and cores of phenocrysts and microphenocrysts, respectively. Gms, crystals in groundmass. Mg# is atomic 100Mg/(Mg+Fe).

Appendix 3 B:. Representative analyses of clinopyroxene from Cascade Head basalt

Sample	SR61-5 R	SR61-5 C	SR61-5 R	SR61-5 C	SR61-5 Gms	SR83-94 R	SR83-94 C	SR83-94 R	SR83-94 Gms	SR83-86 R	SR83-86 C	SR83-86 Gms
SiO_2	48.59	51.07	49.62	48.90	50.02	47.07	49.50	48.38	49.50	48.84	50.61	49.62
TiO_2	2.82	1.46	2.38	2.40	1.96	3.66	1.79	2.48	2.99	2.70	1.58	1.84
Al_2O_3	5.68	4.17	3.69	5.29	3.34	6.69	4.30	5.29	9.67	3.92	3.59	4.07
FeO	7.69	6.21	8.45	7.03	8.71	8.02	6.47	7.13	6.88	8.51	6.07	9.45
Cr_2O_3	0.02	0.33	0.00	0.18	0.01	0.03	0.47	0.04	0.01	0.00	0.48	0.00
MnO	0.16	0.11	0.21	0.12	0.26	0.16	0.12	0.14	0.14	0 .18	0.10	0.21
MgO	13.34	15.06	13.73	14.26	13.19	12.28	14.27	13.47	10.41	13.29	15.10	13.92
CaO	21.86	21.49	21.22	21.59	21.00	21.10	21.45	21.77	19.59	21.79	22.48	20.65
Na_2O	0.48	0.50	0.55	0.55	0.53	0.51	0.47	0.47	1.30	0.47	0.36	0.43
Total	100.64	100.39	99.84	100.31	99.01	99.51	98.83	99.15	100.50	99.68	100.37	100.19
Wo	47.1	45.5	45.2	46.0	45.5	47.5	46.3	47.2	49.7	46.4	46.6	43.6
En	40.0	44.3	40.7	42.3	39.8	38.5	42.8	40.7	36.7	39.4	43.6	40.9
Fs	12.9	10.3	14.1	11.7	14.7	14.1	10.9	12.1	13.6	14.2	9.8	15.6
Mg#	75.6	81.2	74.3	78.3	73.0	73.2	79.8	77.1	73.0	73.5	81.6	72.4

Sample	SR62-160 R	SR62-160 C	SR62-160 Mr	SR62-160 Mc	SR83-48 R	SR83-48 C	SR83-48 R	SR83-48 C	SW56-5 Gms	SW56-5 gms	S91-10 R	S91-10 C
SiO_2	49.81	49.19	49.53	50.58	51.01	50.02	49.28	49.04	48.09	49.95	48.82	48.50
TiO_2	1.91	1.79	1.79	1.61	1.76	1.41	2.39	2.01	2.68	1.81	2.36	1.82
Al_2O_3	4.42	4.35	4.39	3.70	2.33	3.73	3.20	5.18	5.24	3.22	3.78	4.73
FeO	7.43	6.82	7.06	6.91	9.14	6.12	9.44	8.08	10.77	10.24	8.37	7.74
Cr_2O_3	0.01	0.11	0.15	0.15	0.01	0.13	0.01	0.22	0.01	0.03	0.01	0.00
MnO	0.19	0.12	0.15	0.13	0.19	15.50	0.18	0.16	0.24	0.22	0.18	0.20
MgO	14.07	14.19	14.39	14.79	14.24	21.50	12.99	14.00	12.93	14.10	13.89	14.32
CaO	21.85	22.65	21.98	22.08	20.92	21.50	21.07	20.74	20.01	20.23	21.51	21.24
Na_2O	0.51	0.43	0.41	0.42	0.37	0.36	0.41	0.50	0.37	0.32	0.48	0.47
Total	100.20	99.59	99.85	100.35	99.96	99.07	98.95	99.92	100.33	100.12	99.41	99.02
Wo	46.2	47.5	46.3	46.0	43.7	44.9	45.3	44.6	43.1	42.3	45.4	45.0
En	41.5	41.4	42.1	42.8	41.4	45.1	38.9	41.9	38.8	41.0	40.8	42.2
Fs	12.3	11.1	11.6	11.2	14.9	10.0	15.8	13.5	18.1	16.7	13.8	12.8
Mg#	77.1	78.8	78.4	79.2	73.5	81.9	71.0	75.6	68.2	71.1	74.7	76.8

R,C, and Mr, Mc are rims and cores of phenocrysts and microphenocrysts, respectively. Gms, crystals in groundmass. Mg# is atomic 100 Mg/(Mg+Fe).

Appendix 4: Representative olivine analyses

Yachats Basalt

Sample	SR58-17 Mc	SR58-17 Mc	SR58-17 Mc	S89-15 Mc	S89-15 Mc	S89-15 Mc	S89-15 Mc	S89-15 Mc
MgO	35.05	35.16	34.51	29.36	29.19	30.84	31.75	30.98
SiO_2	37.27	37.41	37.36	36.07	36.10	36.45	36.71	36.57
CaO	0.28	0.33	0.31	0.53	0.43	0.36	0.37	0.40
MnO	0.36	0.33	0.37	0.92	0.87	0.83	0.81	0.78
FeO	27.80	27.75	27.37	34.06	34.27	31.79	30.64	31.64
NiO	0.13	0.08	0.11	0.00	0.00	0.02	0.03	0.01
Total	100.88	101.06	100.03	100.92	100.85	100.30	100.30	100.41
Fo (mol.%)	69.2	69.3	69.2	60.6	60.3	63.4	65.1	63.9

Cascade Head basalt

Sample	SR83-86 R	SR83-86 C	SR83-86 R	SR83-86 C	SR83-86 Gms	SR83-86 Gms	SR83-94 R	SR83-94 C
MgO	27.89	39.89	37.55	43.04	23.25	20.91	41.42	43.10
SiO_2	36.59	39.51	37.70	38.03	35.54	35.08	39.35	39.61
CaO	0.33	0.25	0.30	0.28	0.49	0.50	0.25	0.22
MnO	0.63	0.31	0.38	0.27	0.80	0.86	0.35	0.24
FeO	35.46	20.58	24.90	18.39	40.07	43.64	19.67	16.96
NiO	0.03	0.20	0.11	0.21	0.01	0.01	0.10	0.24
Total	100.94	100.73	100.93	100.21	100.15	101.00	101.14	100.36
Fo (mol.%)	58.4	77.5	72.9	80.7	50.9	46.0	79.0	81.9

Sample	SR83-94 R	SR83-94 C	SR83-94 R	SR83-94 C	S91-10 R	S91-10 C	S91-10 Mr	S91-10 Mc
MgO	39.48	40.01	40.04	41.16	35.11	37.19	34.05	34.74
SiO_2	39.42	39.52	39.41	39.77	38.40	39.04	37.32	38.08
CaO	0.22	0.19	0.23	0.20	0.34	0.21	0.40	0.38
MnO	0.39	0.31	0.34	0.29	0.47	0.33	0.49	0.47
FeO	20.83	20.51	20.18	19.18	26.67	24.48	27.52	27.36
NiO	0.09	0.15	0.15	0.19	0.07	0.05	0.05	0.05
Total	100.42	100.69	100.34	100.78	101.06	101.31	100.82	101.06
Fo (mol.%)	77.2	77.7	77.9	79.3	70.1	73.0	68.8	69.3

R, C, rim and core of phenocrysts. Mr, Mc, rim and core of microphenocrysts. Gms, crystals in groundmass.

Appendix 5: Amphibole analyses of Cascade Head basalts

Sample	MR68-80 R	MR68-80 C	MR68-80 R	MR68-80 C	MR68-80 R	MR68-80 C	S79-36 R	S79-36 C	S79-36 R	S79-36 C	S79-36 R	S79-36 C
Na2O	2.60	2.58	2.68	2.64	2.61	2.59	2.63	2.57	2.71	2.63	2.66	2.68
MgO	13.22	13.18	13.08	13.24	13.12	13.19	9.91	10.14	10.26	10.14	10.01	10.51
Al2O3	13.29	13.26	13.04	13.02	13.25	13.35	11.37	11.48	11.43	11.62	11.66	11.67
SiO2	40.87	40.84	40.26	40.54	40.67	40.87	41.67	41.63	41.89	41.30	41.75	41.65
K2O	0.71	0.71	0.70	0.73	0.69	0.71	0.75	0.70	0.74	0.72	0.72	0.68
Cl	0.01	0.01	0.02	0.02	0.01	0.02	0.05	0.04	0.04	0.04	0.05	0.05
CaO	12.14	12.13	12.14	12.04	12.17	12.13	10.50	10.52	10.39	10.52	10.38	10.47
TiO2	5.61	5.69	5.52	5.62	5.63	5.70	3.69	3.76	3.65	3.56	3.69	3.80
Cr2O3	0.01	0.01	0.01	0.00	0.02	0.00	0.01	0.00	0.01	0.00	0.00	0.00
MnO	0.21	0.21	0.19	0.20	0.19	0.20	0.52	0.53	0.57	0.52	0.52	0.53
FeO	11.31	11.29	11.29	11.22	11.19	11.27	17.38	17.22	17.46	17.18	17.38	16.61
Total	100.0	99.91	98.92	99.27	99.55	100.03	98.48	98.60	99.15	98.22	98.81	98.65

R and C, rim and core of phenocrysts.